

REPORT NO.  
EERC 76-27  
NOVEMBER 1976

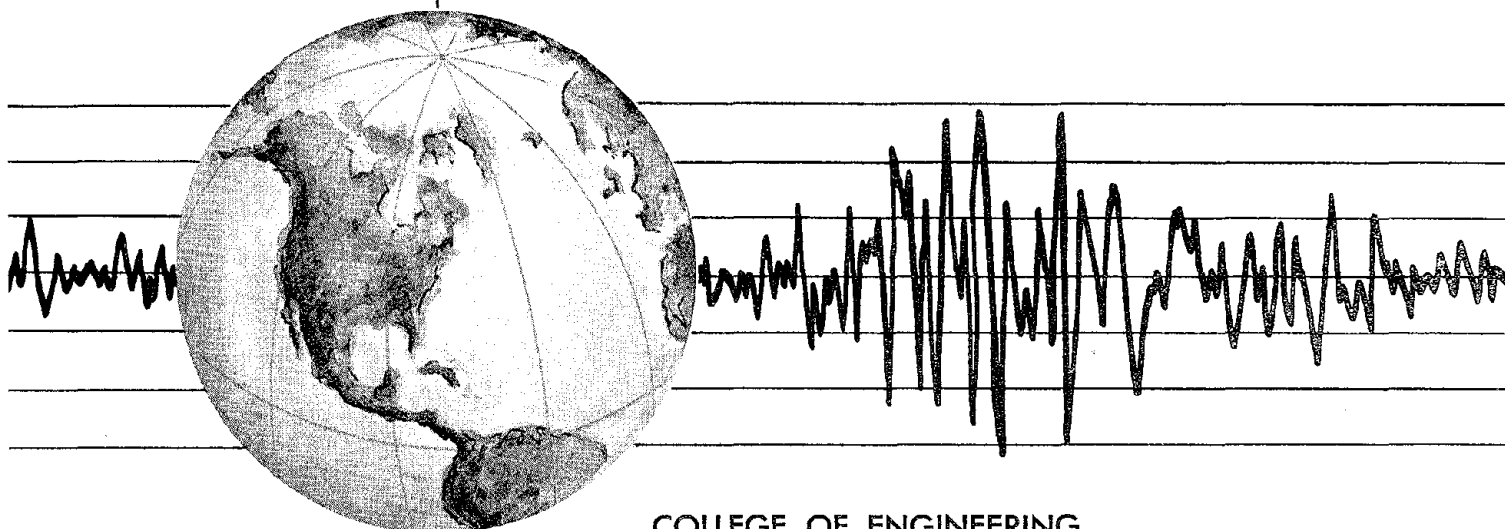
EARTHQUAKE ENGINEERING RESEARCH CENTER

# EARTHQUAKE RESPONSE OF COUPLED SHEAR WALL BUILDINGS

by  
THIRAWAT SRICHATRAPIMUK

Faculty Supervisor:  
ANIL K. CHOPRA

A report on research conducted under  
Grants GI-36387, AEN73-07732 A02 & ENV76-04264  
from the National Science Foundation.



COLLEGE OF ENGINEERING

UNIVERSITY OF CALIFORNIA • Berkeley, California



EARTHQUAKE RESPONSE OF COUPLED  
SHEAR WALL BUILDINGS

Dissertation by  
Thirawat Srichatrapimuk

In Partial Satisfaction of the Requirements  
for the Degree of Doctor of Philosophy

Faculty Supervisor: Anil K. Chopra

Research Conducted under Grants from the  
National Science Foundation  
(Grants GI-36387, AEN73-07732 A02, & ENV76-04264)

Report No. EERC 76-27

Earthquake Engineering Research Center  
University of California  
Berkeley, California

November 1976



BIBLIOGRAPHIC DATA SHEET		1. Report No. EERC 76-27	2.	3. Recipient's Accession No.
4. Title and Subtitle "Earthquake Response of Coupled Shear Wall Buildings"				5. Report Date November 1976
7. Author(s) Thirawat Srichatrapimuk				6.
9. Performing Organization Name and Address Earthquake Engineering Research Center University of California, Berkeley 47th Street and Hoffman Blvd. Richmond, California 94804				8. Performing Organization Rept. No. 76-27
12. Sponsoring Organization Name and Address National Science Foundation 1800 G Street, N.W. Washington, D. C. 20550				10. Project/Task/Work Unit No.
				11. Contract/Grant No. GI 36387 AEN73-07732 A02 ENV76-04264
				13. Type of Report & Period Covered
15. Supplementary Notes				14.
<p>16. Abstracts An efficient analytical technique for determining linear and nonlinear responses of coupled shear wall structures is developed. Walls are assumed to be non-yielding with all inelastic action confined to coupling beams. Structural displacements are then represented as a linear combination of the first few natural mode shapes in both lateral and longitudinal (vertical) vibration of individual walls which are treated as independent cantilevers. The number of degrees of freedom of the system is thereby substantially reduced. With such a reduction technique, vertical inertia need not be neglected and any mechanical model for coupling beams may be incorporated into the analysis.</p> <p>The effectiveness and flexibility of this general approach in reducing the number of degrees of freedom are demonstrated. The technique results in a considerable reduction in computational effort when compared to standard programs used to analyze inelastic structural response.</p> <p>The analytical technique is implemented in earthquake response analyses of two coupled shear wall systems; analytical results are then correlated with observations of earthquake damage in these structures. The earthquake response of coupled shear walls is then interpreted, and design considerations for efficient earthquake resistant shear wall systems are suggested.</p>				
17b. Identifiers/Open-Ended Terms				
17c. COSATI Field/Group				
18. Availability Statement Release Unlimited			19. Security Class (This Report) UNCLASSIFIED	21. No. of Pages 140
			20. Security Class (This Page) UNCLASSIFIED	22. Price PC A07/AF-A01

**INSTRUCTIONS FOR COMPLETING FORM NTIS-35 (10-70)** (Bibliographic Data Sheet based on COSATI Guidelines to Format Standards for Scientific and Technical Reports Prepared by or for the Federal Government, PB-180 600).

1. **Report Number.** Each individually bound report shall carry a unique alphanumeric designation selected by the performing organization or provided by the sponsoring organization. Use uppercase letters and Arabic numerals only. Examples FASEB-NS-87 and FAA-RD-68-09.
2. Leave blank.
3. **Recipient's Accession Number.** Reserved for use by each report recipient.
4. **Title and Subtitle.** Title should indicate clearly and briefly the subject coverage of the report, and be displayed prominently. Set subtitle, if used, in smaller type or otherwise subordinate it to main title. When a report is prepared in more than one volume, repeat the primary title, add volume number and include subtitle for the specific volume.
5. **Report Date.** Each report shall carry a date indicating at least month and year. Indicate the basis on which it was selected (e.g., date of issue, date of approval, date of preparation).
6. **Performing Organization Code.** Leave blank.
7. **Author(s).** Give name(s) in conventional order (e.g., John R. Doe, or J. Robert Doe). List author's affiliation if it differs from the performing organization.
8. **Performing Organization Report Number.** Insert if performing organization wishes to assign this number.
9. **Performing Organization Name and Address.** Give name, street, city, state, and zip code. List no more than two levels of an organizational hierarchy. Display the name of the organization exactly as it should appear in Government indexes such as USGRDR-I.
10. **Project/Task/Work Unit Number.** Use the project, task and work unit numbers under which the report was prepared.
11. **Contract/Grant Number.** Insert contract or grant number under which report was prepared.
12. **Sponsoring Agency Name and Address.** Include zip code.
13. **Type of Report and Period Covered.** Indicate interim, final, etc., and, if applicable, dates covered.
14. **Sponsoring Agency Code.** Leave blank.
15. **Supplementary Notes.** Enter information not included elsewhere but useful, such as: Prepared in cooperation with . . . Translation of . . . Presented at conference of . . . To be published in . . . Supersedes . . . Supplements . . .
16. **Abstract.** Include a brief (200 words or less) factual summary of the most significant information contained in the report. If the report contains a significant bibliography or literature survey, mention it here.
17. **Key Words and Document Analysis.** (a). **Descriptors.** Select from the Thesaurus of Engineering and Scientific Terms the proper authorized terms that identify the major concept of the research and are sufficiently specific and precise to be used as index entries for cataloging.  
(b). **Identifiers and Open-Ended Terms.** Use identifiers for project names, code names, equipment designators, etc. Use open-ended terms written in descriptor form for those subjects for which no descriptor exists.  
(c). **COSATI Field/Group.** Field and Group assignments are to be taken from the 1965 COSATI Subject Category List. Since the majority of documents are multidisciplinary in nature, the primary Field/Group assignment(s) will be the specific discipline, area of human endeavor, or type of physical object. The application(s) will be cross-referenced with secondary Field/Group assignments that will follow the primary posting(s).
18. **Distribution Statement.** Denote releasability to the public or limitation for reasons other than security for example "Release unlimited". Cite any availability to the public, with address and price.
- 19 & 20. **Security Classification.** Do not submit classified reports to the National Technical
21. **Number of Pages.** Insert the total number of pages, including this one and unnumbered pages, but excluding distribution list, if any.
22. **Price.** Insert the price set by the National Technical Information Service or the Government Printing Office, if known.

## ABSTRACT

An efficient analytical technique for determining linear and nonlinear responses of coupled shear wall structures is developed. Walls are assumed to be nonyielding with all inelastic action confined to coupling beams. Structural displacements are then represented as a linear combination of the first few natural mode shapes in both lateral and longitudinal (vertical) vibration of individual walls which are treated as independent cantilevers. The number of degrees of freedom of the system is thereby substantially reduced. With such a reduction technique, vertical inertia need not be neglected and any mechanical model for coupling beams may be incorporated into the analysis.

The effectiveness and flexibility of this general approach in reducing the number of degrees of freedom are demonstrated. The technique results in a considerable reduction in computational effort when compared to standard programs used to analyze inelastic structural response.

The analytical technique is implemented in earthquake response analyses of two coupled shear wall systems; analytical results are then correlated with observations of earthquake damage in these structures. The earthquake response of coupled shear walls is then interpreted, and design considerations for efficient earthquake resistant shear wall systems are suggested.



### ACKNOWLEDGEMENTS

A scholarship from the Thai Government enabled the author to pursue his doctoral studies at the University of California, Berkeley. The research reported herein was made possible through National Science Foundation Grants GI-36387, AEN73-07732 A02, and ENV76-04264.

The author is truly grateful to Professor Anil K. Chopra for his assistance, encouragement, and guidance throughout the course of this research. Invaluable suggestions were offered by Professor Vitelmo V. Bertero at times during the research and preparation of this thesis and are gratefully acknowledged. Professor Bruce A. Bolt has kindly reviewed the manuscript.

Special thanks are due to Dr. Stephen A. Mahin for providing drawings and a photograph of the Banco de America Building, as well as computer input data for the same building. The editorial assistance of Judith Sanders in preparing the manuscript is greatly appreciated. The assistance of Shirley Edwards in typing the final manuscript, and of Al Klash, Gail Feazell, and Lea Rambeau in preparing the drawings is also appreciated.

The author wishes to express his deepest gratitude to his parents for their continual moral support and to his two lovely sisters, Wunpen and Pimjai, who sacrificed so that he might be able to continue his education.



## TABLE OF CONTENTS

	<u>Page</u>
ACKNOWLEDGEMENTS . . . . .	i-D
TABLE OF CONTENTS . . . . .	ii
1. INTRODUCTION . . . . .	1
1.1 Coupled Shear Wall Structures . . . . .	1
1.2 Review of Past Work . . . . .	1
1.3 Objective and Scope . . . . .	3
2. ANALYTICAL PROCEDURE . . . . .	5
2.1 Scope of Chapter . . . . .	5
2.2 Assumptions . . . . .	5
2.3 Equations of Motion in Nodal Point Coordinates . . . . .	7
2.3.1 $i^{\text{th}}$ Story Coupling Beam . . . . .	8
2.3.2 $i^{\text{th}}$ Story Wall Element . . . . .	13
2.4 Reduction of Degrees of Freedom . . . . .	19
2.4.1 Selection of Generalized Coordinates . . . . .	19
2.4.2 Equations of Motion in Generalized Coordinates . . . . .	20
2.5 Mechanical Model for Coupling Beams . . . . .	23
2.6 Step-by-Step Time History Analysis . . . . .	24
2.6.1 Linear Analysis . . . . .	25
2.6.2 Nonlinear Analysis . . . . .	25
2.7 Computer Program . . . . .	26
3. EVALUATION OF REDUCTION TECHNIQUE . . . . .	28
3.1 Scope of Chapter . . . . .	28



	<u>Page</u>
3.2 Mode Shapes and Frequencies . . . . .	28
3.2.1 Case Study of a Coupled Shear Wall Model . . . . .	28
3.2.2 Mode Shapes and Frequencies . . . . .	29
3.3 Modal Stress Resultants . . . . .	30
3.4 Nonlinear Time - History Response . . . . .	33
3.5 Computational Aspect: Reduced System v.s. Original System . . . . .	35
4. ANALYSIS OF EARTHQUAKE-DAMAGED BUILDINGS . . . . .	37
4.1 Scope of Chapter . . . . .	37
4.2 McKinley Building . . . . .	37
4.2.1 Structural System and Design Criteria . . . . .	37
4.2.2 Observed Damage . . . . .	39
4.2.3 Ground Motion . . . . .	40
4.2.4 Analytical Model . . . . .	40
4.2.5 Earthquake Response - Correlation with Observed Damage . . . . .	42
4.3 Banco de America Building . . . . .	46
4.3.1 Structural System and Design Criteria . . . . .	46
4.3.2 Observed Damage . . . . .	47
4.3.3 Ground Motion . . . . .	48
4.3.4 Analytical Model . . . . .	48
4.3.5 Earthquake Response - Correlation with Observed Damage . . . . .	50
4.4 Design Considerations for Coupled Shear Wall Systems . . . . .	53
5. CONCLUSIONS . . . . .	57
REFERENCES . . . . .	61



	<u>Page</u>
TABLES . . . . .	64
FIGURES . . . . .	67
APPENDIX I NOTATION . . . . .	113



## 1. INTRODUCTION

### 1.1 Coupled Shear Wall Structures

Coupled shear walls in high-rise buildings can effectively resist lateral forces from winds and strong ground motions. Such a building performed excellently during a recent earthquake in Managua<sup>(27)</sup>.

Isolated shear walls in high-rise buildings are usually subjected to high overturning moments and high story shears. Allowing such walls to yield might lead to structural instability, while requiring these walls to remain elastic leads to a costly design. Instead, when two shear walls are coupled by a series of floor beams with appropriate stiffness and dimensions, substantial moment couples associated with axial forces in the wall can be created to help resist story overturning moments. Walls therefore need resist only part of the story overturning moment and story shears.

A coupled shear wall can be an efficient seismic resistant system if inelastic yielding is confined to ductile coupling beams. The elastic walls maintain structural stability, while coupling beams dissipate earthquake energy through inelastic action. Walls provide a major part of lateral stiffness, thereby controlling lateral story drift and limiting nonstructural damage during an earthquake.

### 1.2 Review of Past Work

The best-known simplified technique for analyzing the seismic behavior of coupled shear wall structures is the continuous laminae theory<sup>(9)</sup>. Discrete coupling beams are modeled by equivalent continuous media, consisting of independently acting laminae. The system's

equilibrium is governed by a second order differential equation with constant coefficients. The technique has been applied extensively to analyses of coupled shear walls under various types of static lateral loading<sup>(4,8,10,24)</sup>. Satisfactory results have been obtained for systems with a large number of stories, i.e. when interstory height is relatively small when compared to a structure's total height.

This analytical technique has been used to analyze the inelastic response of coupled shear wall systems<sup>(22,32)</sup>. Because coupling beams are modeled by a series of continuous laminae, analytical results do not accurately reflect nonlinear behavior due to cracking of concrete and yielding of reinforcement.

Earlier investigations assumed that wall-beam panel zones were perfectly rigid and that a point of contraflexure occurred at the midspan of each lamina. The deformability of the wall-beam panel zone was later found to affect structural response substantially<sup>(11)</sup>. Also, the contraflexure point does not occur at midspan for systems with unequally sized walls, particularly under dynamic loading when inertial forces are directly proportional to wall weight. If these assumptions are voided, the governing equations of the system can no longer be described simply<sup>(26,29)</sup>, affording no obvious closed-form solution<sup>(26)</sup>. Consequently, coupled shear wall systems have been idealized in the standard manner as an assemblage of one-dimensional elements and equations formulated by matrix methods of structural analysis. Both linear and nonlinear responses of coupling systems to dynamic loadings were obtained<sup>(12,14,18,31)</sup>.

In standard structural analyses, multistory buildings are idealized as having a large number of degrees of freedom. Furthermore,

in determining response to horizontal component ground motion, vertical inertia is conventionally neglected and 'massless' degrees of freedom are condensed out in order to reduce the size of the problem<sup>(14,18,31)</sup>. However, vertical inertia should be considered in analyzing coupled shear wall structures<sup>(26)</sup>.

### 1.3 Objective and Scope

The objectives of this investigation are: (i) to develop an efficient analytical technique for analyzing the response of coupled shear wall structures to earthquake motions; (ii) to study the response of selected structures; and (iii) to suggest design considerations for efficient earthquake resistant coupled shear wall systems.

In a coupling system, walls contribute most to the rigidity of a system, maintaining structural stability and protecting the contents of buildings during severe earthquakes. Such walls should therefore be designed against significant yielding, and in this study have been assumed to be nonyielding.

Walls are idealized as one-dimensional wide-column members and coupling beams as one-dimensional beam elements; wall and beam elements are connected through rigid links, representing effective beam-wall panel zones, to form a two-dimensional in-plane coupling system.

Walls contribute most to the lateral resistance of a structure, thereby controlling structural response. Structural displacements may thus be expressed as a linear combination of natural mode shapes of lateral and vertical vibration modes of individual walls. The original system of equations in physical coordinates is transformed into a reduced

system of substantially fewer equations in generalized coordinates, as described in Chapter 2.

The mode shapes, frequencies, and modal stress resultants computed from the reduced system of equations are evaluated with respect to those obtained from analyzing the original system of equations. The number of generalized coordinates necessary to produce satisfactory results is determined. The time-history response of a system subjected to a simplified ground motion is analyzed by the reduction technique, and the results compared to those obtained by an existing computer program in Chapter 3.

In Chapter 4, the analytical procedure is used to analyze the response of two existing coupled shear wall systems damaged in earthquakes. Results from these analyses are correlated with observed damage. The designs of the coupled shear walls are examined in light of the analytical results and observed damage. Finally, some design considerations for an efficient earthquake resistant coupling system are suggested.

Conclusions drawn from this investigation are presented in Chapter 5.

## 2. ANALYTICAL PROCEDURE

### 2.1 Scope of Chapter

A method for analyzing coupled shear wall systems in which inelastic yielding is assumed to be confined to coupling beams is developed in this chapter. The equations of motion are first formulated in physical coordinates using variational methods. Inertial forces in both horizontal and vertical directions are considered; the latter have been shown to affect the vibration properties of coupled shear wall systems significantly<sup>(26)</sup>.

Structural displacements are expressed as a linear combination of the first few natural mode shapes of walls considered as independent cantilevers. The original system of equations is transformed into a reduced system of equations in these generalized modal coordinates. Although any realistic mechanical model for coupling beams can easily be incorporated, a simple bilinear hysteresis relation between shear and average end rotation has been developed for this investigation.

Finally, the numerical procedure for solving the reduced system of equations by a step-by-step integration procedure to determine the response history is outlined. A computer program (not described here) has been developed to implement the analytical procedure; the program is employed to analyze example structures in Chapter 4.

### 2.2 Assumptions

Walls are coupled in the plane of their neutral axes, i.e., a coupled shear wall forms a two-dimensional in-plane system. Wall sections are modeled as wide columns, located at their respective

neutral axes which together with coupling beams will be represented by an assemblage of one-dimensional members joined at 'nodes' (Fig. 2.1). Three degrees of freedom per nodal point are considered: vertical, horizontal, and rotational (Fig. 2.2).

For the wide columns representing walls, axial and bending deformations are considered, but shear deformations, which are insignificant in wall piers of coupling systems<sup>(11)</sup>, are neglected. In coupling beams, shear deformations resulting from high shear forces are considered as are axial and bending deformations.

At every wall-beam intersection, the stiffness of the panel zone formed by the depth of beam  $d_b^i$  and the depth of the longitudinal axis of symmetry in wall  $w$  (Fig. 2.1) depends on the ratio  $\lambda = w/d_b^i$ ; a small value of  $\lambda$  results in a stiff zone, while a large value of  $\lambda$  gives rise to a flexible zone with substantial in-plane distortion. A one-dimensional rigid link of length  $w$  is usually assumed in modeling the rigidity of this zone (Fig. 2.1). However, Michael<sup>(17)</sup> reduces this value by  $d_b^i/2$ . Effects of various assumptions regarding effective length of the rigid link are shown in Fig. 2.3<sup>(15,16)</sup>. An equivalent wide-column frame which assumes full rigid length  $w$  satisfactorily predicts the top deflection when  $\lambda < 2.0$ , as does the Michael correction when  $\lambda \geq 3.0$ . For  $2.0 \leq \lambda < 3.0$ , the full rigid length assumption is more accurate. In the present formulation, the effective rigid length --  $d_1^i$  or  $d_2^i$  -- will be taken as

$$w ; \quad \text{for } \lambda < 3.0$$

$$w - \frac{d_b^i}{2} ; \quad \text{for } \lambda \geq 3.0$$

Because the greatest part of a coupled shear wall system's stiffness and strength is supplied by walls, they should be designed to remain essentially undamaged in the event of an earthquake. Earthquake energy can be more efficiently dissipated through yielding in coupling beams rather than through significant yielding in walls. Therefore, wall piers in coupled shear walls are assumed to be linearly elastic in the following formulation.

Standard methods of frame analysis<sup>(14,31)</sup> neglect inertial forces in vertical and rotational degrees of freedom in determining response to horizontal component ground motion; by statically condensing these degrees of freedom, the dynamic equations may be formulated in terms of lateral displacements. In coupled shear wall systems, however, vertical inertia significantly influences mode shapes and frequencies, particularly those higher than the fundamental mode<sup>(26)</sup>. Therefore, vertical inertia must be retained and static condensation is not possible.

### 2.3 Equations of Motion in Nodal Point Coordinates

A system of two walls coupled by one row of beams is considered (Fig. 2.1). This system can also represent a substructure of a coupled shear wall system with several walls. The equations of motion can be formulated by applying the Hamilton Variational Principle:

$$\delta \sum_i \int_{t_0}^{t_1} (T_i - U_i) dt = 0 \quad (2.1)$$

in which  $T_i$  and  $U_i$  are the kinetic and strain energy expressions, respectively, for element  $i$  of the system. The equations of motion

for a multiwall system can be assembled from such equations for every substructure in the system.

Equations associated with the nodal point degrees of freedom for the  $i^{\text{th}}$  element of a wall and beam (Fig. 2.2) are derived first. Later, these equations are assembled for all elements, thereby forming the equations of motion for the complete structure.

### 2.3.1 $i^{\text{th}}$ Story Coupling Beam

The kinetic and strain energies for the  $i^{\text{th}}$  story coupling beam are expressed, respectively, as

$$T_b^i = \frac{1}{2} \int_0^s \rho_b^i A_b^i \left[ \left( \frac{\partial \eta(x)}{\partial t} + \dot{v}_g \right)^2 + \left( \frac{\partial \zeta(x)}{\partial t} + \dot{u}_g \right)^2 \right] dx \quad (2.2a)$$

$$U_b^i = \frac{1}{2} \int_0^s \left[ \frac{P^2(x)}{E_b^i A_b^i} + \frac{M^2(x)}{E_b^i I_b^i} + \frac{V^2(x)}{G_b^i \bar{A}_b^i} \right] dx \quad (2.2b)$$

in which for the  $i^{\text{th}}$  beam

$\rho_b^i$  = mass per unit volume;

$E_b^i, G_b^i$  = Young's and shear moduli, respectively;

$A_b^i, I_b^i$  = sectional area and moment of inertia, respectively;

$\zeta(x), \eta(x)$  = longitudinal and transverse displacement fields, respectively, relative to ground motion, along beam axes;

$\dot{v}_g, \dot{u}_g$  = vertical and horizontal ground motion velocities, respectively;

$P(x), M(x), V(x)$  = axial force, bending moment, and shear force along beam axis, respectively; and

$\bar{A}_b^i$  = effective shear area of beam section.

The variation of displacements and forces along the beam can be expressed in terms of relative end deformations  $\delta$ ,  $\theta$ , and  $\Delta$

(Fig. 2.4) as follows:

$$\zeta(x) = \frac{-i}{u_1} + \frac{x}{s} \Delta \quad (2.3a)$$

$$\begin{aligned} \eta(x) = & \frac{-i}{v_1} + \frac{1}{\beta_i^2} \left[ \left( \beta_i^2 - 1 \right) \frac{x}{s} + 3 \left( \frac{x}{s} \right)^2 - 2 \left( \frac{x}{s} \right)^3 \right] \delta \\ & + \frac{1}{2 \beta_i^2} \left[ \left( 1 - \beta_i^2 \right) \frac{x}{s} - \left( 3 - \beta_i^2 \right) \left( \frac{x}{s} \right)^2 + 2 \left( \frac{x}{s} \right)^3 \right] \theta s \end{aligned} \quad (2.3b)$$

$$P(x) = \frac{E_b^i A_b^i}{s} \Delta \quad (2.3c)$$

$$M(x) = \frac{E_b^i I_b^i}{s^2 \beta_i^2} \left[ 6 \delta - \left( 3 - \beta_i^2 \right) \theta s \right] + \frac{E_b^i I_b^i}{s^2 \beta_i^2} \left[ -12 \frac{\delta}{s} + 6 \theta \right] x \quad (2.3d)$$

$$V(x) = \frac{E_b^i I_b^i}{s^2 \beta_i^2} \left[ -12 \frac{\delta}{s} + 6 \theta \right] \quad (2.3e)$$

in which

$$\beta_i^2 = 1 + \frac{12 E_b^i I_b^i}{s^2 G_b^i A_b^i}, \quad (2.4)$$

$s$  = span between end rigid links (effective clear span) of beam,  
and

$\frac{-i}{v_1}$ ,  $\frac{-i}{u_1}$  = vertical and horizontal displacements relative to ground motion at left end of beam's effective clear span.

The deformation quantities for the beam in Eq. (2.3) can further be related to physical nodal deformation coordinates (Figs. 2.2 and 2.4):

$$\frac{-i}{v_1} = \frac{i}{v_1} - d_1^i \theta_1^i \quad (2.5a)$$

$$u_1^{-i} = u_1^i \quad (2.5b)$$

$$\delta = v_2^i - v_1^i + (d_1^i + s) \theta_1^i + d_2^i \theta_2^i \quad (2.5c)$$

$$\theta = \theta_1^i - \theta_2^i \quad (2.5d)$$

$$\Delta = u_2^i - u_1^i \quad (2.5e)$$

where

$v_j^i, u_j^i, \theta_j^i$  = vertical, horizontal, and rotational displacements, respectively, of node at  $i^{\text{th}}$  story of wall  $j$ ; and

$d_1^i, d_2^i$  = effective rigid length at left and right ends of effective clear span.

Energy functionals are expressed in terms of nodal point coordinates  $v_j^i, u_j^i, \theta_j^i$ , by substituting Eq. (2.5) into Eq. (2.3), and then substituting the resulting expression into Eq. (2.2). Because rotational inertia of beams is negligible in comparison to lateral inertia of walls, terms involving rotations will be dropped during evaluation of kinetic energy,  $T_b^i$ . The resulting energy expressions in matrix form are as follows:

$$T_b^i = \frac{1}{2} \left\{ \begin{array}{l} \left[ \begin{array}{cc} \dot{r}_1^i & \dot{r}_2^i \\ \dot{r}_1^i & \dot{r}_2^i \end{array} \right]^T \left[ \begin{array}{cc} m_b^{11} & m_b^{12} \\ m_b^{21} & m_b^{22} \end{array} \right] \left[ \begin{array}{c} \dot{r}_1^i \\ \dot{r}_2^i \end{array} \right] \\ + \left[ \begin{array}{cc} \dot{r}_1^i & \dot{r}_2^i \\ \dot{r}_1^i & \dot{r}_2^i \end{array} \right]^T \left[ \begin{array}{c} F_{-b1} \\ F_{-b2} \end{array} \right] + \rho_b^i A_b^i s \left( \dot{v}_g^2 + \dot{u}_g^2 \right) \end{array} \right\} \quad (2.6a)$$

$$U_b^i = \frac{1}{2} \begin{bmatrix} \underline{r}_1^i & \underline{r}_2^i \end{bmatrix}^T \begin{bmatrix} k_{-b}^{11} & k_{-b}^{12} \\ k_{-b}^{21} & k_{-b}^{22} \end{bmatrix} \begin{bmatrix} \underline{r}_1^i \\ \underline{r}_2^i \end{bmatrix} \quad (2.6b)$$

where

$$\underline{r}_1^i = \begin{bmatrix} v_1^i & u_1^i & \theta_1^i \end{bmatrix}^T \quad (2.6c)$$

$$\underline{r}_2^i = \begin{bmatrix} v_2^i & u_2^i & \theta_2^i \end{bmatrix}^T \quad (2.6d)$$

$$\underline{m}_{-b}^{11} = \underline{m}_{-b}^{22} = \rho_b^i A_b^i s \begin{bmatrix} \xi_i & 0 & 0 \\ 0 & 1/3 & 0 \\ 0 & 0 & 0 \end{bmatrix} \quad (2.6e)$$

$$\underline{m}_{-b}^{12} = \underline{m}_{-b}^{21}{}^T = \rho_b^i A_b^i s \begin{bmatrix} (1-2\xi_i)/2 & 0 & 0 \\ 0 & 1/6 & 0 \\ 0 & 0 & 0 \end{bmatrix} \quad (2.6f)$$

$$\underline{k}_{-b}^{11} = \frac{6 E_b^i I_b^i}{s^3 \beta_i^2} \begin{bmatrix} 2 & 0 & -(2d_1^i + s) \\ 0 & A_b^i s^2 \beta_i^2 / 6 I_b^i & 0 \\ -(2d_1^i + s) & 0 & 2d_1^i (d_1^i + s) + s^2 (3 + \beta_i^2) / 6 \end{bmatrix} \quad (2.6g)$$

$$\underline{k}_{-b}^{12} = \underline{k}_{-b}^{21}{}^T = \frac{6 E_b^i I_b^i}{s^3 \beta_i^2} \begin{bmatrix} -2 & 0 & -(2d_2^i + s) \\ 0 & -A_b^i s^2 \beta_i^2 / 6 I_b^i & 0 \\ 2d_1^i + s & 0 & 2d_1^i d_2^i + s a_1 - s^2 (3 + \beta_i^2) / 6 \end{bmatrix} \quad (2.6h)$$

$$k_{-b}^{22} = \frac{6 E_b^i I_b^i}{s^3 \beta_i^2} \begin{bmatrix} 2 & 0 & (2d_2^i + s) \\ 0 & A_b^i s^2 \beta_i^2 / 6 I_b^i & 0 \\ (2d_2^i + s) & 0 & 2d_2^i (d_2^i + s) + s^2 (3 + \beta_i^2) / 6 \end{bmatrix} \quad (2.6i)$$

$$F_{-b1} = F_{-b2} = \rho_b^i A_b^i s [\dot{v}_g \quad \dot{u}_g \quad 0]^T \quad (2.6j)$$

in which

$$a_1 = d_1^i + s + d_2^i \quad (2.6k)$$

$$\xi_i = (70 \beta_i^4 + 7 \beta_i^2 + 1) / 210 \beta_i^4 \quad (2.6l)$$

and an overdot on the displacement vector represents the time derivative.

Substituting Eqs. (2.6a) and (2.6b) into Eq. (2.1) associated with the  $i^{\text{th}}$  coupling beam results in:

$$\delta \int_{t_0}^{t_1} \left( T_b^i - U_b^i \right) dt = \int_{t_0}^{t_1} \left( \delta \dot{r}_{-b}^i \dot{m}_{-b}^i + \frac{1}{2} \delta \dot{r}_{-b}^i F_b^i - \delta \dot{r}_{-b}^i k_{-b}^i \right) dt \quad (2.7)$$

in which

$$r_{-b}^i = \left[ v_1^i \quad u_1^i \quad \theta_1^i \quad v_2^i \quad u_2^i \quad \theta_2^i \right]^T, \quad \text{nodal point co-}$$

ordinates associated with  $i^{\text{th}}$  coupling beam, and

$\delta \dot{r}_{-b}^i$  its corresponding variation:

$$m_{-b}^i = \begin{bmatrix} m_{-b}^{11} & m_{-b}^{12} \\ m_{-b}^{21} & m_{-b}^{22} \end{bmatrix}, \quad \text{element mass matrix for } i^{\text{th}} \text{ coupling beam;}$$

$$\underline{k}_{-b}^i = \begin{bmatrix} k_{-b}^{11} & k_{-b}^{12} \\ k_{-b}^{21} & k_{-b}^{22} \end{bmatrix}, \text{ element stiffness matrix for } i^{\text{th}} \text{ coupling beam;}$$

and

$$\underline{F}_{-b}^i = \begin{bmatrix} F_{-b1}^i \\ F_{-b2}^i \end{bmatrix}.$$

The first and second terms in Eq. (2.7) are integrated by parts with respect to time, and the displacement conditions at times  $t_0$  and  $t_1$  are imposed. Equation (2.7) then becomes:

$$\delta \int_{t_0}^{t_1} \left( \underline{T}_{-b}^i - U_{-b}^i \right) dt = \int_{t_0}^{t_1} \delta \underline{r}_{-b}^i \text{ }^T \left( -\underline{m}_{-b}^i \ddot{\underline{r}}_{-b}^i - \underline{k}_{-b}^i \underline{r}_{-b}^i + \underline{R}_{-b}^i \right) dt \quad (2.8)$$

in which

$$\underline{R}_{-b}^i = -\frac{1}{2} \rho_b^i A_b^i s \begin{bmatrix} \ddot{v}_g & \ddot{u}_g & 0 & \ddot{v}_g & \ddot{u}_g & 0 \end{bmatrix}^T,$$

is an effective load vector for the  $i^{\text{th}}$  coupling beam; overdots on the displacement vector denote time derivatives.

### 2.3.2 $i^{\text{th}}$ Story Wall Element

The kinetic and strain energies of the  $i^{\text{th}}$  story element of the  $j^{\text{th}}$  wall (Fig. 2.2) are, respectively:

$$T_w^i = \int_0^{h_i} \frac{1}{2} \rho_j^i A_j^i \left[ \left( \frac{\partial \zeta(x)}{\partial t} + \dot{v}_g \right)^2 + \left( \frac{\partial \eta(x)}{\partial t} + \dot{u}_g \right)^2 \right] dx \quad (2.9a)$$

$$U_w^i = \int_0^{h_i} \frac{1}{2} \left[ E_j^i A_j^i \left( \frac{\partial \zeta(x)}{\partial x} \right)^2 + E_j^i I_j^i \left( \frac{\partial^2 \eta(x)}{\partial x^2} \right)^2 \right] dx \quad (2.9b)$$

in which, for the  $i^{\text{th}}$  story of wall  $j$ :

$h_i$  = height of story  $i$ ;

$\rho_j^i$  = mass per unit volume of wall;

$E_j^i$  = Young's modulus;

$A_j^i, I_j^i$  = sectional area and moment of inertia, respectively; and

$\zeta(x), \eta(x)$  = longitudinal and transverse displacements, relative to ground motion, along neutral axis of wall element, respectively.

The displacement functions in Eq. (2.9) are expressed in terms of nodal point displacements through interpolation functions:

$$\zeta(x) = \left(1 - \frac{x}{h_i}\right) v_j^{i-1} + \left(\frac{x}{h_i}\right) v_j^i \quad (2.10a)$$

$$\begin{aligned} \eta(x) = & \left[1 - 3\left(\frac{x}{h_i}\right)^2 + 2\left(\frac{x}{h_i}\right)^3\right] u_j^{i-1} + \left[x - 2\frac{x^2}{h_i} + \frac{x^3}{h_i^2}\right] \theta_j^{i-1} + \\ & + \left[3\left(\frac{x}{h_i}\right)^2 - 2\left(\frac{x}{h_i}\right)^3\right] u_j^i + \left[-\frac{x^2}{h_i} + \frac{x^3}{h_i^2}\right] \theta_j^i \end{aligned} \quad (2.10b)$$

Substituting Eq. (2.10) into Eq. (2.9), the energy expressions for the  $i^{\text{th}}$  story element of wall  $j$  can be expressed in matrix form as follows:

$$T_w^i = \frac{1}{2} \left\{ \begin{aligned} & \left[ \begin{array}{cc} \cdot^{i-1} & \cdot^i \\ r_j & r_j \end{array} \right]^T \left[ \begin{array}{cc} m_{-w}^{11} & m_{-w}^{12} \\ m_{-w}^{21} & m_{-w}^{22} \end{array} \right] \left[ \begin{array}{c} \cdot^{i-1} \\ r_j \\ \cdot^i \\ r_j \end{array} \right] + \left[ \begin{array}{cc} \cdot^{i-1} & \cdot^i \\ r_j & r_j \end{array} \right]^T \left[ \begin{array}{c} F_{-w1} \\ F_{-w2} \end{array} \right] \\ & + \rho_j^i A_j^i h_i \left( \begin{array}{c} \cdot^2 \\ u_g \\ \cdot^2 \\ v_g \end{array} \right) \end{aligned} \right\} \quad (2.11a)$$

$$U_w^i = \frac{1}{2} \left[ \begin{array}{cc} \cdot^{i-1} & \cdot^i \\ r_j & r_j \end{array} \right]^T \left[ \begin{array}{cc} k_{-w}^{11} & k_{-w}^{12} \\ k_{-w}^{21} & k_{-w}^{22} \end{array} \right] \left[ \begin{array}{c} \cdot^{i-1} \\ r_j \\ \cdot^i \\ r_j \end{array} \right] \quad (2.11b)$$

where

$$\underline{r}_j^{i-1} = \left[ \begin{array}{ccc} \cdot^{i-1} & \cdot^{i-1} & \theta_j^{i-1} \\ v_j & u_j & \end{array} \right]^T \quad (2.11c)$$

$$\underline{r}_j^i = \left[ \begin{array}{ccc} \cdot^i & \cdot^i & \theta_j^i \\ v_j & u_j & \end{array} \right]^T \quad (2.11d)$$

$$m_{-w}^{11} = \rho_j^i A_j^i h_i \left[ \begin{array}{ccc} 1/3 & 0 & 0 \\ 0 & 156/420 & 22h_i/420 \\ 0 & 22h_i/420 & 4h_i^2/420 \end{array} \right] \quad (2.11e)$$

$$m_{-w}^{12} = m_{-w}^{21T} = \rho_j^i A_j^i h_i \left[ \begin{array}{ccc} 1/6 & 0 & 0 \\ 0 & 54/420 & -13h_i/420 \\ 0 & 13h_i/420 & -3h_i^2/420 \end{array} \right] \quad (2.11f)$$

$$\underline{m}_{-w}^{22} = \rho_j^i A_j^i h_i \begin{bmatrix} 1/3 & 0 & 0 \\ 0 & 156/420 & -22h_i/420 \\ 0 & -22h_i/420 & 4h_i^2/420 \end{bmatrix} \quad (2.11g)$$

$$\underline{k}_{-w}^{11} = \frac{6 E_j^i I_j^i}{h_i^3} \begin{bmatrix} A_j^i h_i^2 / 6 I_j^i & 0 & 0 \\ 0 & 2 & h_i \\ 0 & h_i & 2h_i^2/3 \end{bmatrix} \quad (2.11h)$$

$$\underline{k}_{-w}^{12} = \underline{k}_{-w}^{21T} = \frac{6 E_j^i I_j^i}{h_i^3} \begin{bmatrix} -A_j^i h_i^2 / 6 I_j^i & 0 & 0 \\ 0 & -2 & h_i \\ 0 & -h_i & h_i^2/3 \end{bmatrix} \quad (2.11i)$$

$$\underline{k}_{-w}^{22} = \frac{6 E_j^i I_j^i}{h_i^3} \begin{bmatrix} A_j^i h_i^2 / 6 I_j^i & 0 & 0 \\ 0 & 2 & -h_i \\ 0 & -h_i & 2h_i^2/3 \end{bmatrix} \quad (2.11j)$$

$$\underline{F}_{-w1} = \rho_j^i A_j^i h_i [\dot{v}_g \quad \dot{u}_g \quad h_i \dot{u}_g / 6]^T \quad (2.11k)$$

$$F_{-w2}^i = \rho_j^i A_j^i h_i [\dot{v}_g \quad \dot{u}_g \quad -h_i \dot{u}_g / 6]^T \quad (2.11\ell)$$

Substituting Eqs. (2.11a) and (2.11b) into Eq. (2.1), associated with the  $i^{\text{th}}$  element of the  $j^{\text{th}}$  wall, results in:

$$\delta \int_{t_0}^{t_1} \left( T_w^i - U_w^i \right)_j dt = \int_{t_0}^{t_1} \left( \delta \frac{\dot{r}_{-w}^i}{r_{-w}^i} \frac{\dot{m}_{-w}^i}{m_{-w}^i} \frac{\dot{r}_{-w}^i}{r_{-w}^i} + \frac{1}{2} \delta \frac{\dot{r}_{-w}^i}{r_{-w}^i} \frac{F_{-w}^i}{m_{-w}^i} - \delta \frac{r_{-w}^i}{r_{-w}^i} \frac{k_{-w}^i}{m_{-w}^i} \frac{r_{-w}^i}{r_{-w}^i} \right)_j dt \quad (2.12)$$

in which, for the  $j^{\text{th}}$  wall,

$$\frac{r_{-w}^i}{r_{-w}^i} = \left[ v_j^{i-1} \quad u_j^{i-1} \quad \theta_j^{i-1} \quad v_j^i \quad u_j^i \quad \theta_j^i \right]^T, \text{ nodal point coordinates}$$

associated with  $i^{\text{th}}$  story wall element, and  $\delta \frac{r_{-w}^i}{r_{-w}^i}$  its

corresponding variation:

$$\frac{m_{-w}^i}{m_{-w}^i} = \begin{bmatrix} m_{-w}^{11} & m_{-w}^{12} \\ m_{-w}^{21} & m_{-w}^{22} \end{bmatrix}, \text{ element mass matrix for}$$

$i^{\text{th}}$  story wall element;

$$\frac{k_{-w}^i}{k_{-w}^i} = \begin{bmatrix} k_{-w}^{11} & k_{-w}^{12} \\ k_{-w}^{21} & k_{-w}^{22} \end{bmatrix}, \text{ element stiffness matrix}$$

for  $i^{\text{th}}$  story wall element;

and

$$F_{-w}^i = \begin{bmatrix} F_{-w1}^i \\ F_{-w2}^i \end{bmatrix}.$$

The first and second terms of Eq. (2.12) are integrated by parts with respect to time, and the condition on prescribed displacement

configuration at times  $t_0$  and  $t_1$  is applied. Equation (2.12) then becomes:

$$\delta \int_{t_0}^{t_1} \left( T_w^i - U_w^i \right)_j dt = \int_{t_0}^{t_1} \left[ \delta \underline{r}_w^i \left( -\underline{m}_w^i \ddot{\underline{r}}_w^i - \underline{k}_w^i \underline{r}_w^i + \underline{R}_w^i \right) \right]_j dt \quad (2.13)$$

in which

$$\underline{R}_w^i = -\frac{1}{2} \rho_j^i A_j^i h_i \left[ \ddot{v}_g \quad \ddot{u}_g \quad h_i \ddot{u}_g / 6 \quad \ddot{v}_g \quad \ddot{u}_g \quad -h_i \ddot{u}_g / 6 \right]^T,$$

an effective load vector for  $i^{\text{th}}$  story wall; overdots on displacement vector denote time derivatives.

Appropriate variational expressions (Eq. (2.8) and Eq. (2.13)) for all beam and wall elements of a system are summed and equated to zero, as required by Eq. (2.1). Equivalently, element mass, stiffness, and effective load matrices in Eq. (2.8) or Eq. (2.13) are assembled by direct stiffness assembly procedures to obtain  $\underline{M}$ ,  $\underline{K}$ , and  $\underline{R}$  --- the mass matrix, the stiffness matrix, and the effective load vector for the entire structure. In addition to the element mass matrices, dead loads tributary to the coupled shear wall model are included in the mass matrix  $\underline{M}$ ; these additional loads appear on the diagonal elements associated with the translational degrees of freedom at the floor levels. The same corresponding additional masses induce inertial forces from ground motion, which consequently add into the effective load vector  $\underline{R}$ . The equations of motion for the structure in nodal point degrees of freedom  $\underline{r}$  is

$$\underline{M} \ddot{\underline{r}} + \underline{K} \underline{r} = \underline{R} \quad (2.14)$$

Because local damping mechanisms in buildings cannot be accurately defined, a damping matrix cannot be formulated through the

energy method. In the present analysis, damping matrix  $\underline{C}$  is defined as a linear combination of mass matrix  $\underline{M}$  and stiffness matrix  $\underline{K}$ , i.e.,

$$\underline{C} = \alpha_m \underline{M} + \alpha_k \underline{K} \quad (2.15)$$

where the values selected for  $\alpha_m$  and  $\alpha_k$  are consistent with measured modal damping ratios from forced vibration tests on similar buildings.

The general equations of motion including damping are

$$\underline{M} \ddot{\underline{r}} + \underline{C} \dot{\underline{r}} + \underline{K} \underline{r} = \underline{R} \quad (2.16)$$

The size of matrices in Eq. (2.16) increases rapidly as the number of walls and stories increases and the solution of Eq. (2.16) may require prohibitive computational effort. It therefore becomes necessary to reduce the number of degrees of freedom.

## 2.4 Reduction of Degrees of Freedom

### 2.4.1 Selection of Generalized Coordinates

Because walls provide a major part of lateral resistance of the building and are assumed to be nonyielding, they control deformations. A comparison of mode shapes of a coupled shear wall system to those of its individual walls considered as cantilevers suggests that linear combination is an effective technique. In Fig. 2.5, the first 10 natural vibration mode shapes of a coupled shear wall system representing the McKinley Apartment Building<sup>(26)</sup> are compared to the vibration mode shapes of individual, uncoupled walls of the system. The general similarity of the two sets of mode shapes suggests that structural deformations may be effectively expressed as a linear combination of the natural mode shapes of vibration of individual walls.

### 2.4.2 Equations of Motion in Generalized Coordinates

Nodal point displacements associated with the  $j^{\text{th}}$  wall in the nodal point coordinate vector  $\underline{r}$  are expressed as a linear combination of the natural mode shapes of the  $j^{\text{th}}$  wall, considered as an individual cantilever, through generalized coordinates as follows:

$$\underline{v}_j = \sum_{m=1}^{NV} \psi_{-Vj}^m z_{Vj}^m \quad (2.17a)$$

$$\underline{u}_j = \sum_{m=1}^{NH} \psi_{-Hj}^m z_{Hj}^m \quad (2.17b)$$

in which

$\underline{v}_j$  = vector of vertical displacements of nodal points in  $j^{\text{th}}$  wall;

$\underline{u}_j$  = vector of horizontal displacements and rotations of nodal points in  $j^{\text{th}}$  wall;

$\psi_{-Vj}^m$  = vector of vertical displacements of nodal points in  $j^{\text{th}}$  wall corresponding to  $m^{\text{th}}$  natural mode shape in longitudinal (vertical) vibration of cantilever wall  $j$ ;

$\psi_{-Hj}^m$  = vector of horizontal displacements and rotations of nodal points in  $j^{\text{th}}$  wall corresponding to  $m^{\text{th}}$  natural mode shape in transverse (horizontal) vibration of cantilever wall  $j$ ;

$z_{Vj}^m$  = generalized coordinate associated with  $\psi_{-Vj}^m$  ;

$z_{Hj}^m$  = generalized coordinate associated with  $\psi_{-Hj}^m$  ; and

$NV, NH$  = number of vertical and lateral uncoupled mode shapes used per each wall, respectively.

In matrix notation, Eq. (2.17) may be expressed as a transformation between nodal point coordinates  $\underline{r}$  and generalized coordinates  $\underline{z}$ :

$$\underline{r} = \underline{H} \underline{z} \quad (2.18)$$

where  $\underline{H}$  is the transformation matrix of which elements in any column denote the nodal point displacements identical to either the lateral or vertical uncoupled mode shape of each individual wall.

Equation (2.18) is substituted into Eq. (2.16), the equations of motion, and the resulting equations are premultiplied throughout by  $\underline{H}^T$  to restore symmetry to the constituent matrices; the reduced system of equations of motion in generalized coordinates  $\underline{z}$  is

$$\underline{\tilde{M}} \ddot{\underline{z}} + \underline{\tilde{C}} \dot{\underline{z}} + \underline{\tilde{K}} \underline{z} = \underline{\tilde{R}} \quad (2.19)$$

in which

$$\underline{\tilde{M}} = \underline{H}^T \underline{M} \underline{H}, \quad \text{reduced mass matrix} \quad (2.20a)$$

$$\underline{\tilde{C}} = \underline{H}^T \underline{C} \underline{H}, \quad \text{reduced damping matrix} \quad (2.20b)$$

$$\underline{\tilde{K}} = \underline{H}^T \underline{K} \underline{H}, \quad \text{reduced stiffness matrix} \quad (2.20c)$$

and

$$\underline{\tilde{R}} = \underline{H}^T \underline{R}, \quad \text{reduced effective load vector} \quad (2.20d)$$

Rather than computing the reduced matrices directly from Eq. (2.20), it is more efficient to proceed as follows. The transformations are written at the element level:

$$\underline{r}_{-b}^i = \underline{h}_{-b}^i \underline{z} \quad \text{for } i^{\text{th}} \text{ beam element;}$$

$$\underline{r}_{-w}^i = \underline{h}_{-w}^i \underline{z} \quad \text{for } i^{\text{th}} \text{ wall element.}$$

in which  $h_{-b}^i$  and  $h_{-w}^i$  are element transformation matrices whose elements in each column are the corresponding values of  $r_{-b}^i$  or  $r_{-w}^i$  in the uncoupled mode shape vectors, either  $\psi_{-Vj}^m$  or  $\psi_{-Hj}^m$ , whichever is compatible with the ordering of associated generalized coordinates in  $\underline{Z}$ . The matrices for each element are determined in generalized coordinates as follows:

$$\text{beam element mass matrix: } \tilde{m}_{-b}^i = h_{-b}^{iT} m_{-b}^i h_{-b}^i ;$$

$$\text{beam element stiffness matrix: } \tilde{k}_{-b}^i = h_{-b}^{iT} k_{-b}^i h_{-b}^i ;$$

$$\text{beam element load vector: } \tilde{R}_{-b}^i = h_{-b}^{iT} R_{-b}^i ;$$

$$\text{wall element mass matrix: } \tilde{m}_{-w}^i = h_{-w}^{iT} m_{-w}^i h_{-w}^i ;$$

$$\text{wall element stiffness matrix: } \tilde{k}_{-w}^i = h_{-w}^{iT} k_{-w}^i h_{-w}^i ;$$

and

$$\text{wall element load vector: } \tilde{R}_{-w}^i = h_{-w}^{iT} R_{-w}^i$$

The element damping matrices in generalized coordinates are from Eq. (2.15):

$$\text{beam element damping matrix: } \tilde{c}_{-b}^i = \alpha_m \tilde{m}_{-b}^i + \alpha_k \tilde{k}_{-b}^i ;$$

and

$$\text{wall element damping matrix: } \tilde{c}_{-w}^i = \alpha_m \tilde{m}_{-w}^i + \alpha_k \tilde{k}_{-w}^i .$$

Each element matrix is then directly assembled into corresponding mass, stiffness, damping, and effective load matrices of the complete system, leading to the reduced matrices  $\tilde{M}$ ,  $\tilde{K}$ ,  $\tilde{C}$ , and  $\tilde{R}$  as in Eq. (2.19).

If a small number of generalized coordinates suffices to predict response satisfactorily, the number of equations in generalized

coordinates (Eq. (2.19)) is much smaller than in nodal point coordinates (Eq. (2.16)). The computational effort required for dynamic analysis will then be reduced considerably, as discussed in Chapter 3.

## 2.5 Mechanical Model for Coupling Beams

Coupling beams in coupled shear wall systems are usually deep and subject to high shear. High shears induce shear cracking, normally accompanied by yielding of stirrups and flexural reinforcement. Cracking of concrete and yielding of reinforcement give rise to nonlinearities or stiffness changes in the load-deformation relation of beams; the order of their occurrence depends on the aspect ratio of and the amount of reinforcement in beams<sup>(21)</sup>.

Shear cracks and subsequent yielding are not localized at end sections of beams, but are spread throughout a substantial portion of the beam's span. Therefore, instead of using the end sectional moment capacities,  $M_{y1}$  or  $M_{y2}$ , to signify a change in beam stiffness, as in flexural beams, the span shear,  $P_y = (M_{y1} + M_{y2})/s$ , which can directly reflect nonlinearities due to diagonal shear cracking or stirrup yielding, is used to decide whether or not a change in stiffness has occurred. A bilinear hysteretic force deformation relation is assumed for coupling beams, controlled by a bilinear hysteresis shear - average end rotations relation (Fig. 2.6) which can be obtained from laboratory experiments as described in Ref. 21.

The above mechanical model is characterized by simultaneous changes in stiffness in the resulting moment-rotation relations at both ends of a beam, reflecting nonlinearities distributed throughout the span and not just at localized span ends. If induced end moments are equal, the assumed mechanical model indicates initial yielding when

moment at each end reaches average yielding capacity,  $(M_{y1} + M_{y2})/2$  (curve (a), Fig. 2.6b); if the induced end moments differ slightly, however, the model indicates initial yielding when moment at one end of the beam is slightly less and at the other end is slightly more than the average sum of respective yielding capacities (curves (b) and (c), Fig. 2.6b). The magnitudes of induced end moments are generally very close, even if rigidities of the two coupled piers differ greatly. Therefore, the moment-rotation relations at the two ends of the beam are averaged by the corresponding relation under equal end moments.

## 2.6 Step-by-Step Time History Analysis

The equations of motion (Eq. (2.19)) are integrated numerically. A suitable time increment is chosen for the numerical scheme used considering the dynamic characteristics of the system; the time step chosen must not induce numerical instability, and must ensure reasonably accurate calculations of response. Within each time step, second order differential equations of motion are transformed into a system of linear algebraic equations in incremental values of generalized coordinates which can be solved for by a standard Gaussian elimination technique. Dynamic equilibrium is satisfied at the end of every time step. Displacement configurations are successively modified from one time step to another, marching throughout the time range. Such a step-by-step analysis is detailed in Ref. 3.

Again, if a small number of generalized coordinates suffices to predict response satisfactorily, the size of the reduced system will be much smaller than that of the original system. Not only does step-by-step integration of the reduced system of equations (Eq. (2.19))

require considerably less computational effort than does the original system (Eq. (2.16)), but a larger integration time step may be used because unwanted higher modes -- those contributing negligibly to structural response -- are eliminated by the transformation to generalized coordinates (Eq. (2.17)).

### 2.6.1 Linear Analysis

Using the procedure described in Ref. 3 together with a special case of Newmark's numerical integration method which is equivalent to the constant average acceleration scheme<sup>(20)</sup>, Eq. (2.19) is transformed into a system of algebraic equations in the incremental vector of  $\underline{Z}$ ,  $\Delta\underline{Z}$ , at each time step. Because the properties of the system ( $\tilde{\underline{M}}$ ,  $\tilde{\underline{C}}$ , and  $\tilde{\underline{K}}$ ) do not change throughout the duration of the response, the resulting algebraic equations are linear. Thus, the solution for  $\Delta\underline{Z}$  always produces a deformation configuration satisfying dynamic equilibrium. Dynamic stress resultants at any time step are obtained by transforming the generalized displacement  $\underline{Z}$  at that time to the nodal displacement  $\underline{r}$ , through the relation in Eq. (2.18), and evaluating element forces using the respective element stiffness matrices.

### 2.6.2 Nonlinear Analysis

The basic step-by-step procedure for linear analysis can, with suitable modifications, be used to handle nonlinearities arising in a system. Nonlinearities due to yielding of coupling beams result in changes in stiffness. Stiffness is assumed to remain constant within each time interval. The same equations of motion (Eq. (2.19)) are then valid at discrete time intervals if the stiffness matrix  $\tilde{\underline{K}}$  is

evaluated according to the current state of yielding in structural members. Within a time step, yielding or unloading may occur in some beams, thus invalidating the assumption of constant structural stiffness. Consequently, results obtained at the end of each time step may not satisfy dynamic equilibrium for the system. An iterative process within each time interval is used to correct the displacement configuration successively until convergence is achieved and equilibrium established<sup>(3)</sup>. When nonlinearities in the structural behavior of beams arise, progressive stages of yielding must be traced and the stiffness in nodal point coordinates correspondingly adjusted. The solution scheme is otherwise similar to that for the linear analysis.

## 2.7 Computer Program

A computer program was developed to implement the technique described above for both linear and nonlinear analyses of coupled shear wall systems. A set of vertical and lateral mode shapes for individual walls was evaluated first, constituting the required family of generalized functions. Element mass, stiffness, damping, and effective load matrices for every beam and wall element were subsequently formed in association with the generalized coordinates used. By directly assembling these element matrices, the reduced mass, stiffness, damping, and effective load matrices of the complete system were obtained. The geometric stiffness of the wide-column walls was neglected in the stiffness formulation.

Nonlinearities were assumed to occur in coupling beams only. The mechanical model for coupling beams described in Section 2.5 was used; however, any mechanical model could easily be incorporated into the program. Using the constant average acceleration method for

numerical integration, a suitable time step was chosen and the step-by-step analysis<sup>(3)</sup> used to solve Eq. (2.19) to determine response to specified earthquake ground motion. In the analysis, any unbalanced load due to nonlinearities within the time step is evaluated at the end of every time step, and constant stiffness iteration used to correct for dynamic equilibrium until convergence is achieved to within an acceptable tolerance.

### 3. EVALUATION OF REDUCTION TECHNIQUE

#### 3.1 Scope of Chapter

In this chapter, the effectiveness of the technique described in Chapter 2 in reducing the number of degrees of freedom is assessed. The ability of the technique in predicting vibrational frequencies and mode shapes, internal mode forces, and nonlinear time-history response is evaluated.

Structural displacements are expressed as a linear combination of the natural mode shapes of individual walls in lateral and longitudinal vibration. The number of these modes necessary to achieve a desired level of accuracy in calculating vibrational frequencies and mode shapes and modal stress resultants for the coupled shear wall system is established, and used to evaluate response history. Finally, computational savings achieved by reducing the number of degrees of freedom are discussed.

#### 3.2 Mode Shapes and Frequencies

##### 3.2.1 Case Study of a Coupled Shear Wall Model

A coupled shear wall model was idealized from the coupled shear wall system at the north end of the McKinley Building by assuming that coupling beams span the two end piers and that the middle pier does not exist. The model was taken from Ref. 26 and idealized as shown in Fig. 3.1. In the model, the wall piers and coupling beams have the following dimensions and material properties:

the rectangular wall section is 12' x 8" ;

the rectangular coupling beam section is 4' x 4";

$$a_1 = 18';$$

$$h_i = 8.5';$$

$$E_1^i = E_2^i = E_b^i = 4.64 \times 10^8 \text{ lb/ft}^2;$$

$$G_b^i = 2.32 \times 10^8 \text{ lb/ft}^2; \text{ and}$$

$$\rho_1^i = \rho_2^i = \rho_b^i = 4.5 \text{ lb-sec}^2/\text{ft}^4.$$

The rigidities of walls and coupling beams are uniform over the height of the structure.

### 3.2.2 Mode Shapes and Frequencies

A reduced system is designated by  $H_m V_n$ , where  $m$  and  $n$  denote the number of uncoupled lateral and vertical modes of vibration per wall, respectively. Mode shapes and frequencies were calculated by solving the eigenvalue problem associated with Eq. (2.19) and comparing results with those obtained by solving the eigenvalue problem associated with the original system of Eq. (2.16).

Mode shapes and frequencies determined from analyses of the  $H_4 V_4$  and  $H_6 H_3$  systems are compared to those of the original system in Figs. 3.2a and 3.2b. The first six mode shapes and frequencies of the structure, including the first four antisymmetric modes, were satisfactorily reproduced by the  $H_4 V_4$  system, whereas the first nine modes were more accurately reproduced by the  $H_6 V_3$  system. The two-to-one combination of lateral and vertical uncoupled modes enabled the  $H_6 V_3$  system to produce significantly better results than the  $H_4 V_4$  system with only one more generalized coordinate per wall. The

more significant displacements in the lower modes of vibration are in the lateral direction; it is therefore effective to include a larger proportion of lateral vibration modes.

A case with linear distribution of beam stiffness along the height of a wall was also considered. The wall piers of the structure described in Section 3.2.1 were coupled by a series of modified floor beams with linearly distributed stiffnesses varying from zero at the ground level to a maximum value (the value for the original model) at the top floor. Yielding in the uniform system usually started at lower story beams, propagating upwards. This case represents the uniform system's properties after yielding has occurred. The eigenvalue problem associated with Eq. (2.19) for the  $H_6 V_3$  reduced system of this coupled shear wall was again solved. The number of accurately reproducible mode shapes and frequencies was found to decrease slightly when compared to that reproduced when the uniform system was analyzed. To achieve better accuracy with this nonuniform system or for other systems with highly nonuniform distribution of beam stiffness, a greater number of generalized functions must be used, proportionally combining two lateral modes to one vertical mode.

### 3.3 Modal Stress Resultants

The accuracy of deflected shapes predicted using the reduced systems described in the previous section does not necessarily guarantee the accuracy of predicted stress resultants, which depend on derivatives of displacement fields. Although the first mode deflected shape of the uniform coupled shear wall (Section 3.2.1) was very accurately reproduced by solving the eigenvalue problem for the  $H_{16} V_8$  reduced system, to within 2%, predictions of associated shear and bending moments were

By applying the above adjustment procedure, the corrected bending moments and shears obtained from analyzing the  $H_6 V_3$  reduced system -- a much less refined system than the  $H_{16} V_8$  -- satisfactorily agreed with 'exact' values, those obtained from analysis of the system using the equations in nodal point coordinates, at every story level except the bottom (Fig. 3.3). However, when the base moment in the wall was corrected by half the incoming beam moment at the first story level, the corrected base moment and corresponding equilibrating shear in the bottom story more closely agreed with 'exact' values (Fig. 3.3). Generally, satisfactory stress resultants can be produced by a simple and inexpensive reduced system, such as the  $H_6 V_3$  system, by adjusting the wall moment at the base and at every story level.

To illustrate the applicability of this adjustment to higher modes of vibration, the adjusted stress resultants associated with the third antisymmetrical mode shape were evaluated using the  $H_6 V_3$  reduced system. The results of this evaluation were then compared to 'exact' values (Fig. 3.5). The ability to produce accurate values for shear and moment in walls, and shear in coupling beams, was not lost, although some deviation was apparent in predictions of wall axial force.

Four other coupled shear wall systems were investigated: a weakly coupled system with more flexible coupling beams; a coupled system with unequal walls; a system with linear distribution of beam stiffness along the height of the structure; and a system with parabolic distribution of beam stiffness along the height of the structure. In all cases, the  $H_6 V_3$  reduced system with adjusted wall moments satisfactorily produced stress resultants for the first three vibrational modes of the structure.

extremely inaccurate (Fig. 3.3). Stress resultants were inaccurate because the moments associated with all generalized functions vary continuously along the height of a wall, whereas actual distribution is discontinuous due to incoming beam moments. However, the predicted bending moment smoothly averaged the discontinuity at interstory levels. Shear and bending moments in coupling beams (Fig. 3.3) deviated only slightly from 'exact' results, those obtained from analyzing the system using the equations in nodal point coordinates.

The stress resultants obtained by analyzing the reduced system were corrected by distributing half of the moment at the end of every incoming beam to the wall moment immediately above and below each beam-wall joint. Defining  $M_D^L$  and  $M_D^R$  as moments at the end of coupling beams connected to the left and right faces of a wall pier (Fig. 3.4), respectively, the moments in the wall --  $M_A$  above and  $M_B$  below that joint -- are corrected as follows

$$\tilde{M}_A = M_A - \frac{M_D^L + M_D^R}{2} \quad (3.1a)$$

$$\tilde{M}_B = M_B - \frac{M_D^L + M_D^R}{2} \quad (3.1b)$$

in which  $\tilde{M}_A$  and  $\tilde{M}_B$  are the corrected moments in the wall above and below that joint, respectively. Shear forces in the wall are then correspondingly adjusted to equilibrate corrected bending moments. Axial forces in the wall remained unadjusted. Similar adjustment is required for other simplified techniques, such as the continuous laminae theory, but inelastic action in coupling beams is more realistically handled by the reduction technique described herein.

The reduction technique, particularly the  $H_6 V_3$  reduced system for the coupled shear wall considered, successfully produced accurate modal values -- mode shapes, frequencies, and stress resultants -- for the above-mentioned coupling systems. The number of generalized functions used, and hence the size of the reduced system, can be selected to achieve specified levels of accuracy. Total dynamic response predicted by the reduced system is best evaluated by a time-history response analysis, described in the following section.

#### 3.4 Nonlinear Time-History Response

A nonlinear time-history response of the coupled shear wall system of the McKinley Apartment Building (Section 3.2.1) subjected to simplified input ground motion was obtained by solving Eq. (2.19) for the  $H_6 V_3$  reduced system, and then comparing that solution to 'exact' response obtained by analyzing equations in nodal point coordinates (Eq. (2.16)). The latter was obtained by using program DRAIN-2D<sup>(14)</sup>.

The elastic properties of walls and coupling beams were essentially the same as those described in Section 3.2.1. In addition, a 40-kip shear at initial flexural yielding was assumed for all coupling beams; the bilinear mechanical model described in Section 2.5, together with a strain-hardening of 10%, was also assumed.

The simplified input ground motion was taken from Ref. 30 (Fig. 3.6). The horizontal ground acceleration input (Fig. 3.6) was derived from a simple half-cycle displacement, with a maximum acceleration of 0.5g and a period of  $\sqrt{2} t_1$  in which  $t_1$  is an adjustable constant representing the half-cycle duration of the corresponding

velocity. Vertical acceleration was also considered, with a time variation identical to that of the horizontal component, but with only 1/3 the acceleration value.

No damping was assumed and  $t_1$  was taken as 0.292 seconds, the fundamental period of vibration of the system. With a time step interval of 0.01425 seconds, the computer program described in Section 2.7 was used to analyze the system's nonlinear response. The same numerical integration method and time step interval were used to solve the equations of motion in nodal point coordinates in program DRAIN-2D. No dynamic equilibrium iteration is performed in DRAIN-2D, while dynamic equilibrium iteration by a constant stiffness method is economically handled in the reduction technique analysis. Results from the two analyses are compared in Figs. 3.7-3.9.

Lateral displacement histories of wall 1 at the fourteenth and seventh floor levels are shown in Fig. 3.7. Results from both DRAIN-2D and the  $H_6 V_3$  reduction technique essentially agree as do the vertical displacement histories of the roof level (Fig. 3.7).

When the base axial forces of wall 1 are compared (Fig. 3.8), discrepancies in the results of the two analyses occur late in the time history, with the response from DRAIN-2D analysis oscillating about that from analysis of the  $H_6 V_3$  reduced system. The discrepancies become more apparent when base shear histories are compared (Fig. 3.8). The oscillation was in part due to the lack of equilibrium iteration in the DRAIN-2D analysis. By reducing the time step size to 0.007125 seconds for the analysis by program DRAIN-2D, and hence doubling computational effort, the discrepancies in base shear were

reduced, but the oscillation in shear history of the fourth floor beam was not effectively reduced (Fig. 3.8).

Along the height of the structure, ductility requirements in coupling beams derived from analyses using the  $H_6 V_3$  reduction and DRAIN-2D basically agree in magnitude and distribution (Fig. 3.9).

From the preceding evaluation, the  $H_6 V_3$  reduced system satisfactorily predicted nonlinear response of the coupled shear wall system. The size of the reduced system is not only significantly smaller than that of the original system, but is adjustable to suit the problem under consideration as well as to achieve a desired level of solution accuracy. Furthermore, a larger integration time step may be used in the procedure presented here because unwanted higher modes -- those negligibly contributing to structural response -- have been eliminated in the reduced system. Therefore, the reduction technique is efficient, economical, and flexible. The effectiveness of the reduction technique in reducing computational effort over the original system will be demonstrated through an operational count in the following section.

### 3.5 Computational Aspects: Reduced System v.s. Original System

The reduced system contains far fewer equations of motion than does the original system. Consequently, during the equation-solving process, considerable effort in triangularization, forward reduction, and back substitution is saved in the response analysis of the reduced system. However, the reduction technique has some disadvantages; each time the stiffness matrix is modified to account for nonlinear effects, generalized coordinates must be transformed to physical coordinates (Eq. (2.18)).

For the earthquake response analysis of the coupled shear wall system of Fig. 3.1, the number of computational operations necessary for the step-by-step analysis of the  $H_6 V_3$  reduced system of equations (Eq. (2.19)) and the original system of equations (Eq. (2.16)) is given in Table 3.1.

The computational effort required to solve the generalized coordinate equations (Eq. (2.19)) is much less than that required to solve the original system of equations in nodal point coordinates (Eq. (2.16)), about 50% less for each linear step, and about 80% less for each nonlinear step. The major saving is in triangularization which is always required whenever structural stiffness changes from one time step to another. If dynamic equilibrium were used in the analyses of both systems, the savings afforded by the reduction technique would be even greater.

The reduction technique is applicable to both linear and nonlinear time-history response analyses. The greater the number of nonlinear events occurring during a response, the greater the computational savings, especially in retriangularization of new effective stiffness matrices (Chapter 2). The relatively smaller size of the reduced system in comparison with the original system allows economical equilibrium iteration with which larger step sizes may be used. A lesser number of integration steps is therefore required.

## 4. ANALYSIS OF EARTHQUAKE-DAMAGED BUILDINGS

### 4.1 Scope of Chapter

A computer program developed to implement the analytical technique described in Chapter 2 is used to analyze the earthquake response of coupled shear wall structures damaged during earthquakes in Anchorage, Alaska, and Managua, Nicaragua. The earthquake response of the main coupled shear wall system is investigated and analytical results compared to observed damage. Predictions and observations of the earthquake behavior of the coupled shear wall systems are correlated, and general considerations suggested for the design of such coupling systems.

Two coupled shear wall structures are analyzed: the McKinley Building in Anchorage, Alaska, and the Banco de America Building in Managua, Nicaragua.

### 4.2 McKinley Building

#### 4.2.1 Structural System and Design Criteria

The McKinley Building is a fourteen-story reinforced concrete structure, 52'-4" by 129'-8" in plan, oriented with side walls in the north-south and end walls in the east-west direction (Fig. 4.1). The center core consists of a detached stairwell and a composite core of the elevator shaft, stairwell, and ventilation duct. One-way floor slabs are supported by interior floor beams, which lie in the north-south direction on supporting columns, and exterior reinforced concrete bearing walls, coupled in their plane by deep spandrel beams. Twelve-inch wall sections of the center core are designed as columns, and

two interior square columns are integrated with the core. Most interior walls are nonbearing. Exterior walls between windows and entrance openings are also designed as columns. The exterior coupled wall and core constitute the lateral force-resisting system of the building.

The building was constructed in 1950-51. The building will be assumed to conform to the 1949 edition of the Uniform Building Code, with a seismic Zone 2 factor which was in force in Anchorage until approximately 1954.

In the north end coupled shear wall system, three wall piers, two identical 12'-4" wide end piers at 23'-7" center-to-center apart and one 4'-6" wide middle pier between them, are coupled by 4' deep, 3'-4 - 1/2" span beams at all fourteen stories. The interstory height is 8'-6" (Fig. 4.2).

For wall piers of the north end coupled wall system, sectional dimensions, reinforcement details, and schedule are shown in Fig. 4.3. The thickness of the rectangular sections varies from 8" to 12". Vertical reinforcement is arranged in a double curtain for the first four stories and in a single curtain for the remaining stories. Number 5 bars are spaced identically in both horizontal and vertical directions in all wall sections, except for the eighth story section in which horizontal reinforcement is spaced slightly farther apart than vertical reinforcement. Flexural reinforcement is uniformly spread throughout wall sections rather than being concentrated at the ends, resulting in a relatively small flexural capacity.

All coupling beams in this coupled wall system were 4' deep with various widths and reinforcing details; sectional details are shown in Fig. 4.4. Beams with rustications (Figs. 4.2 and 4.4) are normally 1" thinner than the dimension shown in Fig. 4.4 and the

rustications are generally 1" deep. The rusticated beams are therefore effectively 2" less thick than indicated in Fig. 4.4. In all beams, number 5 round bars are used as both longitudinal and transverse reinforcement, arranged either in single or double curtains. An additional longitudinal reinforcement of number 5 round bars is provided at both extreme faces of beam sections having single curtains of reinforcement (Fig. 4.4).

#### 4.2.2 Observed Damage

Principal damage to the McKinley Building was in the exterior coupled shear wall system, with damage concentrated in the rusticated coupling beams<sup>(28)</sup>. In the east and west end coupled walls, a similar pattern of damage to rusticated coupling beams was observed, starting in the second story and continuing to the twelfth story. The spandrel beams at the corner of the building exhibited x-cracking as well as pronounced horizontal movement along construction joints at the floor level.

In the north end coupled shear wall, the main system considered in this analysis, the rusticated coupling beams on either side of the middle wall pier generally suffered severe x-cracking failure in shear (Fig. 4.5). These cracks were principally concentrated in beams from the third to ninth stories, with some light x-cracks extending to beams in the second and eleventh stories. A severe break along the third story, apparently a combined axial and bending failure, was observed in the east end pier. This failure pattern did not occur in another identical coupling system in the south end of the structure; the failure of the first story supporting column of the south wall was believed to have contributed to such a difference in behavior.

#### 4.2.3 Ground Motion

Because records of ground motion were obtained neither in Anchorage, nor in other areas experiencing strong ground shaking during the 1964 Alaskan Earthquake, a simulated ground acceleration constructed by Housner and Jennings<sup>(13)</sup>, with motion for the first 30 seconds (Fig. 4.6), was used as input for the earthquake analysis. The simulated ground acceleration contains two phases of strong shaking: one of 30 seconds duration with 14% gravity peak acceleration, and a second of 20 seconds duration with 9% gravity peak acceleration. The response spectrum for the simulated ground motion is presented in Fig. 4.7 for 0% and 5% critical damping.

#### 4.2.4 Analytical Model

The analytical model for the north end coupled shear wall (Fig. 4.8) consists of three wide-column lines, located at the respective neutral axes of the walls, and beams at every floor level coupling adjacent walls; the corner spandrel beams are neglected. Rigid links represent the wall-beam panel zone according to the assumption adopted in Chapter 2.

Material properties were calculated in accordance with the Uniform Building Code, based on a 28-day compressive strength for concrete of 3,000 psi and a yielding strength for reinforcement of 50,000 psi. Sectional area and moment of inertia for walls were calculated based on the building's design, assuming uncracked sections. Because x-cracks could be expected to develop early during the earthquake and to remain open during most of the response, the stiffnesses of all coupling beams were calculated assuming cracked sections. Using the mechanical model described in Section 2.5, yielding of beams was

assumed to have been initiated at a shear corresponding to flexural capacity,  $P_y = 60.58$  kips; a 5% strain-hardening factor was also assumed.

Floor slabs were neglected in calculating beam stiffness. Story masses calculated from drawings of the building were adopted from Ref. 7. One-fourth of each story's mass was lumped at the floor level of the model. Based on these assumed masses and stiffnesses, the elastic vibrational periods of the analytical model are very close to those calculated for the total structure in the east-west direction<sup>(7)</sup>, as follows:

<u>Period</u>	<u>Analytical Model</u>	<u>Total Structure (Ref. 7)</u>
$T_1$	0.849	0.875
$T_2$	0.199	0.207
$T_3$	0.089	0.093

Using a computer program developed by Mahin and Bertero<sup>(18)</sup>, the moment-axial force interaction capacity of wall sections was calculated (Fig. 4.9), based on monotonic loading to an ultimate concrete strain of 0.0035. The interaction curves clearly reflect the relatively small percentage of flexural reinforcement area with respect to wall section area, leading to low interacting sectional moment capacity and negligible axial tension capacity (Fig. 4.9). Flexural reinforcement was not detailed to confine the enclosed concrete effectively, and wall sections therefore have relatively low ductility capacities.

All coupling beams in the structure are deep members, having depth to span ratios over 1.00. Flexural reinforcement area ranges from 0.14% to 0.23% of the cross-sectional area, whereas shear

reinforcement area ranges from 0.34% to 0.43% (Table 4.1). The ACI Code<sup>(1)</sup> calculation for such beams indicates that shear capacity for these sections would be in excess of shear at ultimate flexural capacity. Laboratory experiments by Paulay<sup>(21)</sup>, however, indicated that under reversal of loads the shear capacity of such deep beams is significantly less than that predicted by the ACI Code. He also demonstrated that brittle shear failure can only be avoided if web reinforcement alone is sufficient to resist the entire shear at flexural capacity. The web reinforcement in most coupling beams of this building was not sufficient (Table 4.1), and coupling beams would therefore be expected to fail in shear eventually, although initial flexural yielding is indicated.

The original system of equations of motion was reduced to a  $H_6 V_3$  reduced system in which step-by-step integration was used to solve for nonlinear response. Mass proportional damping corresponding to 5% of the first mode critical damping was assumed.

#### 4.2.5 Earthquake Response - Correlation with Observed Damage

Based on preliminary studies, the maximum response of the structure was expected to occur during the first 20 seconds of the simulated motion. The response over this duration was determined by the step-by-step integration procedure mentioned in Chapter 2 with a time step of 0.02 seconds. Analysis of the idealized system by the computer program mentioned earlier to the simulated motion of Fig. 4.6 led to the results presented in Figs. 4.10 to 4.16.

The yielding history in the coupling beams is presented in Fig. 4.10. The third story beam began to yield at 7.38 seconds after the start of the excitation. With the exception of a few minor

excursions into the inelastic range, the system responded elastically during the first 13.16 seconds. Inelastic action then intensified among the third to eighth story coupling beams and occasionally progressed to upper story beams. A typical yielding cycle started at the second story beam and propagated upwards; beams at lower stories typically did not begin to unload until yielding reached beams around the tenth story. Major inelastic action occurred during the seventeenth and eighteenth seconds of the excitation. Such a yielding history indicates that during most inelastic cycles, more than half of the beams remained in yielding stages.

Beams from the first to tenth stories underwent more than 10 inelastic yielding cycles. The most intensive inelastic yielding was confined to beams on the second through eighth stories, each of which accumulated a total plastic rotation of more than 0.02 radians during more than 20 yielding excursions (Figs. 4.11 and 4.12). Cyclic rotation ductility demand, defined as in Ref. 18, was also in excess of 10, an excessive demand for an ordinarily reinforced deep beam. The analysis thus predicted severe inelastic action in these beams which undoubtedly failed due to inadequate ductility. The prediction was generally consistent with the observed damage, beams from the second through ninth stories having been severely distressed by the earthquake.

Axial force envelopes for walls (Fig. 4.13) indicate no resulting axial tension, and therefore no possibility of uplifting of the foundation or failure of walls in tension. A significant difference in magnitude of developed axial compression in two identical end wall piers gave rise to substantially different interacting sectional moment capacities (Fig. 4.9). Therefore, one of the two

identical piers with smaller moment capacity was more vulnerable to yielding than the other pier; this was, in fact, confirmed by observed damage.

Although yielding in walls was not permitted in the analysis, it can be traced through the response history by studying the mechanics of force distribution in the system at certain time steps. Two such time steps were selected:  $t = 7.40$  seconds, when yielding first occurred in beams at the second to sixth stories, and  $t = 16.90$  seconds, when the eleventh story beam began to yield after beams in the third through eighth stories had undergone more than three consecutive large yielding cycles. At  $t = 7.40$  seconds, investigation revealed that wall sections had ample moment capacity, even if all yielding beams were assumed to have failed and walls to have resisted the total story overturning moment. Therefore, the wall piers did not undergo inelastic yielding at this moment.

At  $t = 16.90$  seconds, beams in the third through eighth stories had just undergone 3 large consecutive yielding reversal cycles. They were assumed to fail at this point and part of the resistance to story overturning moment formerly offered by wall axial couples was then no longer available at certain stories. Wall sections across affected stories had therefore to resist more moment to compensate for the loss of axial couple. This additional moment was assumed to be supplied equally by wall sections of the two end piers. The resulting moment distribution is illustrated in Fig. 4.14, indicating that wall sections from the fourth story down were stressed beyond yielding capacity. Although actual redistribution of resisting axial couple after some beams failed is much more complicated, this simple redistribution of

moment indicates a yielding tendency in these lower story wall sections which, in fact, did occur in the third story wall section. The investigation thus suggested that yielding in the wall occurred at approximately  $t = 16.90$  seconds, and that damage in the remaining elastic beams which would otherwise have yielded was mitigated (see Figs. 4.11 and 4.12).

The story shear envelope (Fig. 4.15) indicates that a relatively low shear developed as compared to the capacity offered by the walls. The minimum available capacity of one wall pier interacting with existing axial forces, according to ACI-71 Code, nearly suffices to resist the total developed story shear. Shear failure, against which the walls of the structure were designed, was not a threat to the building's structural integrity. In the middle wall pier, the distribution of developed shear, which was approximately of the same magnitude as in the upper story of the end pier, was very uniform over the height.

Envelopes of maximum bending moment in walls are illustrated in Fig. 4.16. Maximum moments developed in the middle pier were low and uniform over the height, whereas those in end piers were low in the upper stories and increased rapidly from the sixth story down. In the lower stories, a substantial part of the story overturning moment was effectively resisted by the moment couples formed by axial forces in the two end piers, on the order of up to 60%.

Two sets of moment capacities, one associated with the maximum axial compression envelope and the other with the minimum axial compression envelope, are also shown in Fig. 4.16. Again, moment over-stresses were predicted in the lower story wall sections, indicating

yielding in the third, second, and first stories. Observed yielding in the third story wall section was repeatedly predicted by the analysis.

### 4.3 Banco de America Building

#### 4.3.1 Structural System and Design Criteria

The Banco de America Building consists of an 18-story tower and two basements; a general view of the building is shown in Fig. 4.17. The tower consists of four shear wall cores, symmetrically located with respect to the N-S and E-W axes through the center of the 22.68 meter square floor plan (Fig. 4.18). A pair of coupling girders connects two adjacent cores in both directions. The square floor slab is supported externally by a series of peripheral columns closely spaced at 2.30 meters. Even-numbered floor slabs have central openings measuring 3.45 meters square. In addition to this 18-story tower, rising 68.65 meters above street level, the building has two basements extending beyond the square perimeter of the tower in the east-west direction. The tower portion of this building is of particular concern in this investigation.

The building was designed between 1963 and 1967 under the working stress provisions of the UBC, with the structure classified as a box system with a horizontal force factor,  $K$ , of 1.33. The coupled shear core system was assumed to resist all lateral loads -- wind and seismic -- whereas the perimeter columns were designed to support vertical load. Various combinations of dead, live, wind, and seismic loads were considered. More details regarding the procedure and assumptions made in the design of this building have been reported in Ref. 18.

Intermediate grade reinforcement and stone concrete with an ultimate strength of 4000 psi were specified in the design. Sectional dimensions and details of reinforcement for the shear cores are shown in Figs. 4.19 and 4.20. Coupling girders vary in dimension and reinforcing detail (Fig. 4.21). In every girder above those on the first floor, there is an air-conditioning duct, measuring 20 cm deep by 40 cm wide, located immediately below the floor slab. All coupling girders, except those at the first and top floor levels, were under-designed in shear (Table 4.2). Even neglecting the capacity reduction resulting from duct openings, shear capacity of the girders (ACI-71 Code) was much lower than corresponding shear at flexural capacity.

#### 4.3.2 Observed Damage

Damage to the Banco de America Building from the Managua Earthquake<sup>(25)</sup> was predominantly in the east-west direction, and primarily confined to the coupling girders. Damage in walls was restricted to hairline cracks at tapered sections and one-way diagonal cracks on the south faces of south piers at the fifth, sixth, eighth, twelfth, thirteenth and fourteenth stories. Overall, damage to walls was considered to be light.

Damage in coupling girders was mainly concentrated in the north and south girders, with girders in the east and west suffering only slight damage. Parallel pairs of girders in both directions were equally damaged. Shear failure in girders from the third through seventeenth stories was typical: concrete in the section below duct openings failed in shear and spalled. The heaviest damage occurred in the penthouse girders; no damage was observed in the second story girder<sup>(25)</sup>.

Floor slabs cracked at connections to the shear core, to perimeter columns, and to coupling girders which failed in shear. There was no visible damage to perimeter columns.

#### 4.3.3 Ground Motion

There was no record of the ground motion at the site of the building during the earthquake. The only strong motion accelerograms of the Managua earthquake were recorded at the ESSO Refinery<sup>(23)</sup>, about 3.1 miles from the building. The east-west component of this accelerogram was therefore used as an input ground motion for the earthquake analysis. The first 15 seconds duration of this motion is shown in Fig. 4.22, indicating a maximum acceleration of 0.38g. The corresponding velocity response spectrum is shown in Fig. 4.23 for 5% critical damping.

#### 4.3.4 Analytical Model

Since equal damage in parallel pairs of girders indicated a translational response free of torsional effects, the building was idealized by a two-dimensional plane model representing half of the building plan. Also, since the coupling girders oriented in the east-west direction suffered the heaviest damage, the east-west orientation of the plane model was of primary concern in this investigation. The analytical model is shown in Fig. 4.24.

Only core walls and coupling girders in the east-west direction were included in the model, neglecting perimeter columns and floor slabs. Core walls were assumed to be fixed at the street level and were idealized as wide-column members, located at the respective neutral axes of the core sections. Rigidities of the coupling girders

were considered, including the effective width of the connecting slab. Stiffnesses of all members were approximated based on sectional areas and moment of inertia of uncracked sections and on the design-specified strength of concrete and reinforcement; the values were essentially the same as those used in Ref. 19.

Using the mechanical model described in Section 2.5, shears at initial yielding for all girders except those at the first and top floors were determined by the corresponding shear capacities which are smaller than shear at flexural capacity (Table 4.2), and a strain-hardening of 5% was assumed. Yielding in the first and top floor girders was assumed to be initiated by shears at flexural capacity because they were smaller than shear capacities; strain-hardening of 2% was assumed. All girders were assumed to have unlimited ductility capacity and duct openings were neglected.

All dead loads tributary to the structural model were lumped at floor level and the corresponding mass was used in the dynamic analysis. Damping was assumed to be a linear combination of original stiffness and mass matrices, and was chosen to produce 5% critical damping for the first and third modes.

Since the distribution of stiffness in the system was not uniform, and the contribution from higher modes was likely to be significant, a more refined reduced system,  $H_8 V_3$ , was chosen for this investigation. Preliminary study of elastic base shear participation of the first five modes indicated that the strongest contribution was from the second mode, and that there was significant participation up to the third mode. In addition, under shifting of periods due to inelastic yielding, participation of higher modes would be even greater.

Accurate reproduction of higher modes was therefore essential, and the  $H_8 V_3$  system was chosen to analyze the behavior of the Banco de America Building rather than the  $H_6 V_3$  system used to investigate the behavior of the McKinley Building.

#### 4.3.5 Earthquake Response - Correlation with Observed Damage

Using the computer program described earlier (Section 2.7), the nonlinear response of the coupled wall model of the Banco de America Building to the ESSO Refinery ground motion was analyzed using the  $H_8 V_3$  reduced system with a time step of 0.02 seconds. The response was terminated at 12 seconds after the excitation, when major inelastic action was expected to have ended. Results from this analysis are presented in Figs. 4.25 to 4.32.

Yielding histories of coupling girders are illustrated in Fig. 4.25. During a typical yielding cycle, the lower story girders began to yield and did not unload until yielding had propagated towards upper story girders. Immediately after a large acceleration pulse at about  $t = 6.10$  seconds (Fig. 4.22), yielding and unloading alternated rapidly between girders at upper and lower stories. The same alternation was observed during the response from  $t = 10.5$  seconds to  $t = 11.5$  seconds. During such a major yielding cycle, unloading of yielding girders was not always immediate, and one-third of all girders usually remained in yielding stages, indicating an insignificant loss of coupling effect. Although such rapid alternation reduced the possibility of simultaneous yielding in many girders, thus maintaining the coupling effect, the corresponding rapid reversal of high shear in girders would require much more careful detailing of reinforcement to achieve sufficiently high ductility capacity.

The analysis indicated increasingly inelastic yielding from lower to upper story girders; a total plastic rotation of 0.025 radians was accumulated in the sixth story girders and increased to 0.035 radians in the top girder (Fig. 4.26). The girders at levels four through eighteen underwent an average of 30 cycles of inelastic excursion. Cyclic rotation ductility demand (defined in Ref. 18) increased from 8 at the sixth story girders to 24 at the top girder (Fig. 4.27). Overall, the analysis predicted increasing damage in girders from the fourth to top stories. General consistency with observed damage in girders was obtained (Section 4.3.2). The envelope of maximum shear force in girders (Fig. 4.28) also indicates excessive stressing in upper story girders.

Even if the openings in the original design of the coupling system were filled and web reinforcement increased to suppress shear failure, resulting flexural yielding would not be accompanied by high ductility capacity as a result of associated high shear. The intensity of girder shear could be effectively reduced by decreasing the flexural strength of coupling girders. Also, stiffness reductions in all girders could, for this strongly coupled system, reduce elastic shear in all beams. Such reductions in both flexural strength and stiffness would result in more flexible girders with less induced shear. These girders would be easier to design and detail for ductile behavior, provided that shear reinforcement were adequate.

Higher mode effects were, as would be expected, carried over to the stress resultant in the girders. Response histories of shear in coupling girders located at the fourth, tenth, and eighteenth floors are shown in Fig. 4.29. Shear histories for the fourth and eighteenth

story girders oscillated predominantly at the second mode period, with some higher mode effects. Although the tenth story girder was located near a node in the third structural mode shape, second mode effects were still apparent.

The envelope of maximum story shear (Fig. 4.30) exhibits an irregular pattern due to the effects of higher modes. A large jump in shear at the third story can be traced back to the time at which it occurred,  $t = 6.20$  seconds. A pulse with a large peak acceleration had just caused all girders in the system, except those in the first and third stories, to yield (Fig. 4.25). The original system was therefore transformed into a moderately weak coupling of the upper sixteen stories, with a clamp end cantilever representing the coupling of the lower three stories. Higher mode shapes would be required to produce the dynamic deflected shape of such a system, particularly at the lower three stories. The system thereby demands large equilibrating inertial forces proportional to the square of the vibrational frequencies of the participating higher modes. Investigation of dynamic displacement at this time step ( $t = 6.20$  seconds) revealed significant contributions of higher modes in the lower three stories.

Maximum developed moments in core walls were well under corresponding capacities, with the least margin at the eleventh story (Fig. 4.31). However, the analysis predicted no flexural yielding in walls, with observed damage generally corroborating this prediction. The distribution of story overturning moment indicated that axial couples contributed substantial resistance (Fig. 4.31) without which the moment capacity of walls could not have sufficed to resist the induced dynamic story overturning moment.

The envelope of maximum axial force in the core wall (Fig. 4.32) indicates that tension forces developed within middle to upper stories (stories six to sixteen). A maximum axial tension of 556 kips was developed in the twelfth story wall section, not approaching the sectional tension capacity that would fracture reinforcing steel at 973 kips. The analysis predicted no failure in the shear core due to fracture of reinforcing steel; observed damage also did not indicate such failure. Although this relatively high maximum axial tension could result in minor concrete cracking, it did not cause any yielding of flexural reinforcement, clearly demonstrated by the interacting moment capacity shown in Fig. 4.31. The distribution and magnitude of axial force along the height of the wall, directly governing the strength and ductility capacities of wall sections, were highly dependent on induced shear in coupling girders and could be effectively controlled by appropriately selecting coupling girder stiffness and strength.

#### 4.4 Design Considerations for Coupled Shear Wall Systems

In designing an effective coupling system, walls must not be too strongly coupled by both strong and stiff beams, as were the two coupling systems considered in this chapter. The flexural strength of coupling beams controls the magnitude of ultimate beam shear, whereas the stiffness of coupling beams, relative to the stiffness of coupled wall piers, effectively determines beam shear distribution along the height of the structure.

If coupling beams are strong and stiff, shear will be high and concentrated in lower story coupling beams, resulting in axial force couples which contribute to the walls' resistance to story overturning

moment primarily at lower stories. On the other hand, if coupling beams are flexible and have moderate strength capacity, beam shear will be smaller and more evenly distributed throughout upper story beams. Large axial force couples are therefore created within a greater number of stories as a result of evenly distributed beam shear, effectively assisting walls at a greater number of stories to resist overturning moment. Such a difference in the distribution of assisting axial force couple is demonstrated in comparing Fig. 4.31 to Fig. 4.16, reflecting the lower relative beam-to-wall stiffness of the Banco de America Building than of the McKinley Building. Therefore, coupling systems with flexible and moderately strong coupling beams would be more effective than coupling systems with stiff and strong coupling beams. However, walls should not be so weakly coupled that degrading elastic stiffness in a few coupling beams results in substantial reductions in lateral stiffness of the structure.

The walls in a coupling system should not be designed to undergo significant inelastic yielding during an earthquake excitation. Since the magnitude of developed moment in walls heavily depends on the assistance of story axial couple created by shear in coupling beams, unexpected brittle failure of any coupling beam would require that walls resist additional story moment formerly resisted by the axial couple generated from shear of that beam, possibly increasing wall moment beyond anticipated yielding capacity. Therefore, in addition to reinforcing walls for elastic behavior, some ductility capacity should also be provided as a second line of defense. In walls, developed moment as well as strength and ductility are highly dependent on the magnitude of induced axial force. Although high axial forces form large resisting

axial couples, thereby reducing the required resisting moment in walls, flexural ductility capacity is generally reduced by an increase in axial compression, and fracture or moment capacity reduction may occur as the result of an increase in axial tension<sup>(18)</sup>.

For a planar wall with a rectangular section, a strong and ductile wall can be achieved by concentrating flexural reinforcement and confining enclosed concrete at the ends of wall sections<sup>(2)</sup>, and possibly by forming edge columns to accommodate reinforcing details required to confine concrete effectively.

Coupling beams usually undergo numerous cycles of large yielding reversal under high shear. Consequently, deep coupling beams which cannot normally sustain large ductility under high reversal shear should be avoided. Although deep beams can create large axial couples across stories to assist walls in resisting external story moment, they are generally brittle. If these deep beams fail, high moment couples will be redistributed back, increasing wall moment possibly beyond yielding capacity. However, if the thickness of beams is limited by the thickness of planar walls to be coupled -- such as in the McKinley Building -- a deep beam may be required in order to maintain low nominal shear stress, say less than  $5\sqrt{f'_c}$ <sup>(5)</sup>. Such a limitation on beam thickness can be obviated by forming columns at the edges of wall sections, thus providing flexibility in choices of sectional dimensions of connecting beams. Such end columns also enable stronger and more ductile walls as described above, and maintain a nominal shear stress across wall sections equal to or lower than  $10\sqrt{f'_c}$ .

As small a value as is compatible with the design of an effective coupling system (described earlier in this section) should

be selected for the strength and stiffness of coupling beams relative to the stiffnesses of and distance between the two walls. In addition, specially detailed and sufficient shear reinforcement must be provided to ensure that full flexural capacity can be developed in all coupling beams; no openings in beams, which can be detrimental to shear strength, should be permitted.

## 5. CONCLUSIONS

This study and its principal conclusions may be summarized as follows:

1. With the assumption that inelastic action is confined to coupling beams, the dynamic deflections of a coupled shear wall system may be effectively represented as a linear combination of the first few natural mode shapes in both lateral and longitudinal (vertical) vibration of individual nonyielding walls treated as independent cantilevers. A considerable reduction of the number of degrees of freedom of the system is thereby realized. Vertical inertia, which is important in the dynamic response of coupled shear wall systems, need not be neglected in the reduction formulation, and any mechanical model of the coupling beams can be incorporated into the analytical technique.
2. The reduction technique is flexible; the number of uncoupled mode shapes used -- hence the size of the reduced system -- can be selected to achieve any desired solution accuracy, to handle systems with an irregular distribution of rigidity, or to cope with the effects of higher modes in dynamic response. However, for response to the horizontal component of an earthquake excitation, the best combination of these uncoupled mode shapes is one that includes more modes in lateral vibration than in vertical vibration, preferably in a proportion of 2 to 1.
3. Numerical results have demonstrated the effectiveness of this reduction technique in applications to systems with both uniform

and nonuniform distributions of coupling beam stiffness along the heights of walls, as well as to a system coupling nonidentical wall piers. Satisfactory modal values - mode shapes, frequencies, and modal stress resultants - are produced using relatively few uncoupled mode shapes. However, the derived stress resultants in walls must be adjusted by distributing half of each incoming beam moment at every beam-wall joint to the wall bending moment immediately above and below that joint; the base moment is also adjusted by half of the incoming beam moment at the first story beam-wall joint.

4. The analysis procedure leads to a considerable reduction in computational effort when compared to standard computer programs for analyzing inelastic structural response. The reduction technique is efficient for nonlinear earthquake analysis of a multistory coupling of a multiwall system; the greater the number of changes in beam stiffness during rapid load reversals, the greater the computational savings over the standard analytical technique - especially in the retriangularization of the stiffness matrix. In the time-history analysis, not only is the step-by-step integration performed on a substantially reduced system of equations, a larger integration time step may be used because unwanted higher mode effects have been eliminated in the reduction process, leading to a totally economical analysis.
5. Earthquake response analysis of the McKinley Building and the Banco de America Building, using the analytical technique developed in this study, predicted damage patterns which generally agreed with observed damage. Coupling beams in both buildings underwent extensive inelastic yielding, whereas only one wall pier of the

McKinley Building suffered a tensile break across the section. The excellent performance of the Banco de America Building suggested that the walls of an effective coupling system should not undergo significant inelastic yielding, justifying the analytical assumption of nonyielding walls.

6. In the coupling of shear walls, the strength of coupling beams effectively determines the ultimate value of beam shear, whereas the stiffness of coupling beams, with respect to the stiffness of wall piers, effectively determines the distribution of induced beam shear along the height of walls. In a system in which walls are strongly coupled by strong and stiff coupling beams, such as in the McKinley Building, high shears are induced and concentrated among lower story coupling beams. Subsequently, high axial forces are created in lower story walls, forming large moment couples across the stories, assisting walls to resist story overturning moments only at these lower stories. In a coupling system with less relative beam-to-wall stiffness, such as the Banco de America Building, on the other hand, induced beam shear is more evenly distributed throughout higher stories. Significant assistance from axial couples in resisting story overturning moments therefore becomes available for a greater number of stories. Therefore, shear walls will be more effectively coupled by flexible coupling beams with moderate strength capacity.
7. It is desirable to design walls to maintain elastic behavior throughout an earthquake response, and to ensure moderate ductility capacity as a second line of defense. A strong and ductile wall can be designed by concentrating flexural reinforcement at the two

extreme ends of the section and detailing transverse reinforcement to confine concrete effectively. End columns on the rectangular section can accommodate such reinforcing details, remove geometric constraints on the thickness of coupling beams, hence avoiding the use of deep beams, and maintain a low nominal shear stress ( $\leq 10\sqrt{f'_c}$ ) across wall sections.

8. Coupling beams in both the McKinley Building and the Banco de America Building generally underwent numerous cycles of large inelastic yielding reversal. To reduce the possibility of significant yielding in walls, coupling beams must be capable of sustaining large ductility under induced shear without brittle shear failure. Openings in coupling girders of the Banco de America Building reduced the strength and stiffness of girders and invited shear failure. Coupling beams should be selected so as to be flexible and moderately strong in flexure in order to render an effective coupling system as described in Conclusion No. 6. These beams should have an adequate amount of web reinforcement, and should be carefully detailed for ductile behavior under a large number of reversals.

REFERENCES

1. ACI Committee 318, Building Code Requirements for Reinforced Concrete (ACI-318-71), American Concrete Institute, Detroit, Michigan, 1971.
2. Allen, C. M., Jaeger, L. G. and Fenton, V. C., "Ductility in Reinforced Concrete Shear Walls," Response of Multistory Concrete Structures to Lateral Forces, Special Publication SP-36, American Concrete Institute, Detroit, Michigan, 1973, pp 97-118.
3. Bathe, K. J., Ozdemir, H. and Wilson, E. L., "Static and Dynamic Geometric and Material Nonlinear Analysis," SESM Report No. 74-4, Division of Structural Engineering and Structural Mechanics, Dept. of Civil Engineering, University of California, Berkeley, Feb. 1974.
4. Beck, H., "Contribution to the Analysis of Coupled Shear Walls," Journal of the American Concrete Institute, Vol. 59, No. 8, 1962, pp 1055-1069.
5. Bertero, V. V., "Experimental Studies Concerning Reinforced, Prestressed and Partially Prestressed Concrete Structures and Their Elements," Symposium on Resistance and Ultimate Deformability of Structures Acted on by Well-Defined Repeated Loads, International Association of Bridge and Structural Engineering, Lisbon, Preliminary Report, 1972.
6. Bertero, V. V., Mahin, S. A. and Hollings, J. P., "Seismic Analysis of the Banco de America," Earthquake Engineering Research Center, Report in Preparation, University of California, Berkeley.
7. Blume, J. A., "A Structural Dynamic Analysis of an Earthquake Damaged 14-story Building," The Prince William Sound, Alaska Earthquake of 1964 and Aftershocks, F. J. Wood, ed., Vol. II, Part A, Publication 10-3 (C & GS), U. S. Department of Commerce, Washington, D. C., 1967, pp 357-382.
8. Burns, R. J., "An Approximate Method of Analysis of Coupled Shear Walls Subjected to Triangular Loading," Proceedings of the Third World Conference on Earthquake Engineering, Auckland, New Zealand, 1965.
9. Chitty, L., "On the Cantilever Composed of a Series of Parallel Beams Inter-Connected by Cross Bars," Phil. Magazine (London), Vol. 38, Oct., 1947.
10. Coull, A. and Choudhury, J. R., "Stresses and Deflections in Coupled Shear Walls," Journal of the American Concrete Institute, Vol. 64, No. 2, pp 65-72.

11. Coull, A. and Puri, R. D., "Analysis of Pierced Shear Walls," Journal of the Structural Division, ASCE, Vol. 94, No. ST1, Proc. Paper 5710, Jan. 1968, pp 71-32.
12. Hisatoka, T. and Matano, H., "Aseismic Analysis of the Tall Building Structure with Coupled Shear Wall," Proceedings of the Fifth World Conference on Earthquake Engineering, Rome, 1973.
13. Housner, G. W. and Jennings, P. C., "Reconstituted Earthquake Ground Motion at Anchorage," The Great Alaska Earthquake of 1964 - Engineering, Committee on the Alaska Earthquake of the Division of Earth Sciences, National Academy of Sciences, Washington D. C., 1973, pp 43-48.
14. Kanaan, A. E. and Powell, G. H., "General Purpose Computer Program for Inelastic Dynamic Analysis of Plane Structures," Earthquake Engineering Research Center Report No. EERC 73-6, University of California, Berkeley, April 1973.
15. MacLeod, I. A., "Lateral Stiffness of Shear Walls with Openings," Proceedings Symposium on Tall Building, University of Southampton, England, 1967, pp 223-243.
16. MacLeod, I. A., discussion of "The Effect of Local Wall Deformations on the Elastic Interaction of Cross Walls Coupled by Beams," by D. Michael, Proceedings, Symposium on Tall Building, University of Southampton, England, 1967, p 271.
17. Michael, D., "The Effect of Local Wall Deformations on the Elastic Interaction of Cross Walls Coupled by Beams," Proceedings, Symposium on Tall Building, University of Southampton, England, 1967, pp 253-270.
18. Mahin, S. A. and Bertero, V. V., "An Evaluation of Some Methods for Predicting Seismic Behavior of Reinforced Concrete Building," Earthquake Engineering Research Center Report No. EERC 75-5, University of California, Berkeley, Feb. 1975.
19. Mahin, S. A. and Bertero, V. V., "Nonlinear Seismic Response of a Coupled Shear Wall System," Preprint 2621, ASCE National Convention, Denver, Colorado, Nov. 3-7, 1975.
20. Newmark, N. W., "A Method of Computation for Structural Dynamics," Journal of the Engineering Mechanics Division, ASCE, Vol. 85, No. EM3, Proc. paper 2094, July 1959, pp 67-94.
21. Paulay, T., "The Coupling of Shear Walls," Vols, I & II, thesis presented to the University of Canterbury at Christchurch, New Zealand, for the degree of Doctor of Philosophy.
22. Paulay, T., "An Elasto-Plastic Analysis of Coupled Shear Walls," Journal of the American Concrete Institute, Vol. 67, No. 11, Nov. 1970, pp 915-922.

23. Perez, V., "Time-Dependent Spectral Analysis of Four Managua Earthquake Records," Conference Proceedings on the Managua, Nicaragua Earthquake of December 23, 1972, Earthquake Engineering Research Institute, Vol. 1, San Francisco, Nov. 29-30, 1973.
24. Rosman, R., "Approximate Analysis of Shear Walls Subjected to Lateral Loads," Journal of the American Concrete Institute, Proceedings, Vol. 61, No. 6, 1964, pp 717-733.
25. Selna, L. F. and Cho, M. D., "Banco de America, Managua--A High Rise Shear Wall Building Withstands a Strong Earthquake," Conference Proceedings on the Managua, Nicaragua Earthquake of December 23, 1972, Earthquake Engineering Research Institute, San Francisco, Vol. II, Nov. 29-30, 1973, pp 551-570.
26. Skattum, K. S., "Dynamic Analysis of Coupled Shear Walls and Sandwich Beams," thesis presented to California Institute of Technology, Pasadena, Calif., in 1971, in partial fulfillment of the requirements for the degree of Doctor of Philosophy.
27. Sozen, M. A. and Shibata, A., "An Evaluation of the Performance of the Banco de America Building Managua, Nicaragua," Conference Proceedings on the Managua, Nicaragua Earthquake of December 23, 1972, Earthquake Engineering Research Institute, San Francisco, Vol. II, Nov. 29-30, 1973, pp 529-550.
28. Steinbrugge, K. V., Manning, J. M. and Degenkolb, H. J., "Building Damage in Anchorage; Part II: Performance of Specific Buildings," The Prince William Sound, Alaska Earthquake of 1964 and After-shocks, F. J. Wood, ed., Vol. II, Part A, Publication 10-3 (C & GS), U. S. Department of Commerce, Washington D. C., 1967, pp 76-95.
29. Tso, W. K. and Chan, H. B., "Dynamic Analysis of Plane Coupled Shear Walls," Journal of the Engineering Mechanics Division, ASCE, Vol. 97, No. EMI, Proc. paper 7899, Feb. 1971, pp 33-48.
30. Veletsos, A. S. and Vann, W. P., "Response of Ground Excited Elastoplastic Systems," Structural Report No. 6, Dept. of Civil Engineering, Rice University, Houston, Texas, Dec. 1969.
31. Wilson, E. L. and Dovey, H. H., "Static and Earthquake Analysis of Three-Dimensional Frame and Shear Wall Buildings," Earthquake Engineering Research Center, Report No. EERC 72-1, University of California, Berkeley, Calif., May 1972.
32. Winokur, A. and Gluck, J., "Ultimate Strength Analysis of Coupled Shear Walls," Journal of the American Concrete Institute, Proceedings Vol. 65, No. 12, Dec. 1968, pp 1029-1036.

TABLE 3.1 OPERATION COUNT

OPERATIONS	ORIGINAL SYSTEM	$H_6 V_3$ REDUCED SYSTEM
(1) Number of equations, n	84	18
(2) Half bandwidth, b	9	Full, symmetric matrices
(3) Triangularization	$84 \times (9)^2 = 6804$	$(18)^3 / 6 = 972$
(4) Forward reduction and back substitution	$2 \times 84 \times 9 = 1512$	$(18)^2 = 324$
(5) Coordinate Transformation	None	$14 \times 2 \times (3 + (2 \times 6)) = 420$
Each linear step = (4) + (5)	1512	744
Each nonlinear step		
= (3) + (4) + (5)	8316	1716

TABLE 4.1 STRENGTH CAPACITY OF COUPLING BEAMS

BEAM AT STORY NO.	REINFORCEMENT RATIO		SHEAR CAPACITY, KIPS (ACI-71)			SHEAR AT FLEXURAL YIELDING, KIPS
	FLEXURAL	WEB	CONCRETE ONLY	WEB REINF. ONLY	TOTAL	
9-14	.002324	.003408	34.20	44.98	79.18	60.59
8	.002324	.00426	31.06	56.25	87.31	60.59
5-7	.001742	.003196	40.27	56.23	96.50	60.59
3-4	.001742	.004268	36.41	74.99	111.40	60.59
1-2	.001394	.003409	45.58	75.00	120.58	60.59

TABLE 4.2 STRENGTH CAPACITY OF PAIR OF COUPLING GIRDERS [Ref. 6]

PAIR OF GIRDERS AT LEVEL	YIELDING MOMENT CAPACITIES		SHEAR AT FLEXURAL CAPACITIES (KIPS)	SHEAR CAPACITIES BY ACI - 71 (KIPS)
	+ $M_P$ (K-FT)	- $M_P$ (K-FT)		
1	1265	1995	316	337
2-4	1205	1495	262	207
5-11	1300	1667	296	202
12-17	1077	1372	238	150
18	333	254	58	72

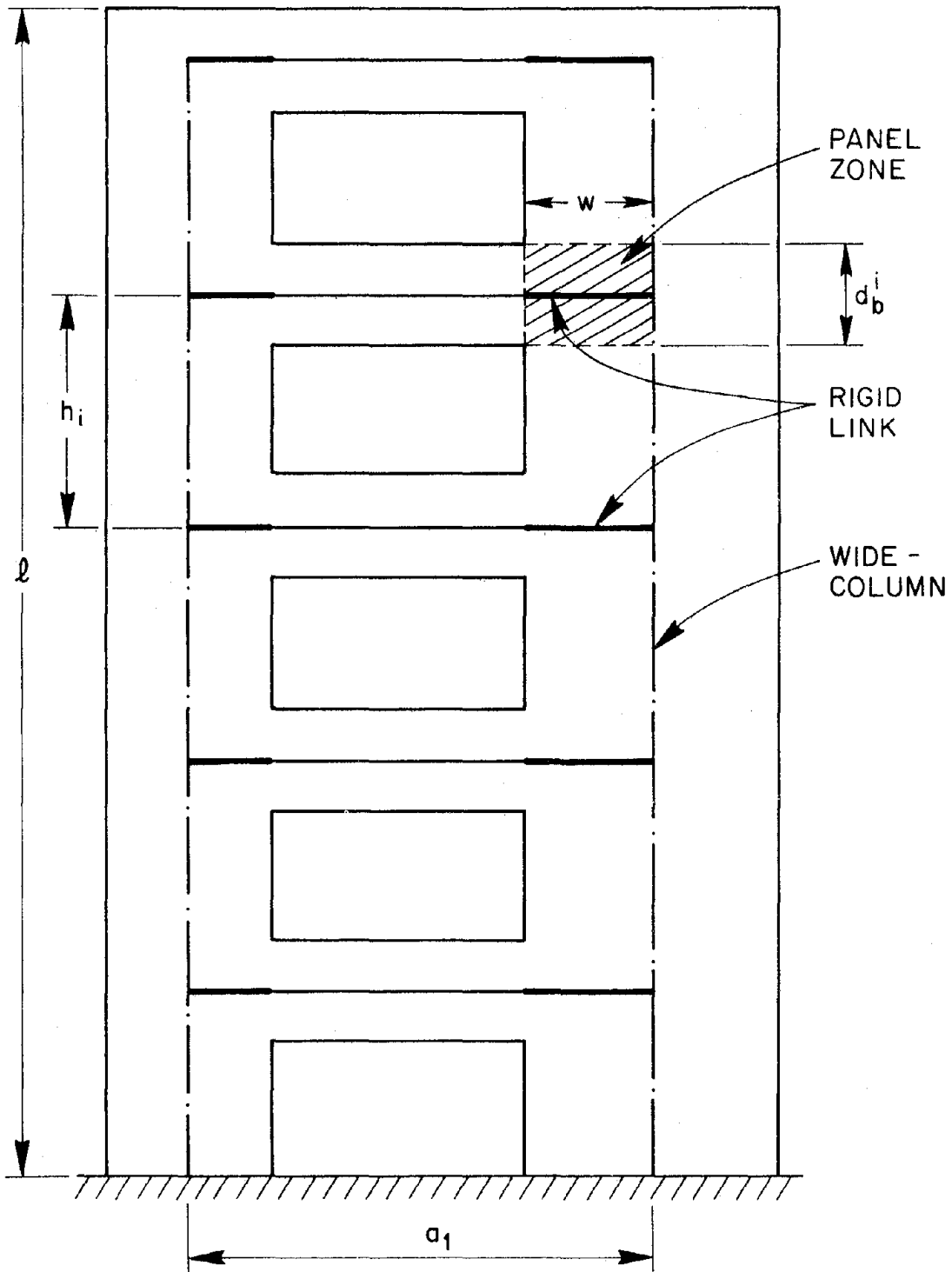
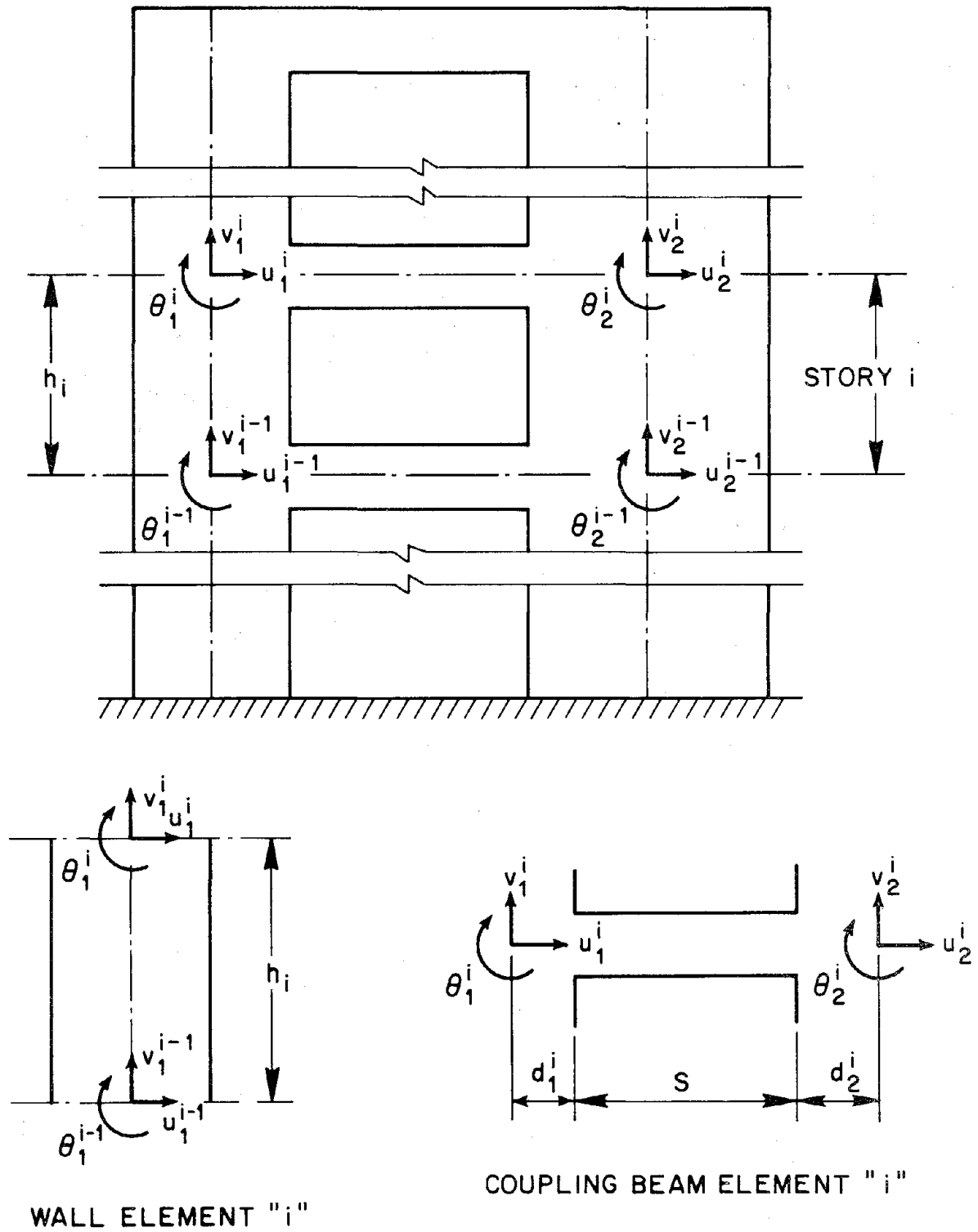


FIG. 2.1 IDEALIZATION OF A COUPLED SHEAR WALL

FIG. 2.2 WALL AND BEAM ELEMENTS OF STORY  $i$

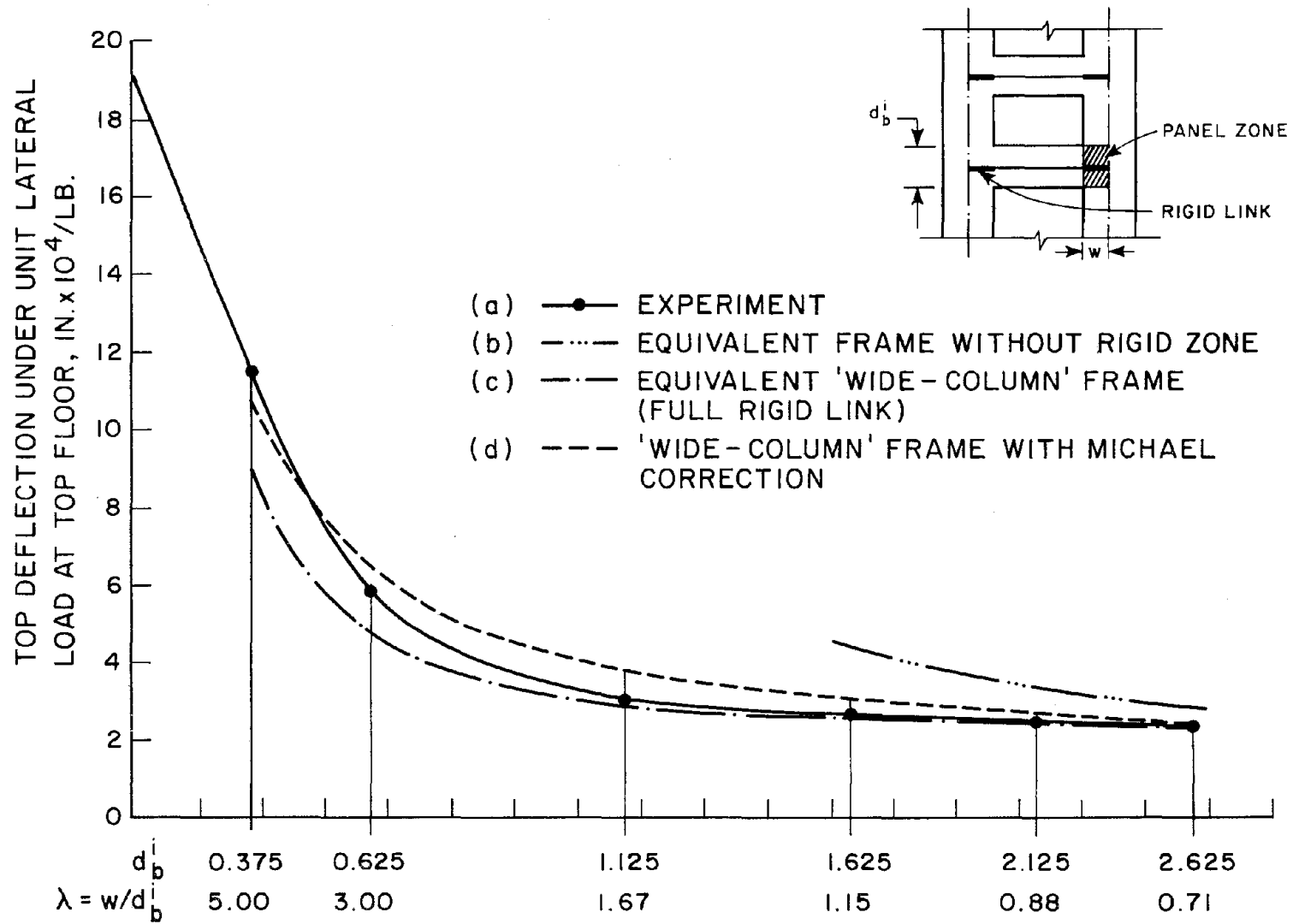


FIG. 2.3 ACCURACY OF VARIOUS ASSUMPTIONS ON LENGTH OF RIGID LINKS [REFS. 15 & 16]

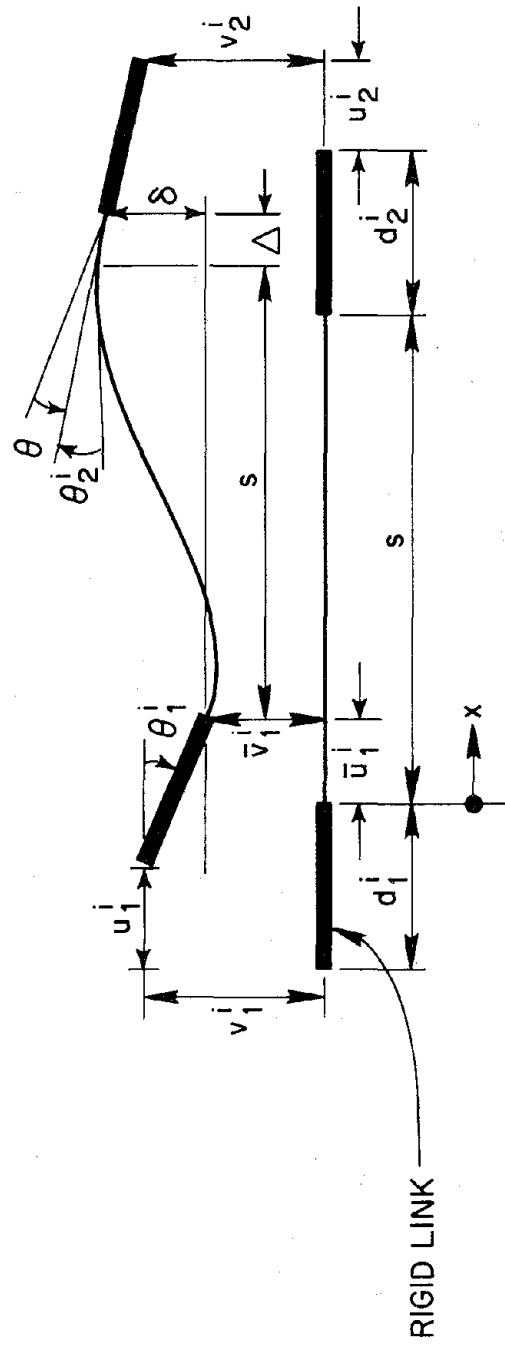
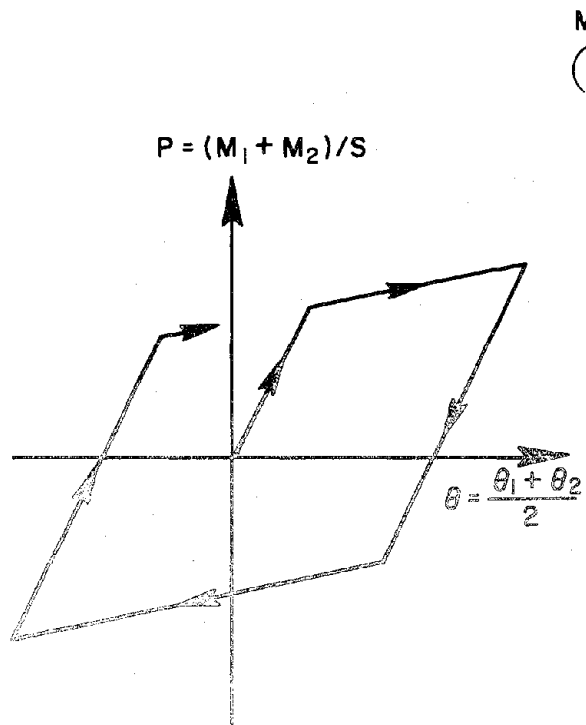
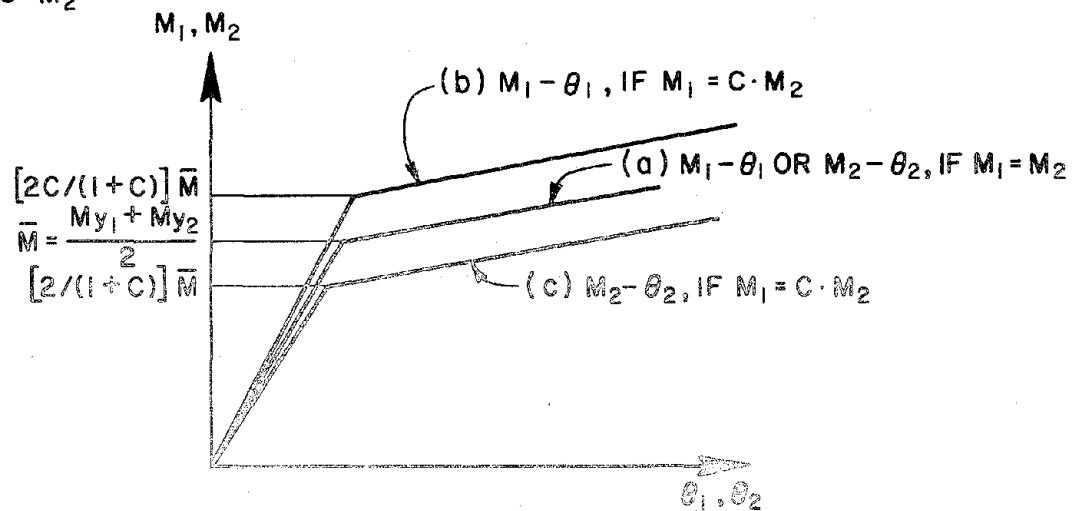
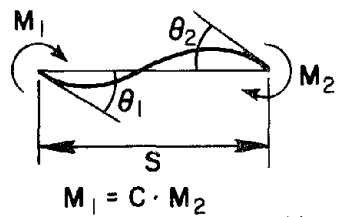


FIG. 2.4 DEFORMATION COORDINATES OF A COUPLING BEAM.





(a) SHEAR-AVERAGE END ROTATION RELATION



(b) INITIAL YIELDING OF MOMENT-END ROTATION CURVES

FIG. 2.6 MECHANICAL MODEL OF COUPLING BEAM

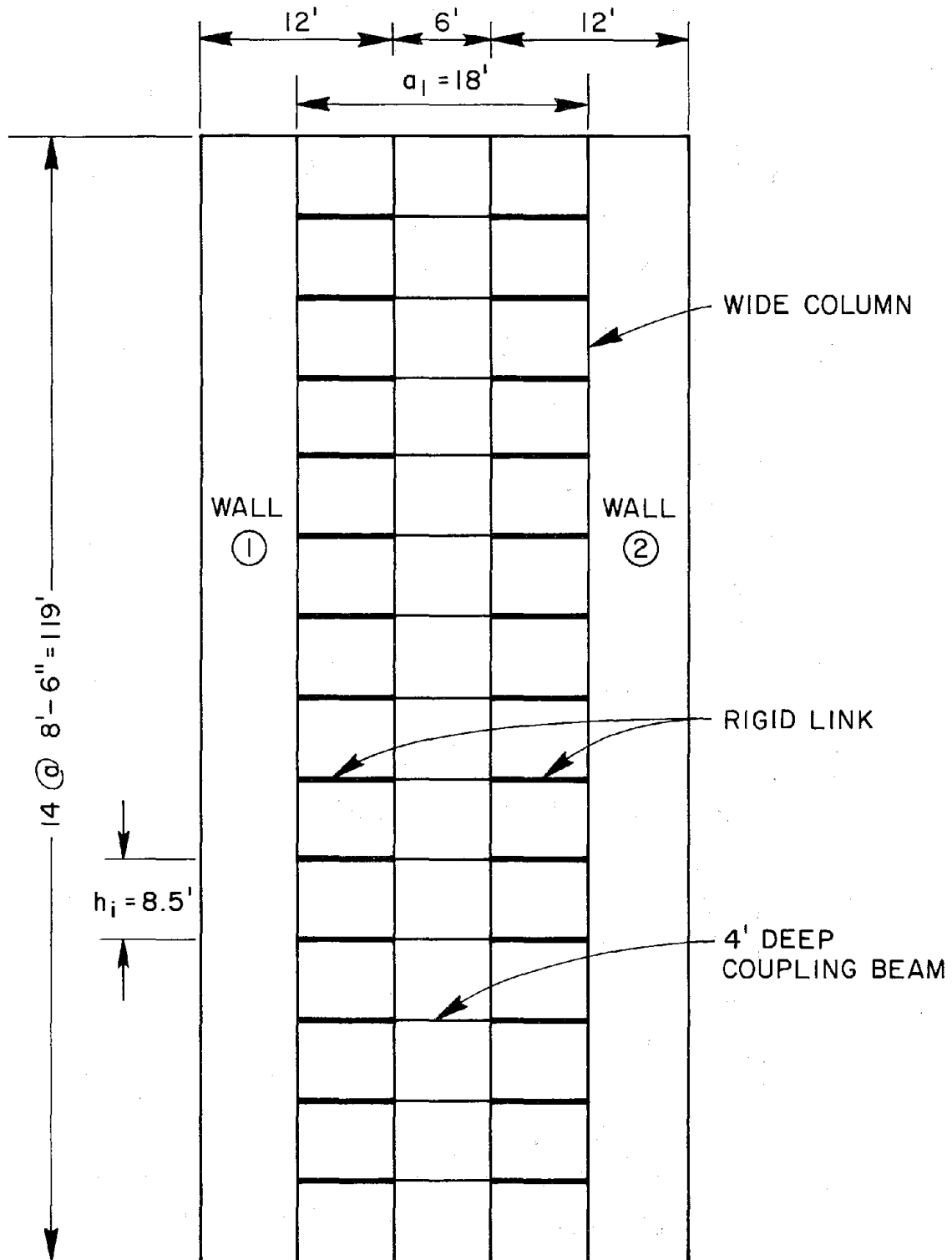
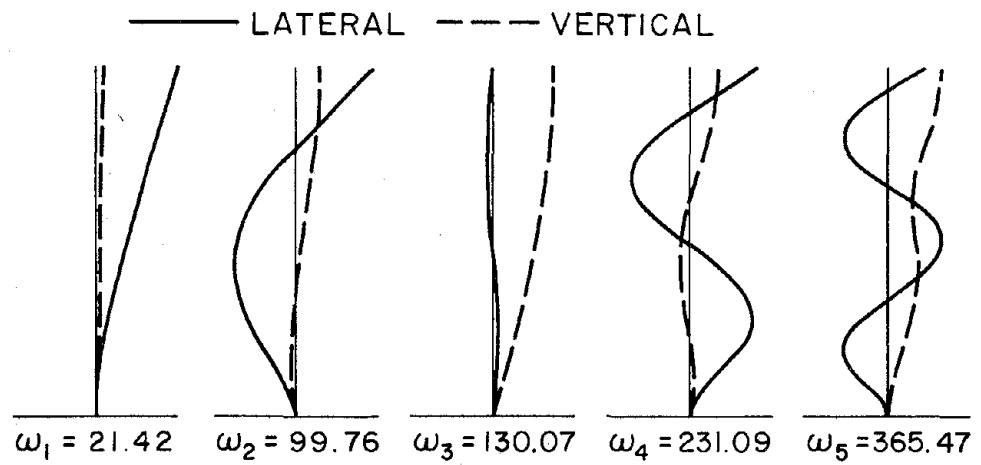
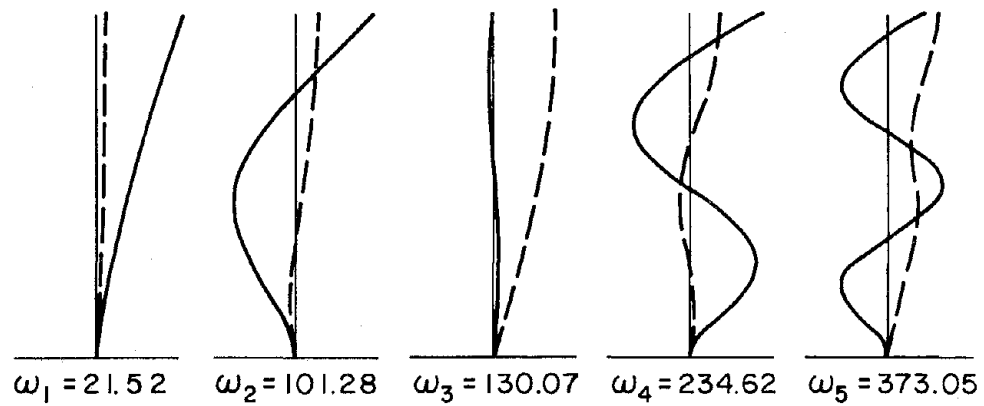


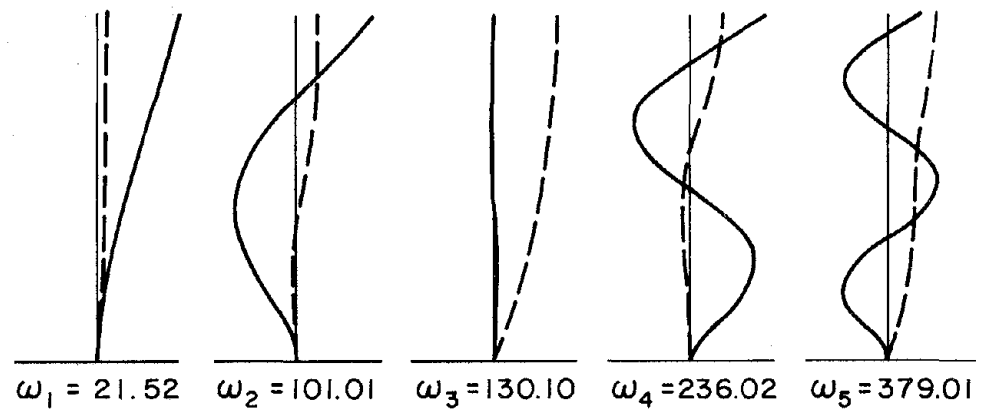
FIG. 3.1 COUPLED SHEAR WALL AND ITS IDEALIZATION



'EXACT' ANALYSIS



ANALYSIS OF  $H_4 V_4$  REDUCED SYSTEM



ANALYSIS OF  $H_6 V_3$  REDUCED SYSTEM

MODE NO. 1

2

3

4

5

FIG. 3.2(A) NATURAL FREQUENCIES AND MODE SHAPES OF VIBRATION

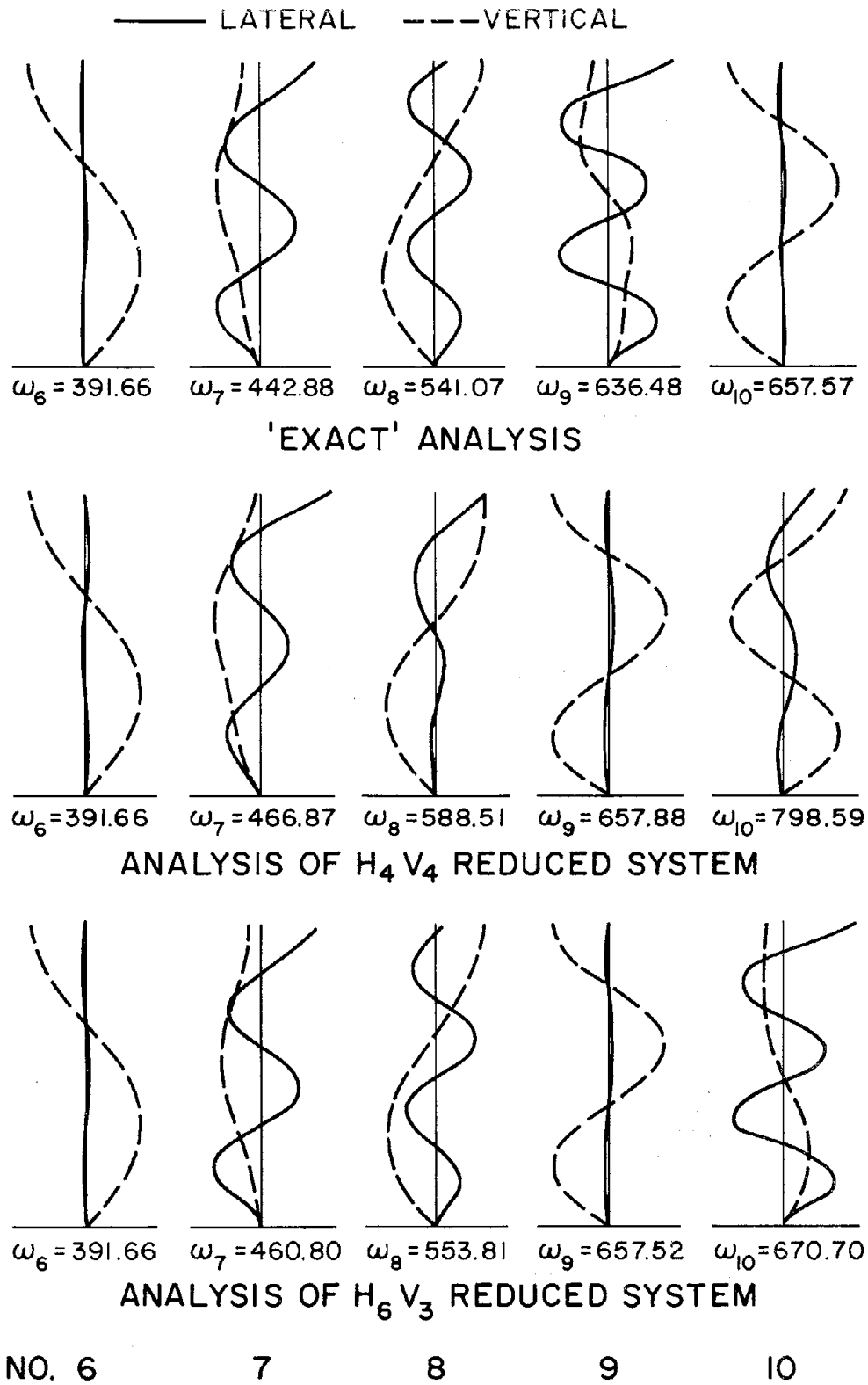


FIG. 3.2(B) NATURAL FREQUENCIES AND MODE SHAPES OF VIBRATION

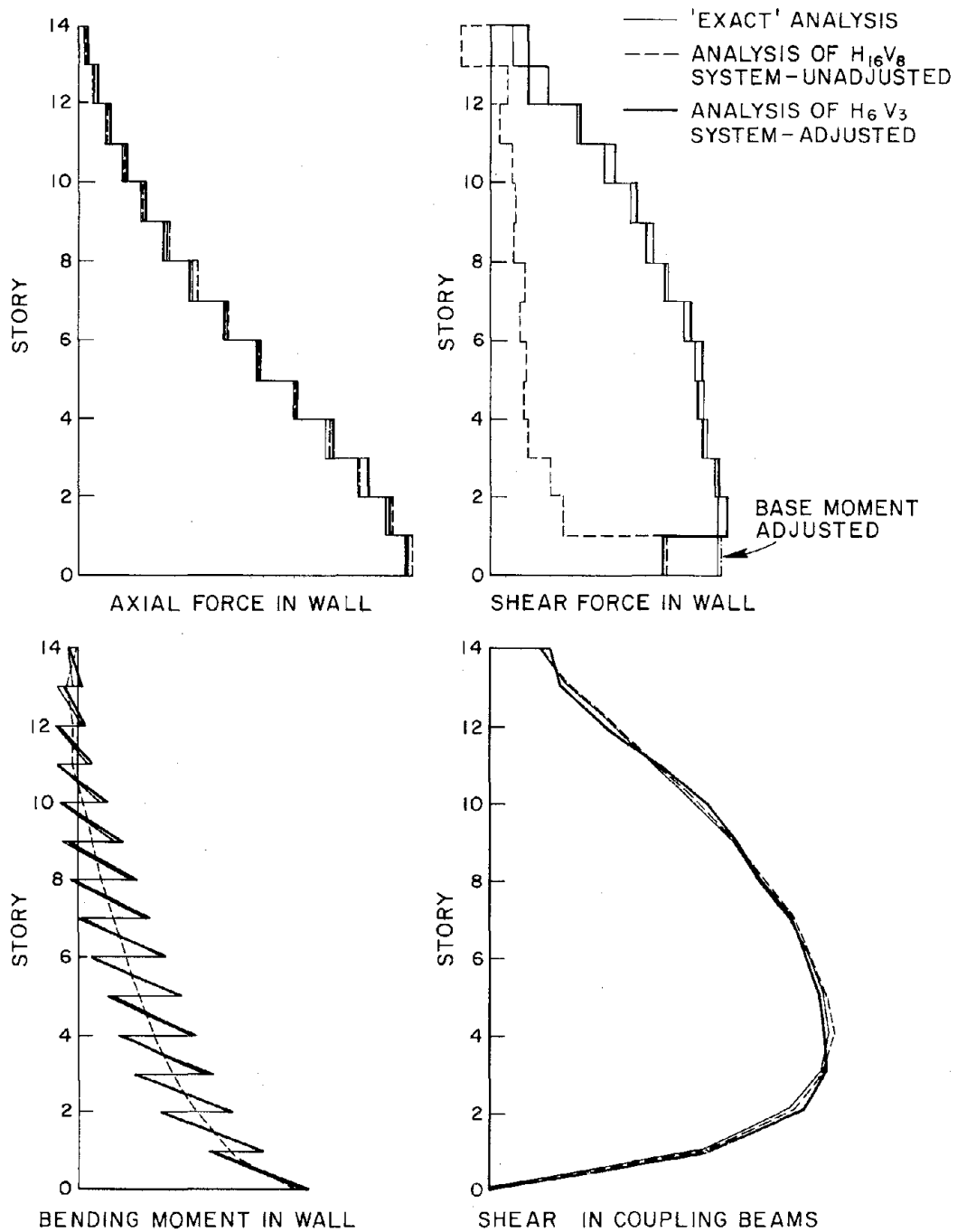
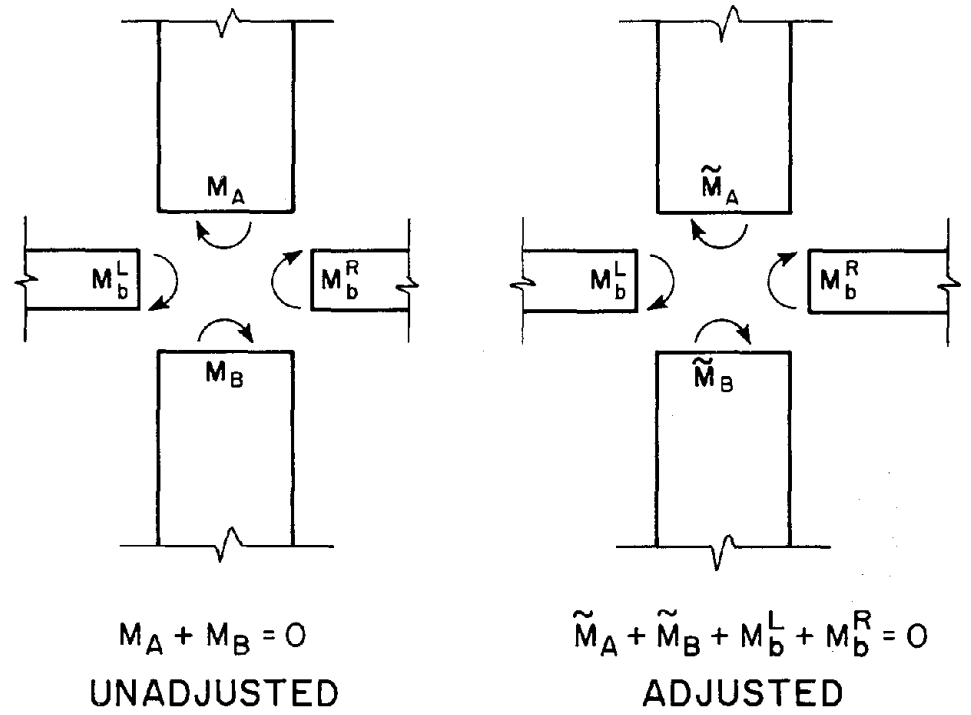
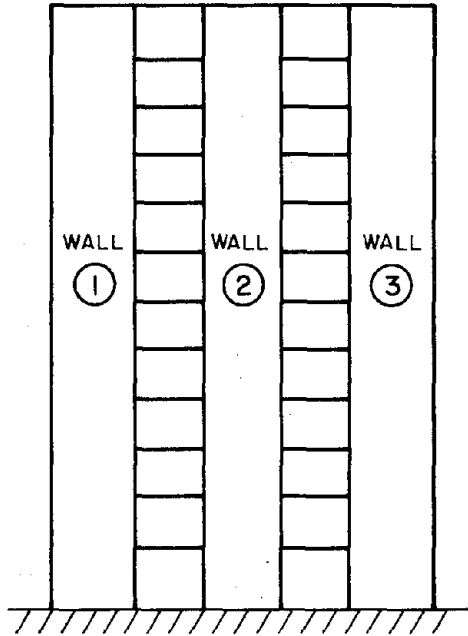


FIG. 3.3 STRESS RESULTANTS IN FIRST MODE OF VIBRATION



ADJUSTMENT :

$$\tilde{M}_A = M_A - \left( \frac{M_b^L + M_b^R}{2} \right)$$

$$\tilde{M}_B = M_B - \left( \frac{M_b^L + M_b^R}{2} \right)$$

FIG. 3.4 ADJUSTMENT OF BENDING MOMENT IN WALL

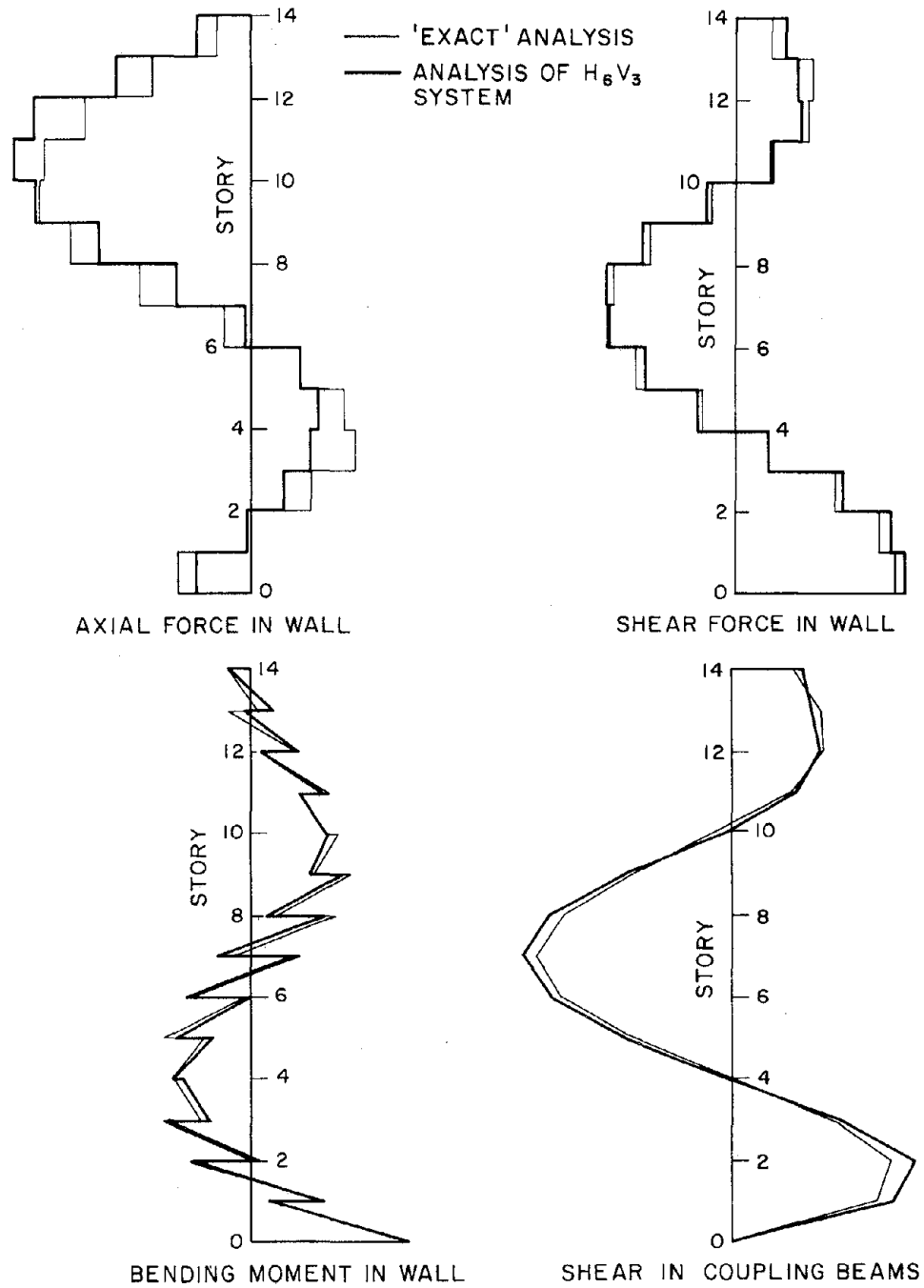


FIG. 3.5 STRESS RESULTANTS IN THIRD MODE OF VIBRATION

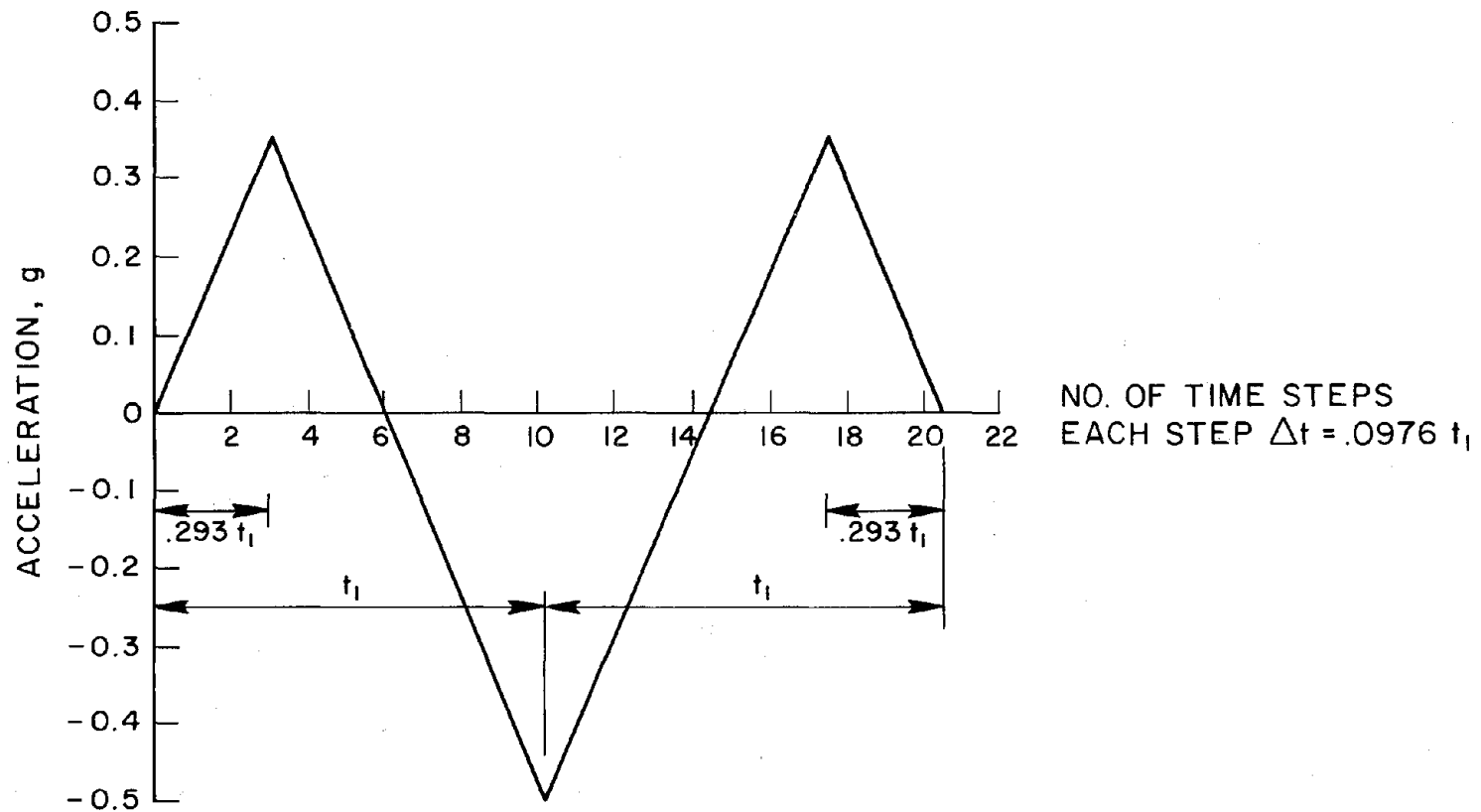


FIG. 3.6 HORIZONTAL COMPONENT OF SIMPLIFIED GROUND ACCELERATION [REF. 30]

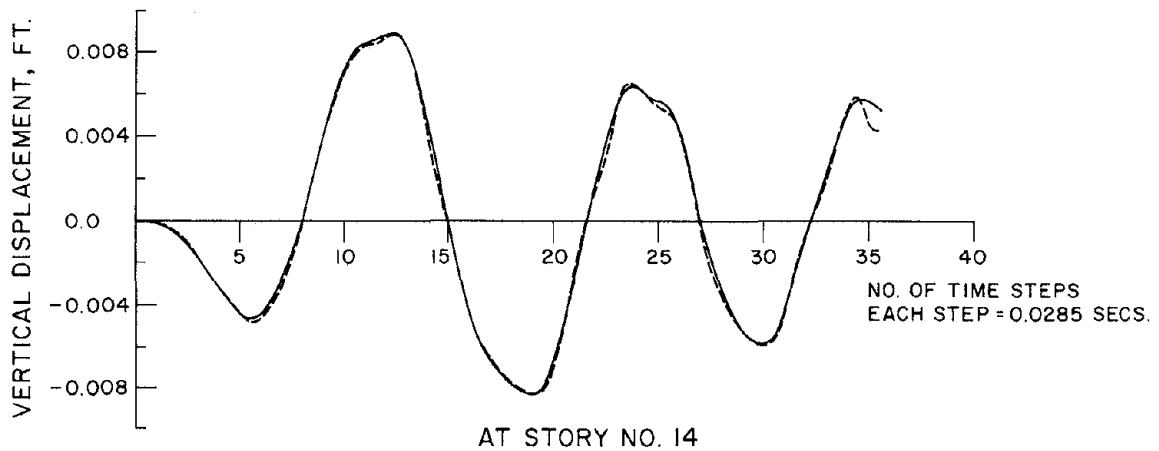
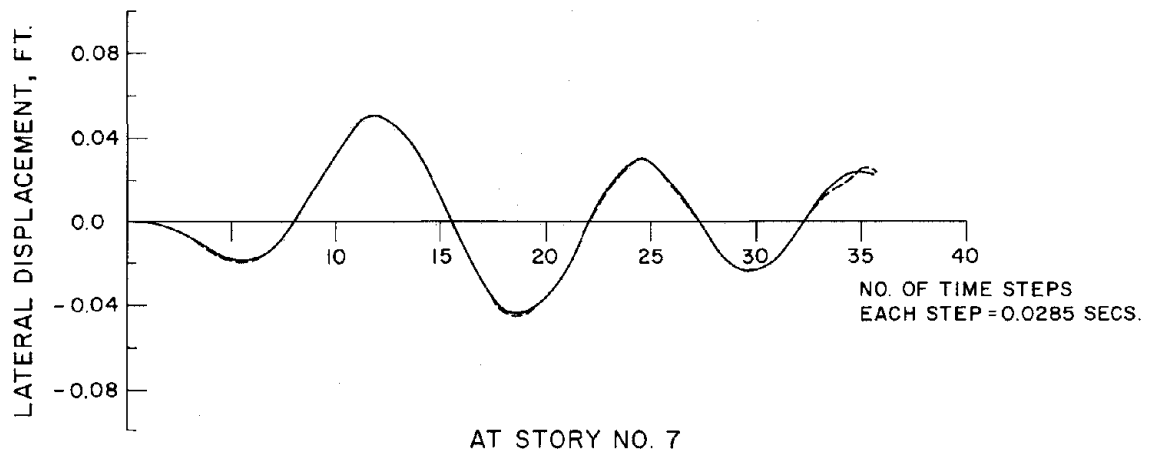
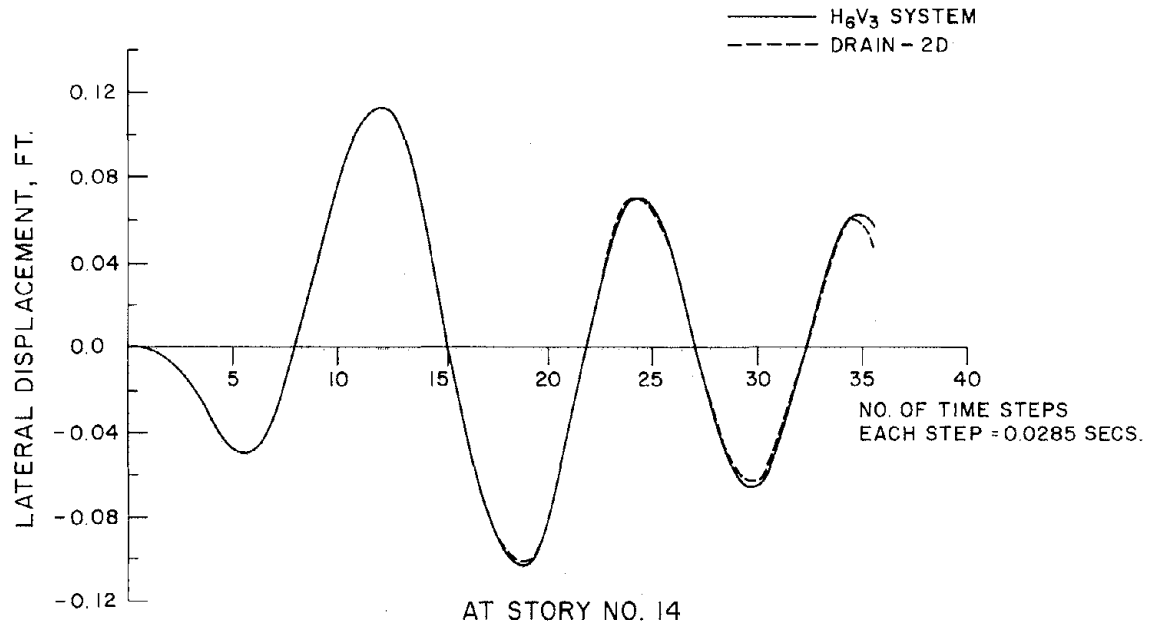


FIG. 3.7 DISPLACEMENT HISTORY OF WALL 1

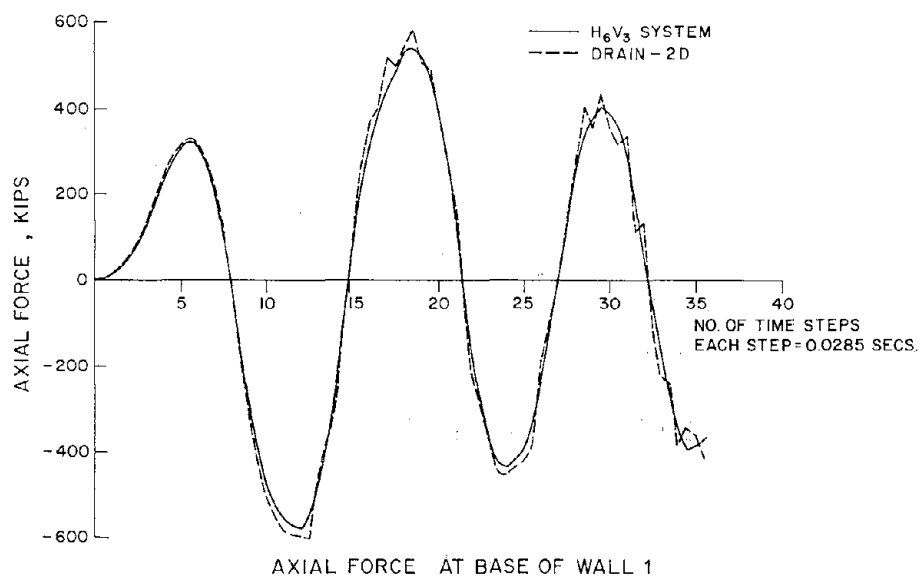
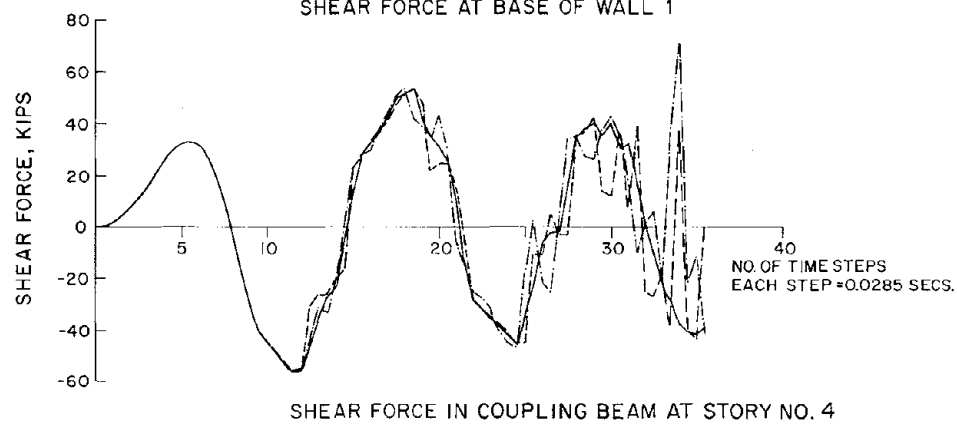
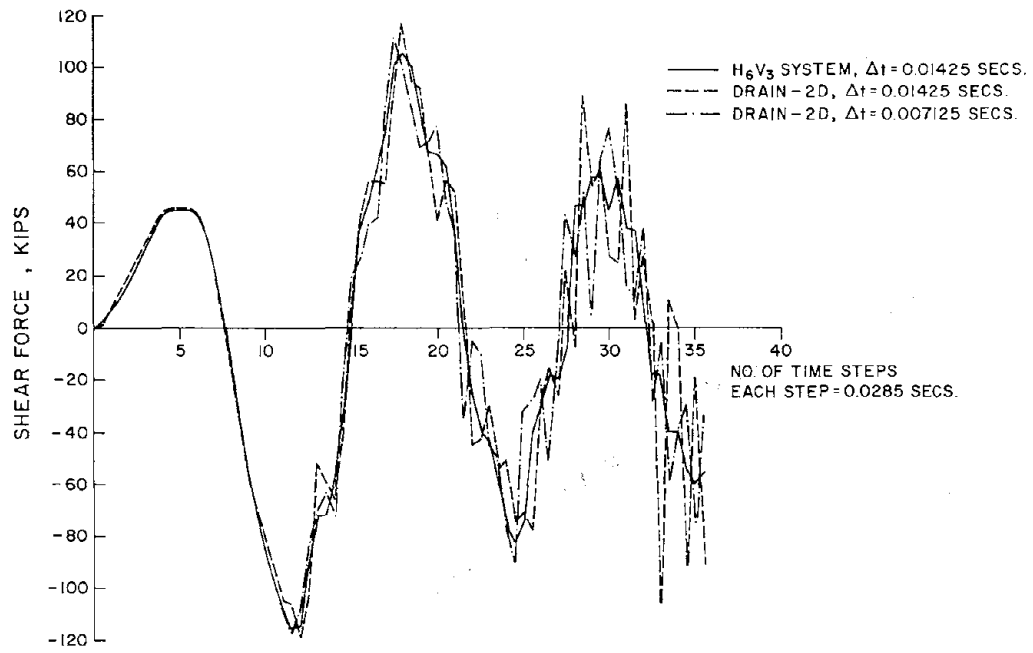


FIG. 3.8 STRESS RESULTANT HISTORY

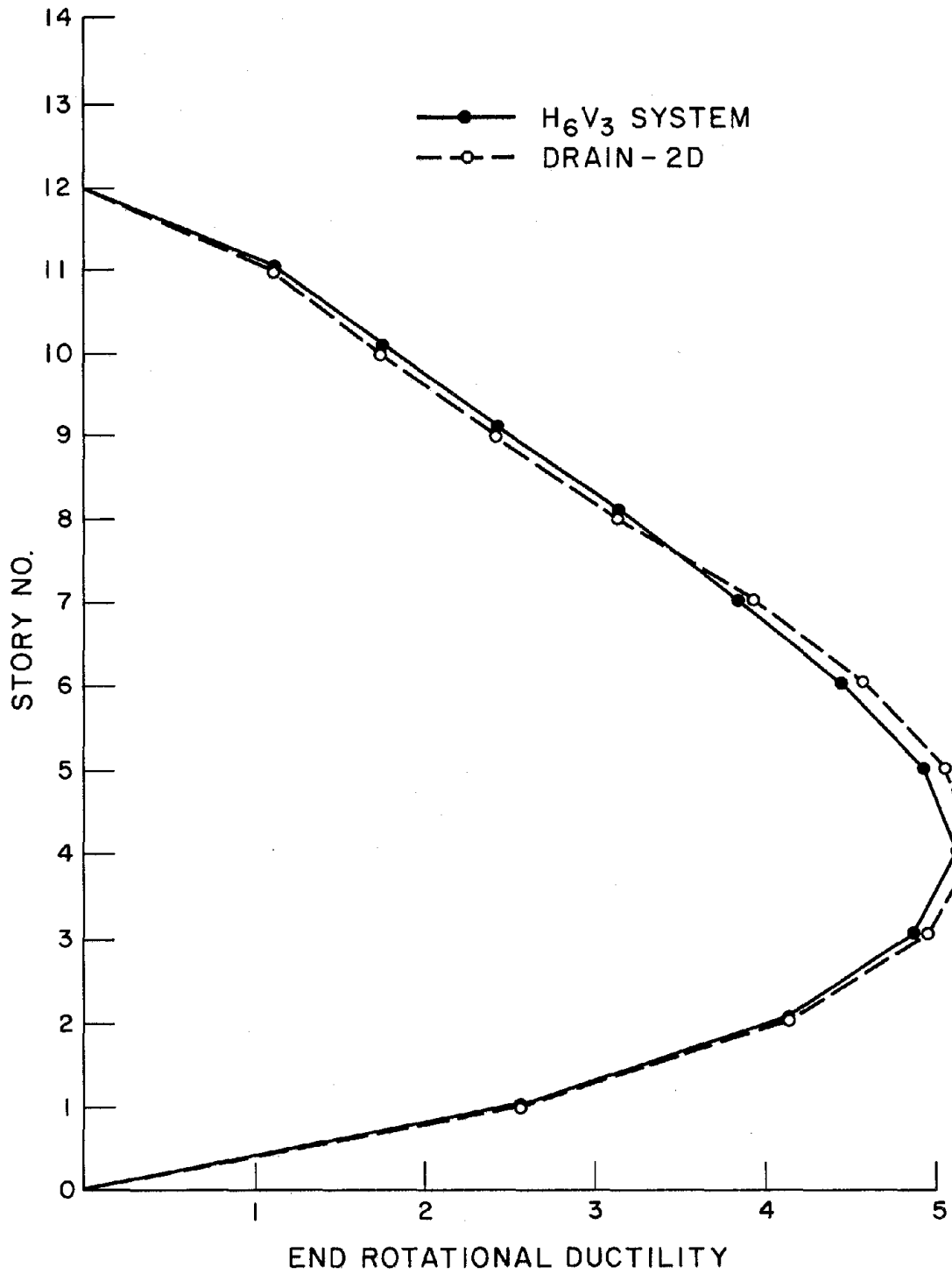


FIG. 3.9 ENVELOPES OF MAXIMUM ROTATIONAL DUCTILITY REQUIREMENTS OF COUPLING BEAMS

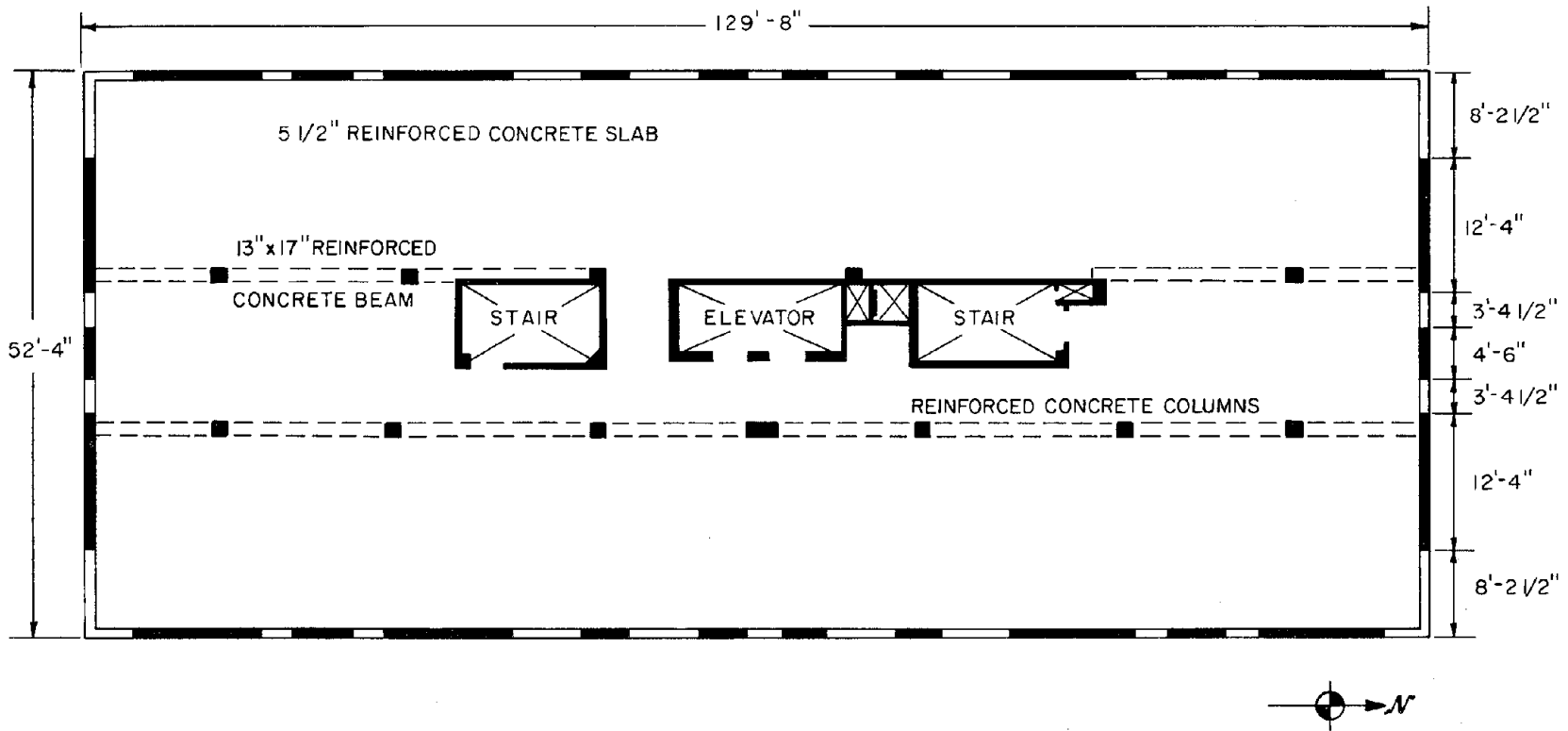


FIG. 4.1 MCKINLEY BUILDING: TYPICAL FLOOR PLAN

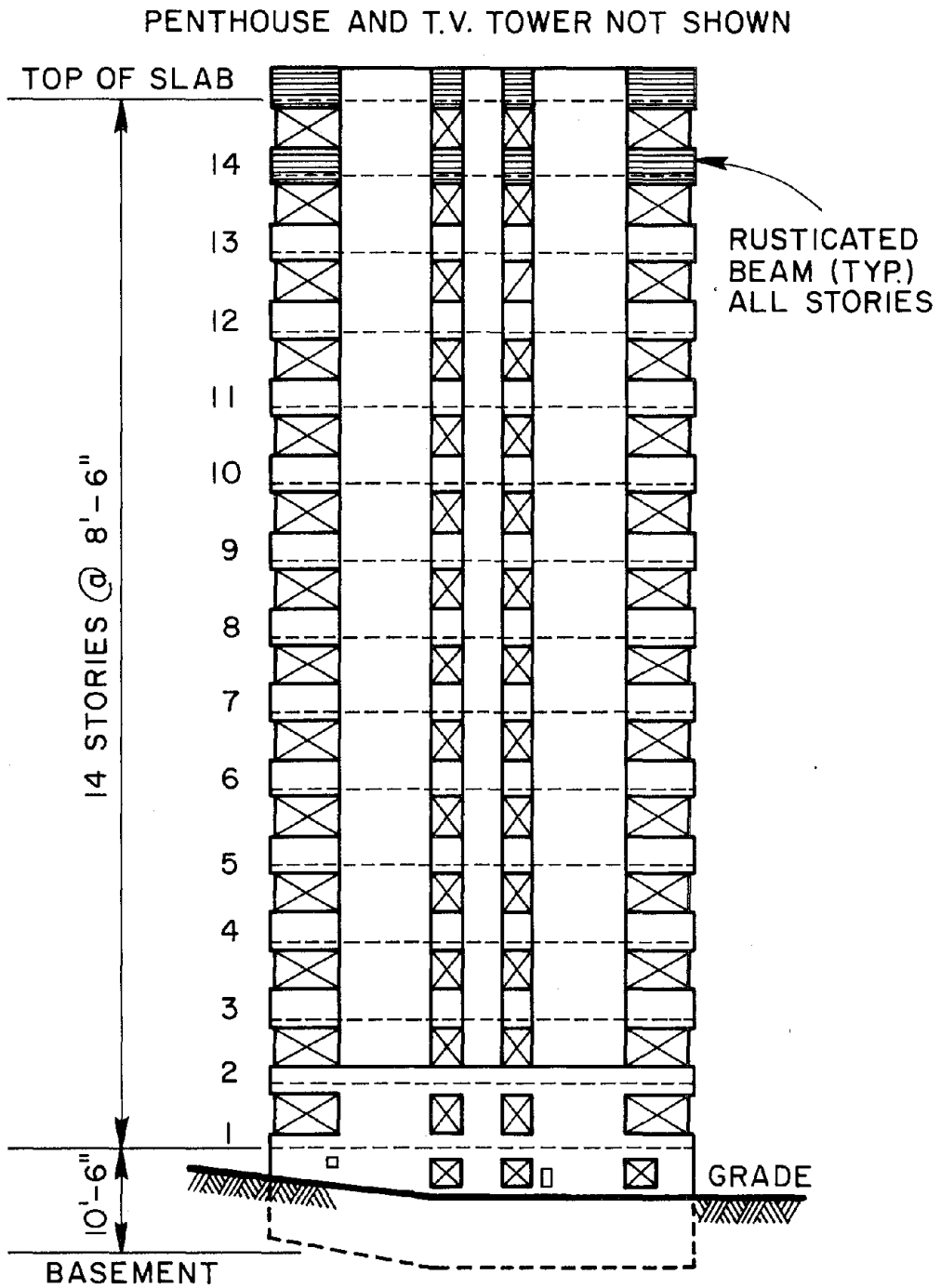
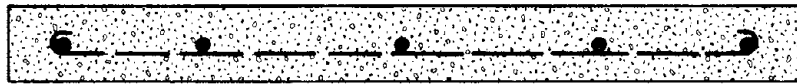
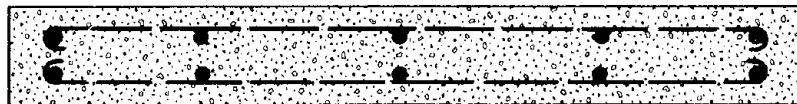


FIG. 4.2 MCKINLEY BUILDING: NORTH ELEVATION

STORY	WALL THICKNESS	REINFORCING DETAILS		
		TYPE	HORIZONTAL	VERTICAL
9 - 14	8"	X	#5 @ 15"	#5 @ 15"
8	8"	X	#5 @ 15"	#5 @ 12"
5 - 7	10"	X	#5 @ 12"	#5 @ 12"
2 - 4	10"	Y	#5 @ 18"	#5 @ 18"
1	12"	Y	#5 @ 18"	#5 @ 18"



TYPE X SINGLE CURTAIN OF STEEL



TYPE Y DOUBLE CURTAIN OF STEEL

FIG. 4.3 MCKINLEY BUILDING: SCHEDULE OF REINFORCING IN WALLS AT NORTH END

STORY	THICKNESS $t$	REINFORCING DETAILS		
		TYPE	HORIZONTAL	WEB
9 - 14	8"	A	#5 @ 15"	#5 @ 15"
8	8"	A	#5 @ 15"	#5 @ 12"
5 - 7	10"	A	#5 @ 12"	#5 @ 12"
3 - 4	10"	B	#5 @ 18"	#5 @ 18"
1 - 2	12"	B	#5 @ 18"	#5 @ 18"

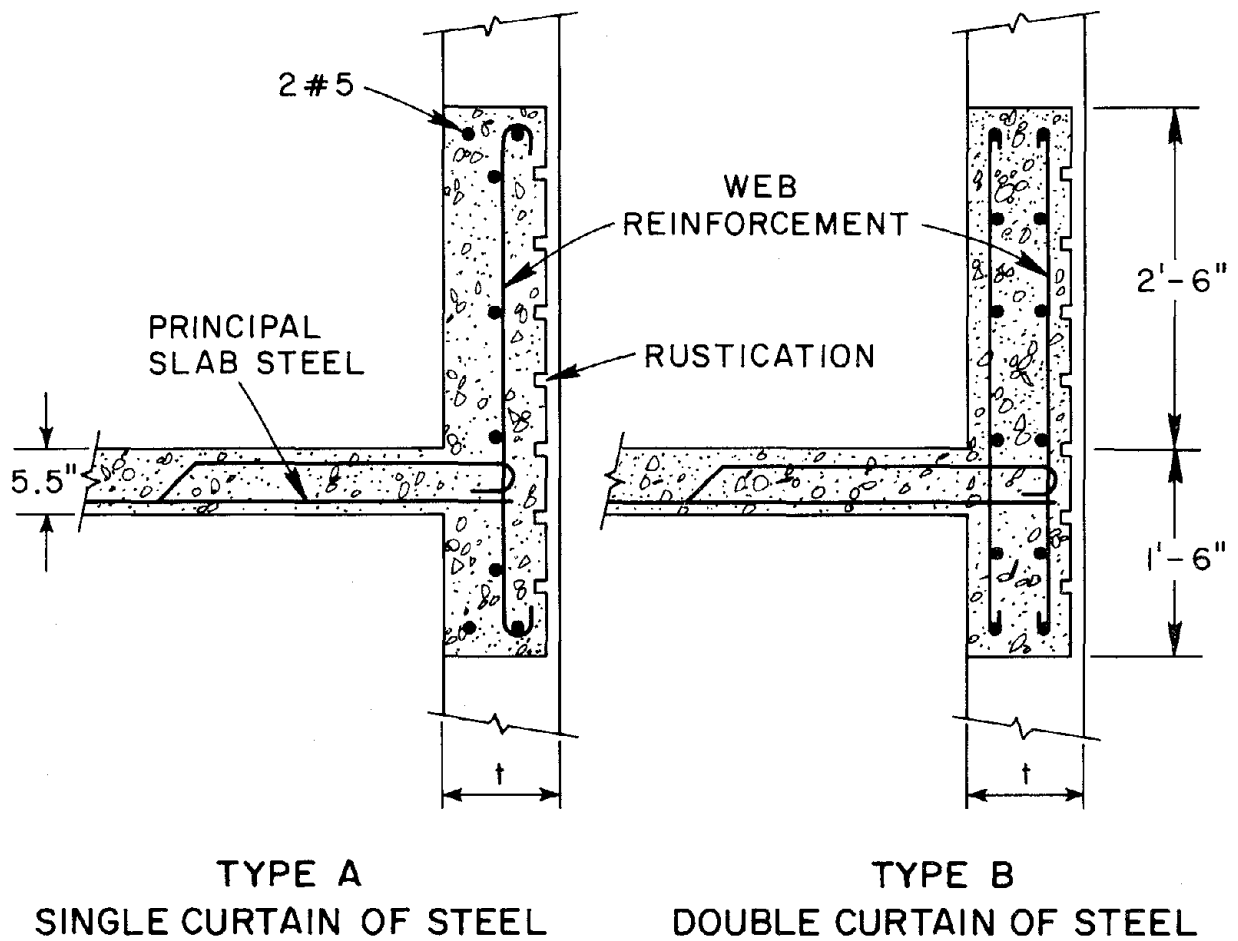


FIG. 4.4 MCKINLEY BUILDING: SECTIONAL DETAILS OF COUPLING BEAMS



FIG. 4.5 MCKINLEY BUILDING: EARTHQUAKE DAMAGE IN NORTH END WALL

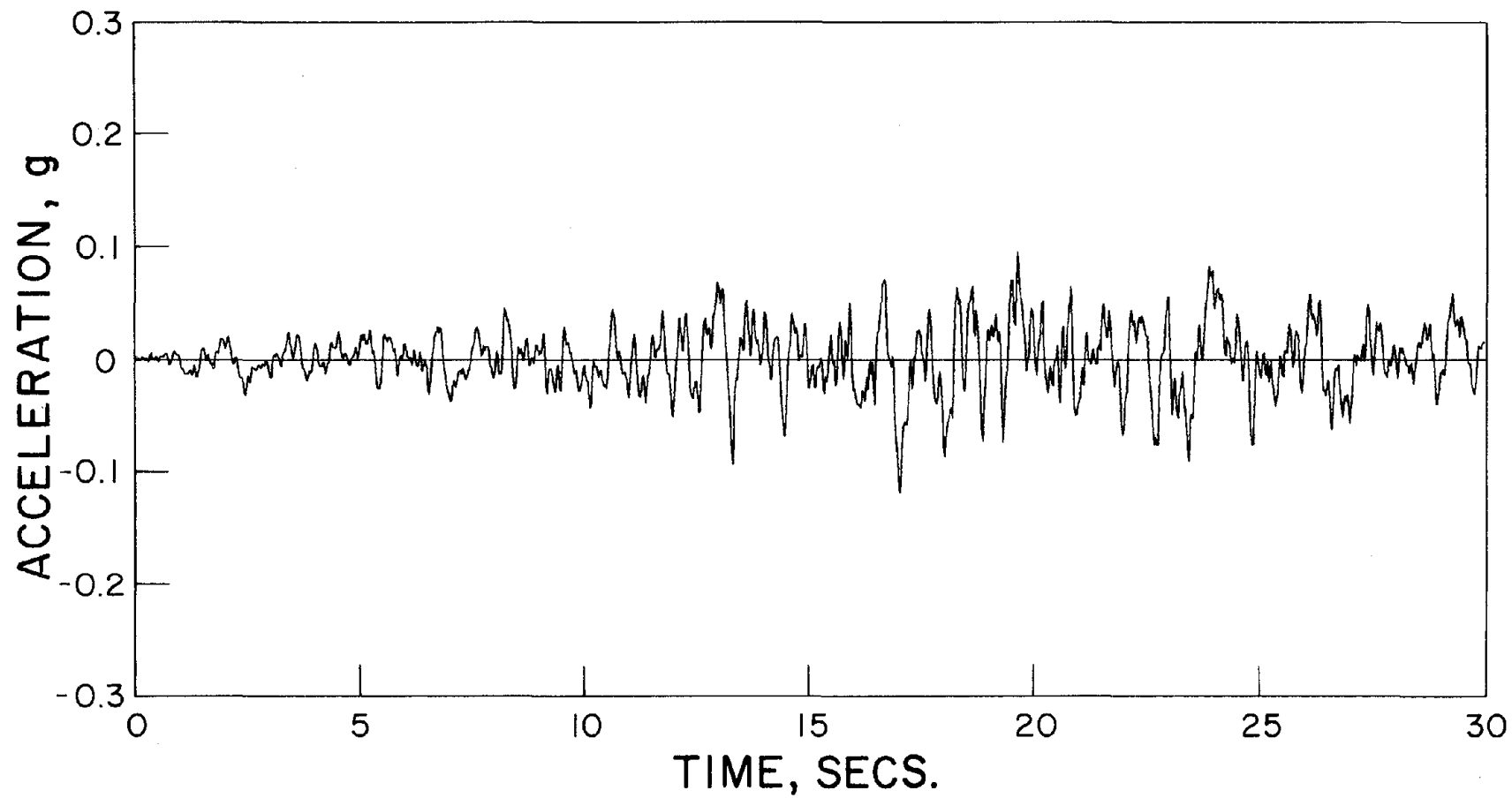


FIG. 4.6 HORIZONTAL COMPONENT OF SIMULATED ALASKAN GROUND MOTION, 1964 [REF. 13]

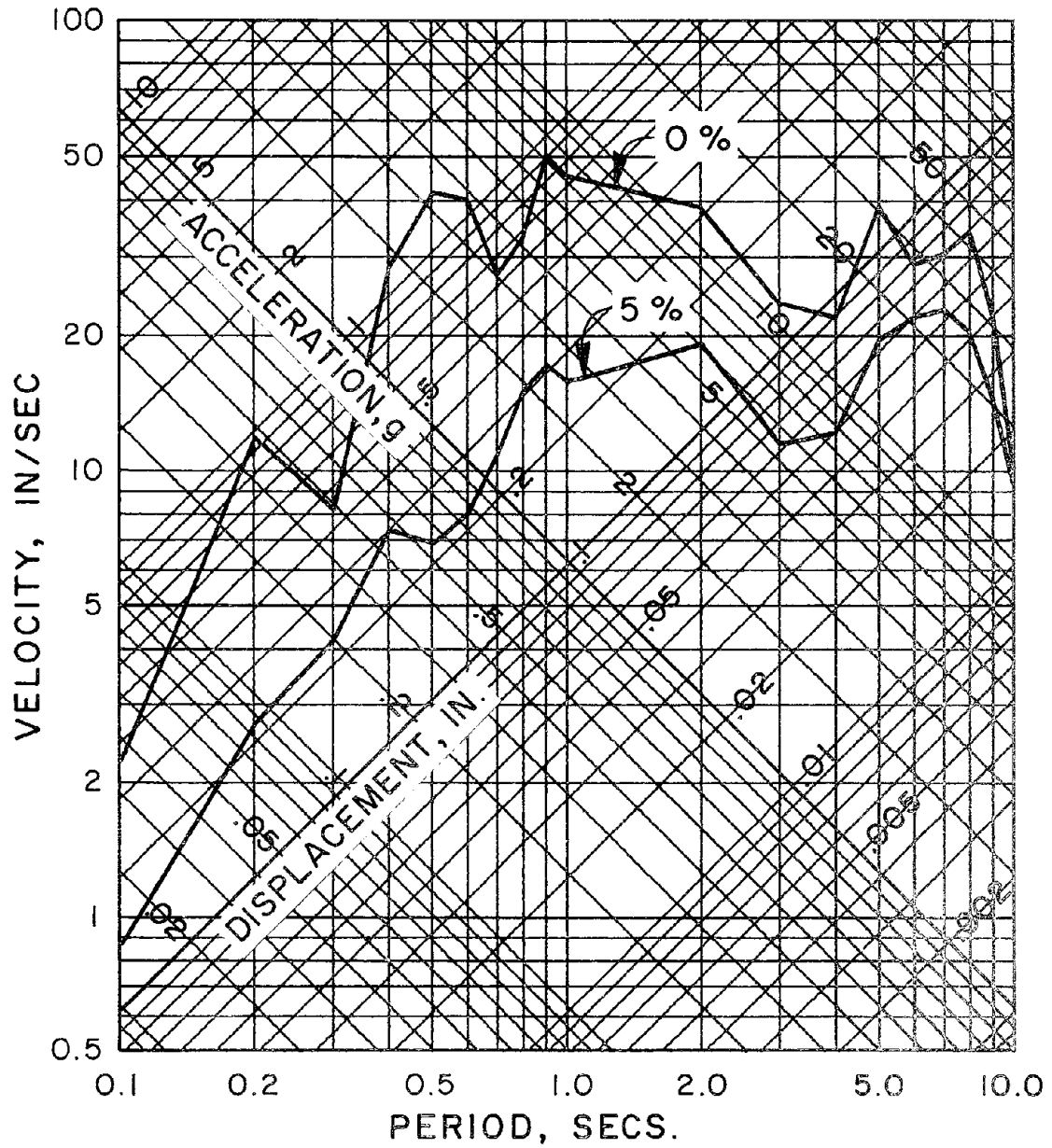


FIG. 4.7 RESPONSE SPECTRUM FOR GROUND MOTION OF FIG. 4.6

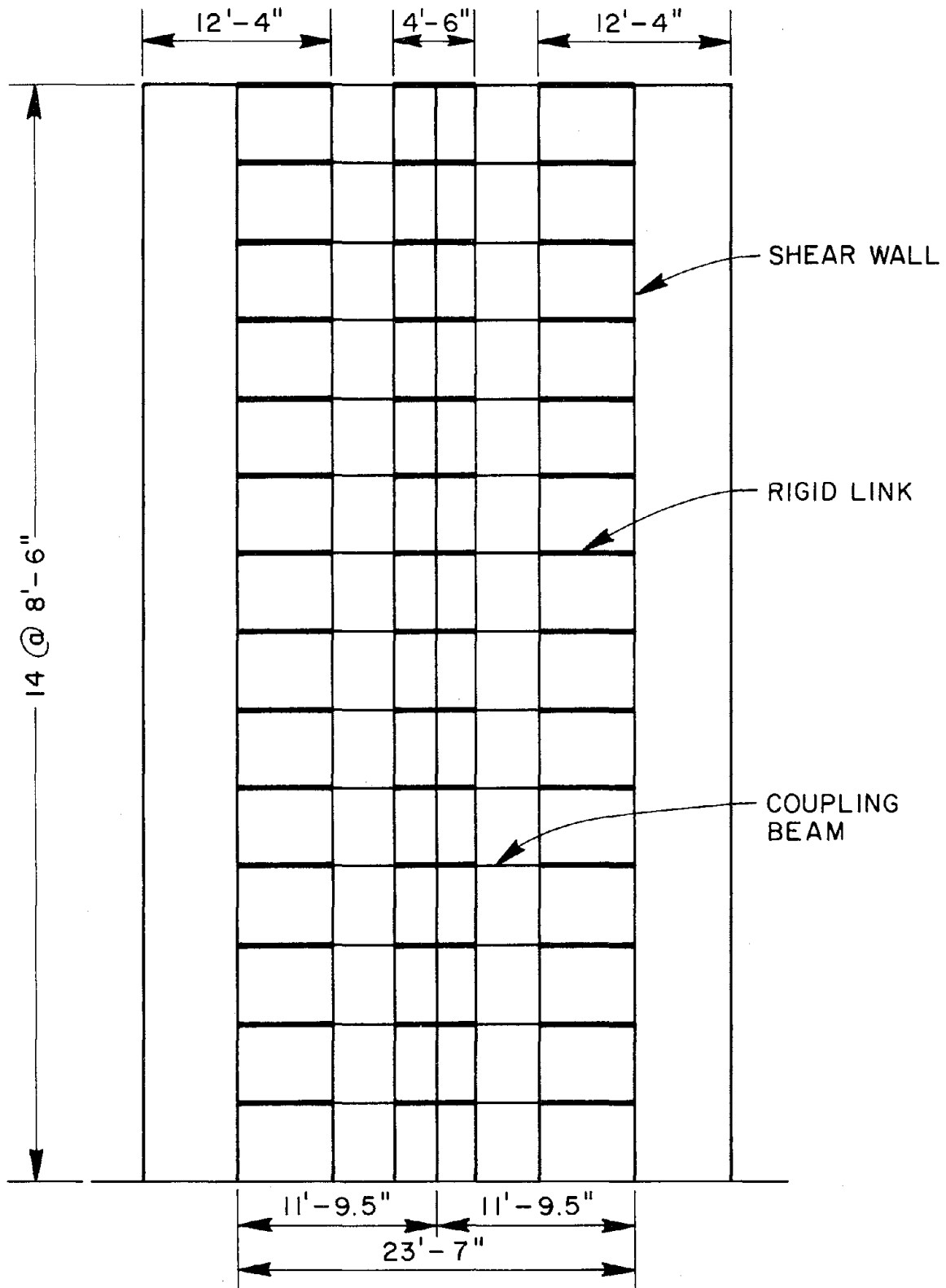


FIG. 4.8 MCKINLEY BUILDING: STRUCTURAL IDEALIZATION OF NORTH END WALL

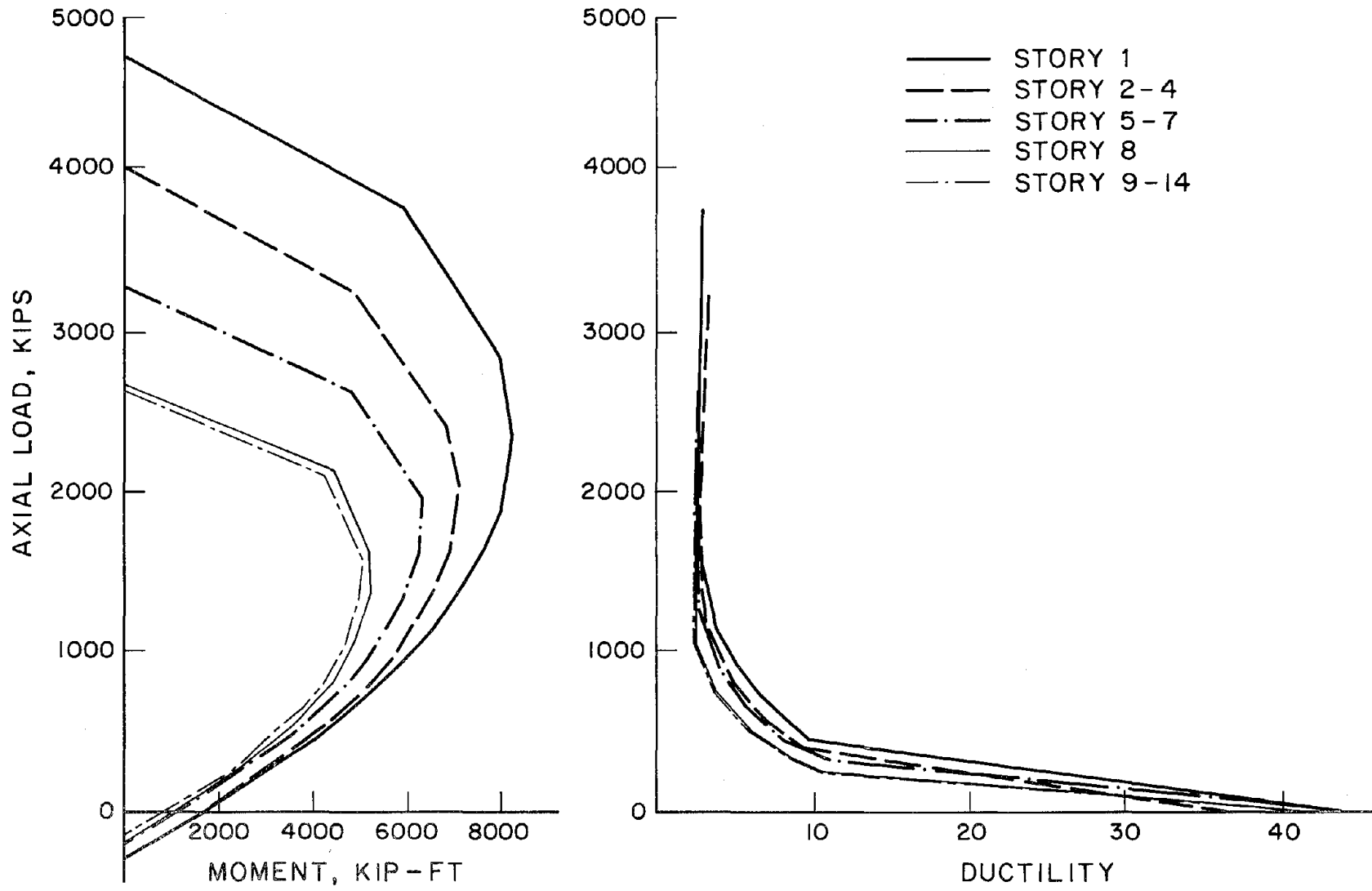


FIG. 4.9 MCKINLEY BUILDING: STRENGTH AND DUCTILITY OF END WALL PIERS

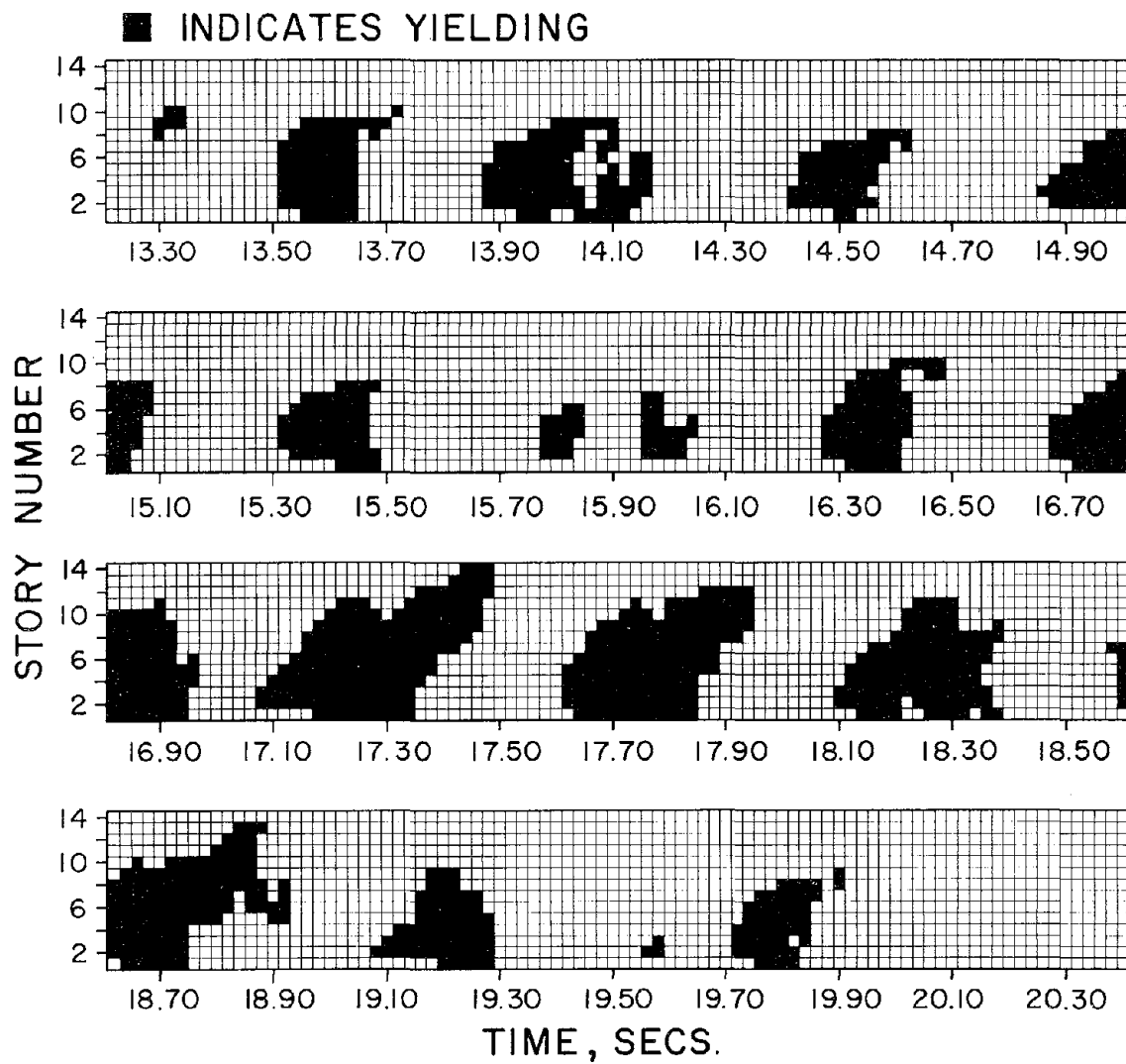


FIG. 4.10 MCKINLEY BUILDING: YIELDING HISTORY OF COUPLING BEAMS

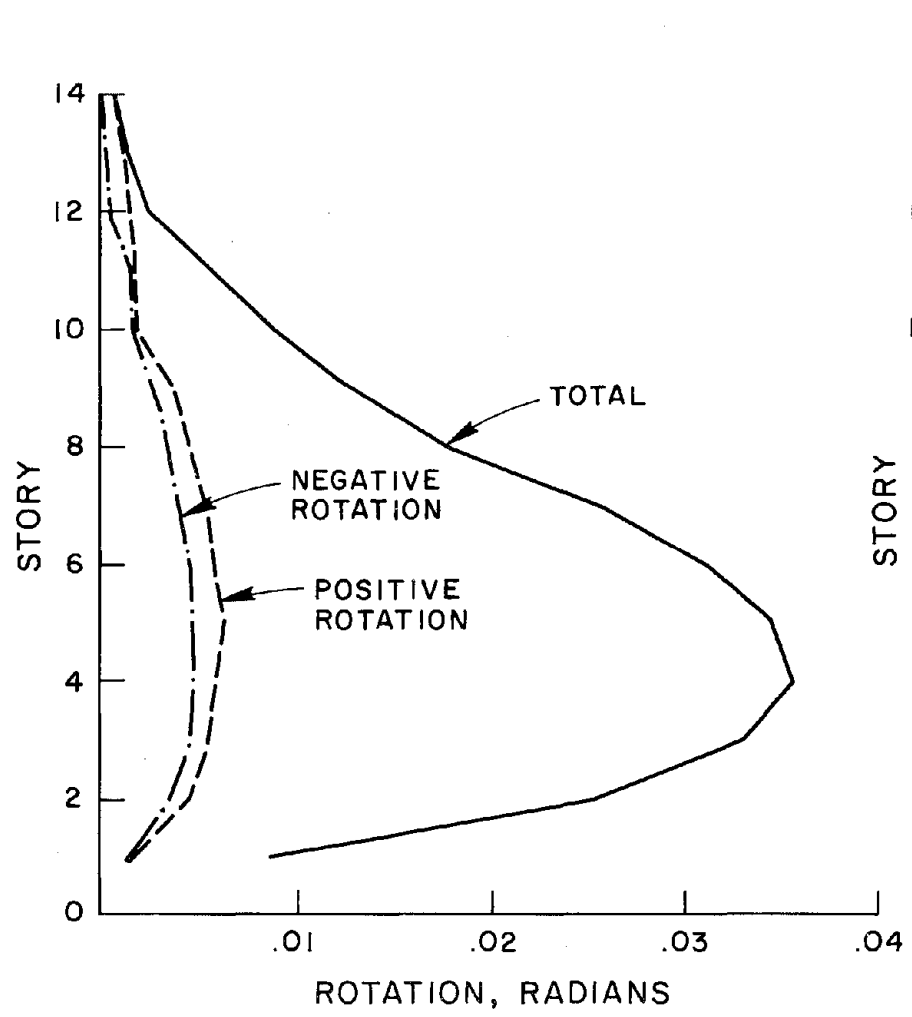


FIG. 4.11 PLASTIC END ROTATION IN COUPLING BEAMS OF MCKINLEY BUILDING

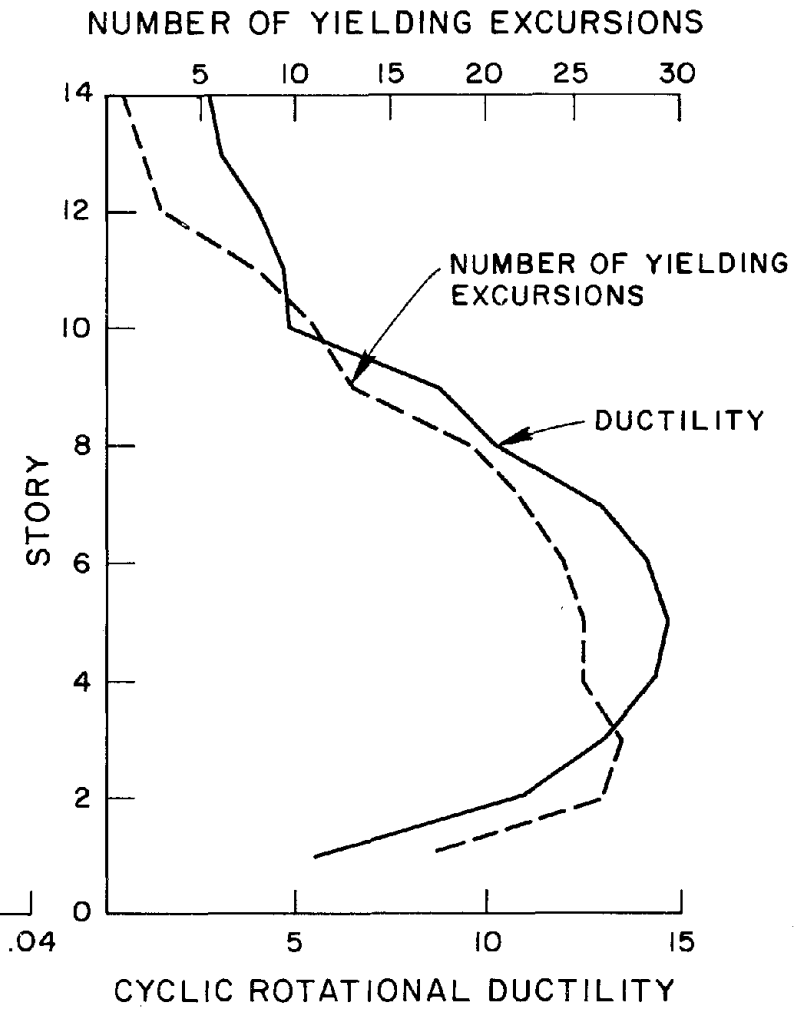


FIG. 4.12 CYCLIC ROTATIONAL DUCTILITY REQUIREMENTS AND NUMBER OF YIELDING EXCURSIONS OF COUPLING BEAMS OF MCKINLEY BUILDING

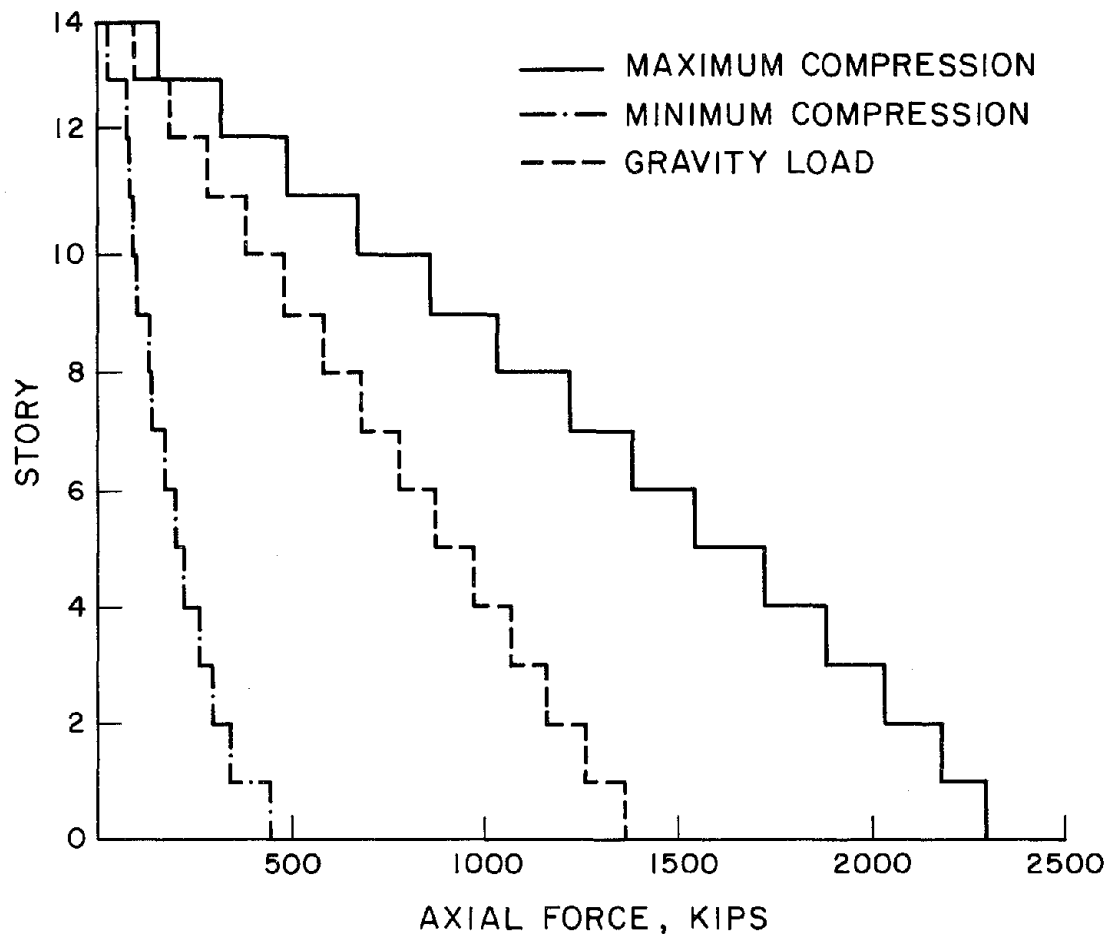


FIG. 4.13 MCKINLEY BUILDING: ENVELOPES OF AXIAL FORCES IN AN END WALL

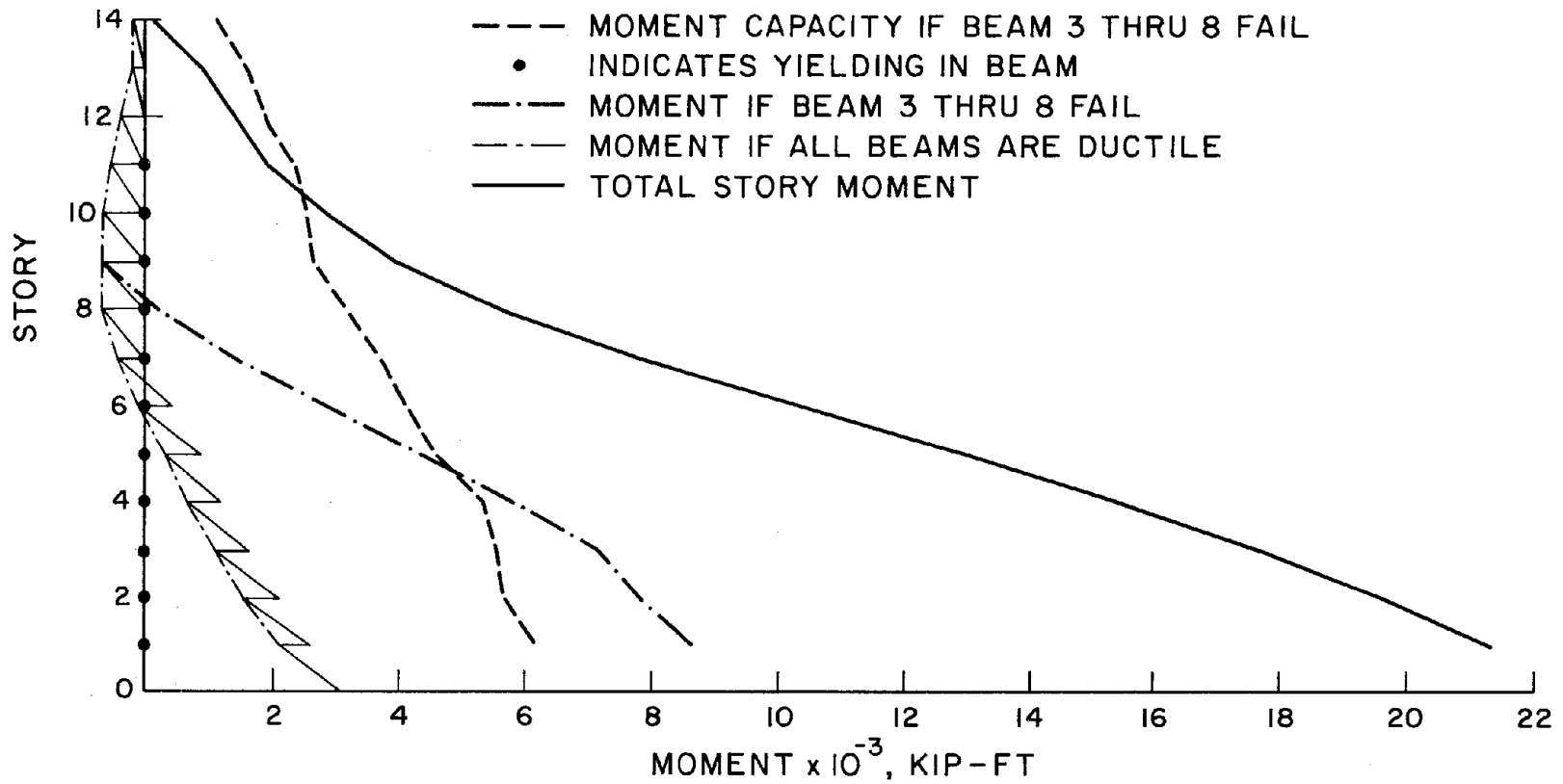


FIG. 4.14 DISTRIBUTIONS OF MOMENT IN AN END PIER AT TIME = 16.90 SECS.



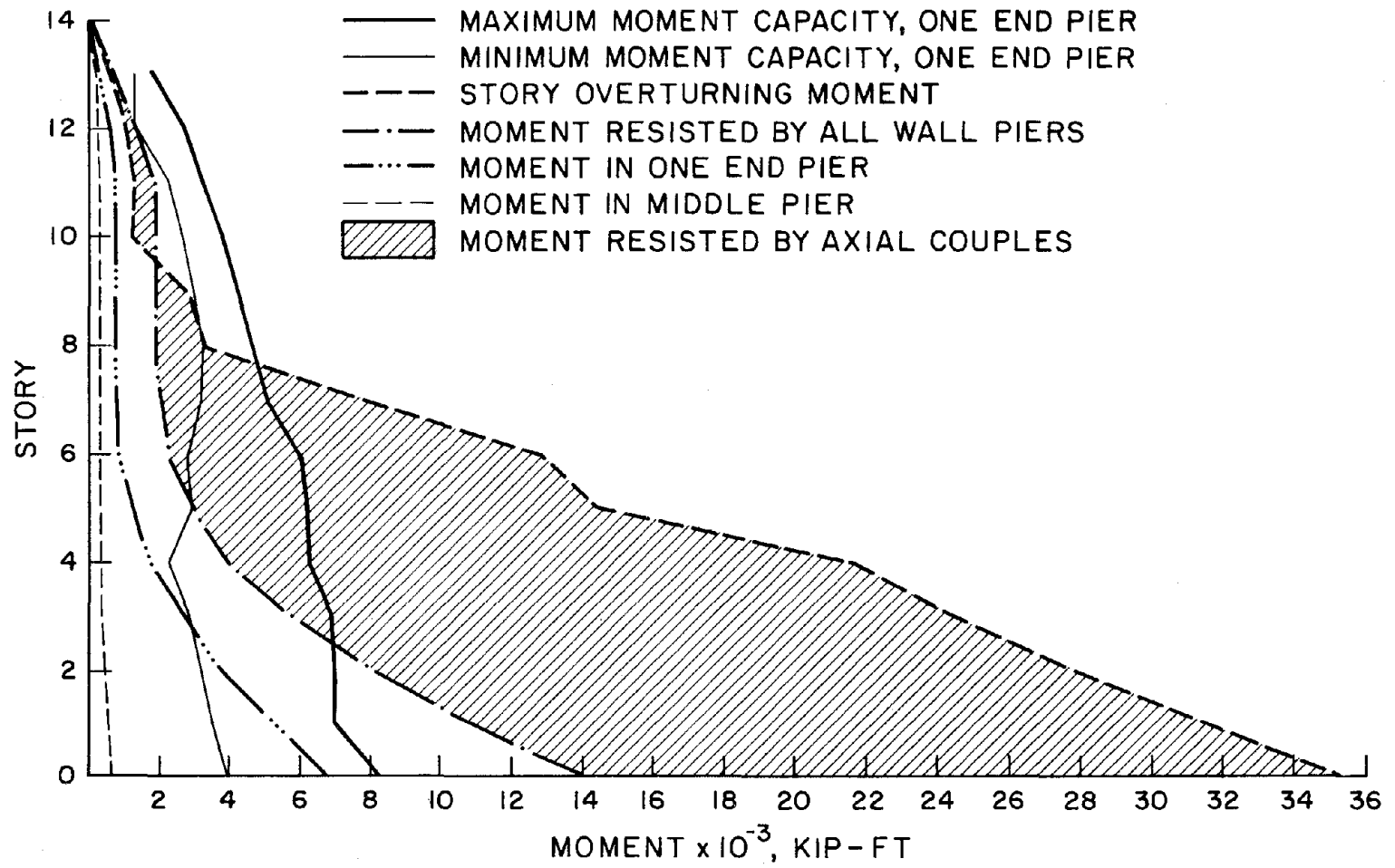


FIG. 4.16 ENVELOPES OF WALL BENDING MOMENT AND STORY OVERTURNING MOMENT

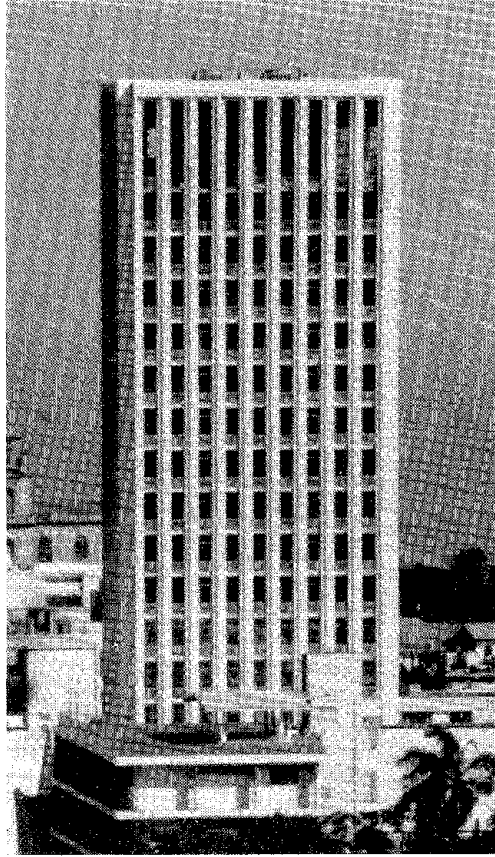
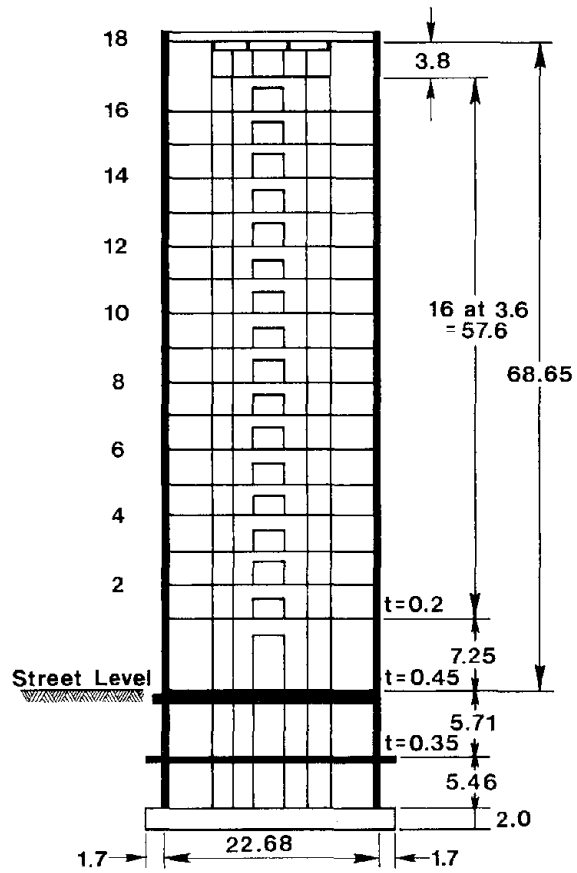
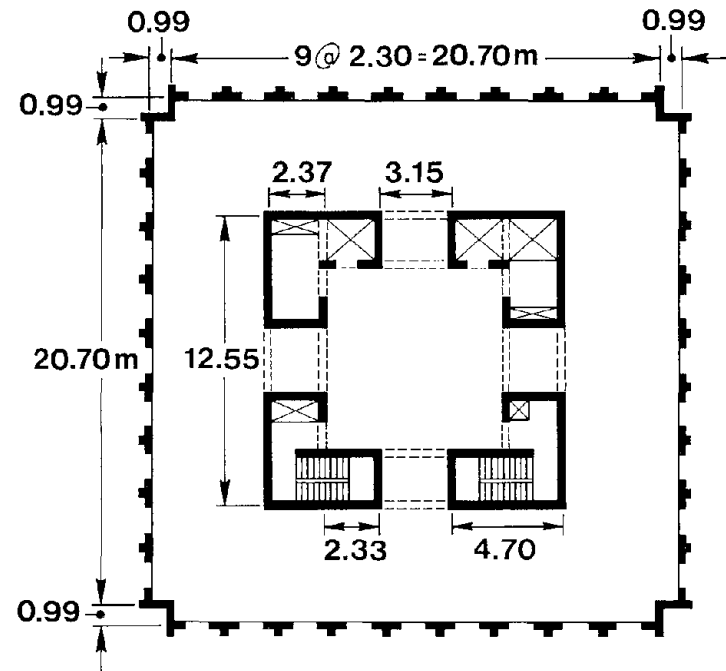


FIG. 4.17 GENERAL - BANCO DE AMERICA BUILDING



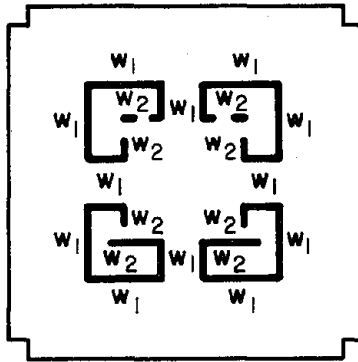
(a) VERTICAL SECTION



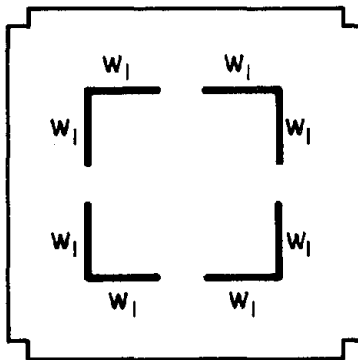
(b) TYPICAL FLOOR PLAN OF TOWER

FIG. 4.18 BANCO DE AMERICA BUILDING: SECTION AND PLAN (UNITS IN METERS)

STORY 1 TO 17



STORY 18



CORE WALL THICKNESS, cm

STORY	$w_1$	$w_2$
1-4	30	25
5-11	25	25
12-17	20	25
18	20	0

FIG. 4.19 BANCO DE AMERICA: DIMENSIONS OF CORE SHEAR WALL

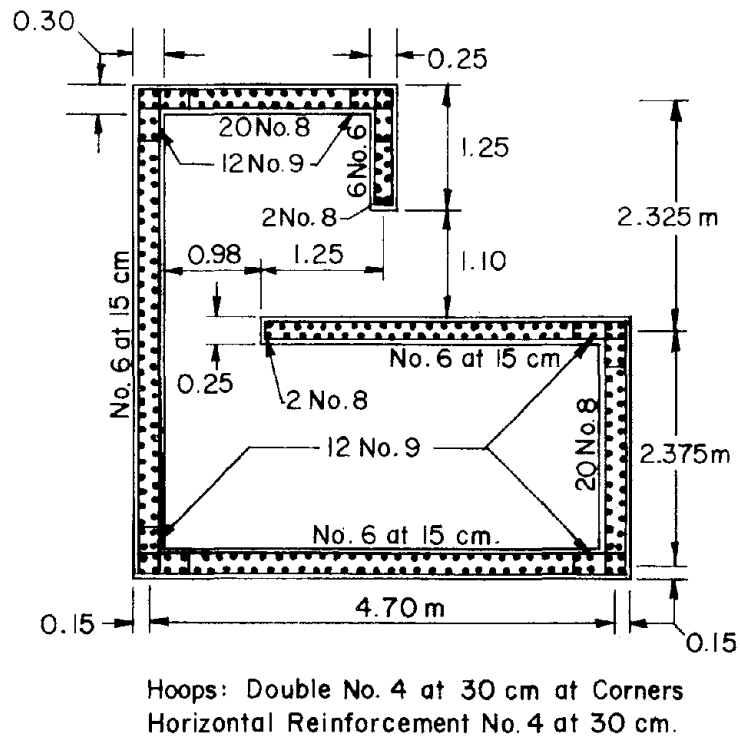
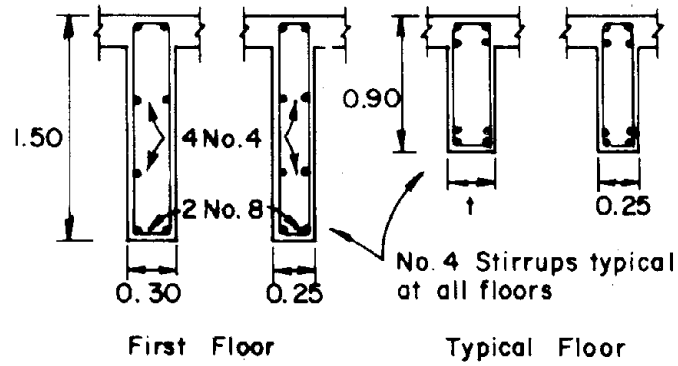


FIG. 4.20 BANCO DE AMERICA BUILDING: DETAILS OF CORE SHEAR WALL REINFORCEMENT - STORIES 1 - 4



FLOOR	REINFORCEMENT		STIRRUP SPACING	EXTERIOR GIRDER THICKNESS, †
	TOP	BOTTOM		
2-4	4 No. 10	4 No. 10	0.25m	0.30m
5-11	4 No. 11	4 No. 11	0.25	0.25
12-16	2 No. 10+	2 No. 10+	0.40	0.20
	2 No. 9	2 No. 9		
17	2 No. 10+	2 No. 10+	0.30	0.20
	2 No. 9	2 No. 9		
18	—	4 No. 6	0.30	0.20

FIG. 4.21 BANCO DE AMERICA BUILDING: COUPLING GIRDER DETAILS

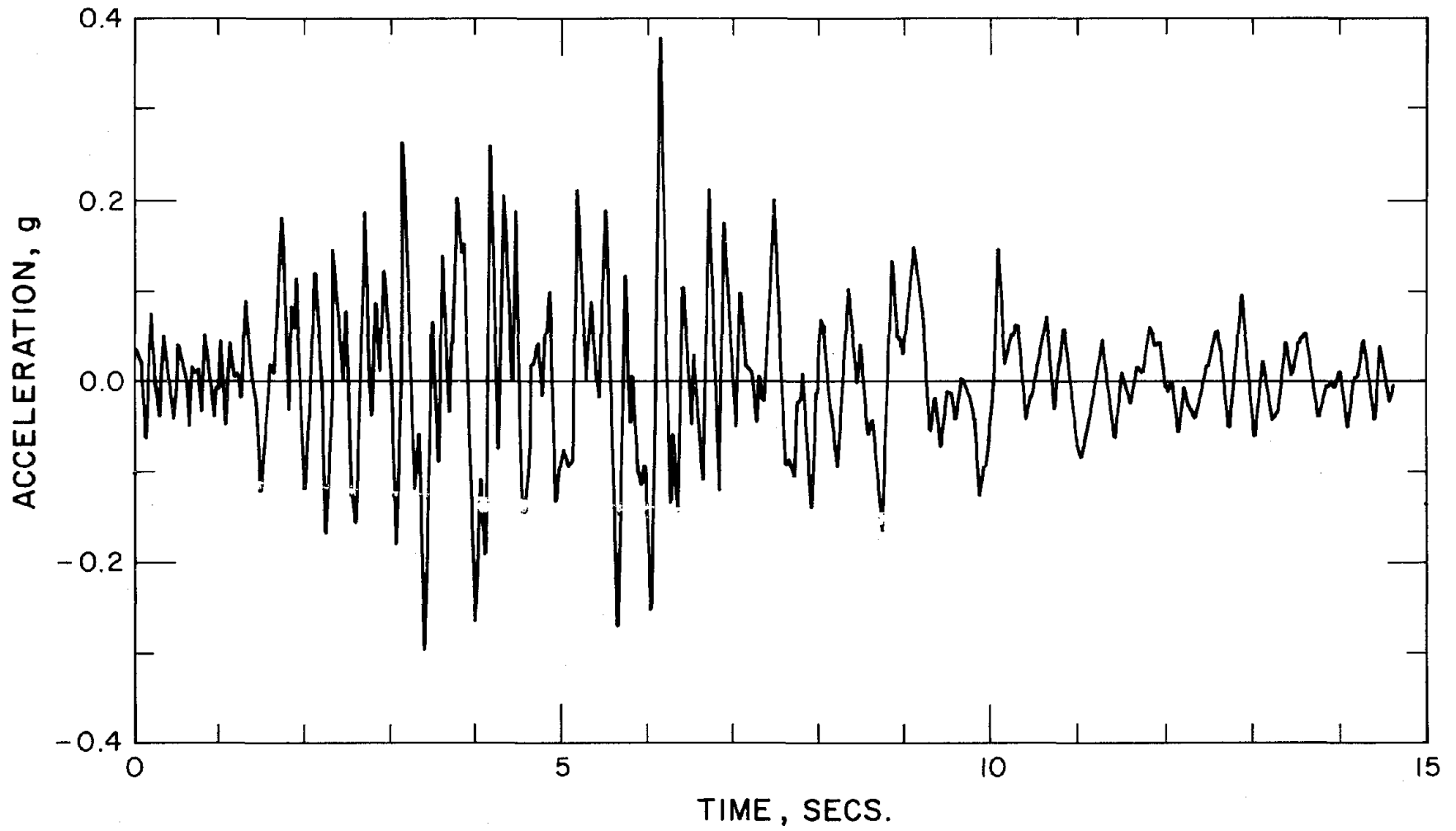


FIG. 4.22 ESSO REFINERY ACCELEROGRAM, EAST - WEST COMPONENT,  
MANAGUA EARTHQUAKE OF DECEMBER 23, 1972

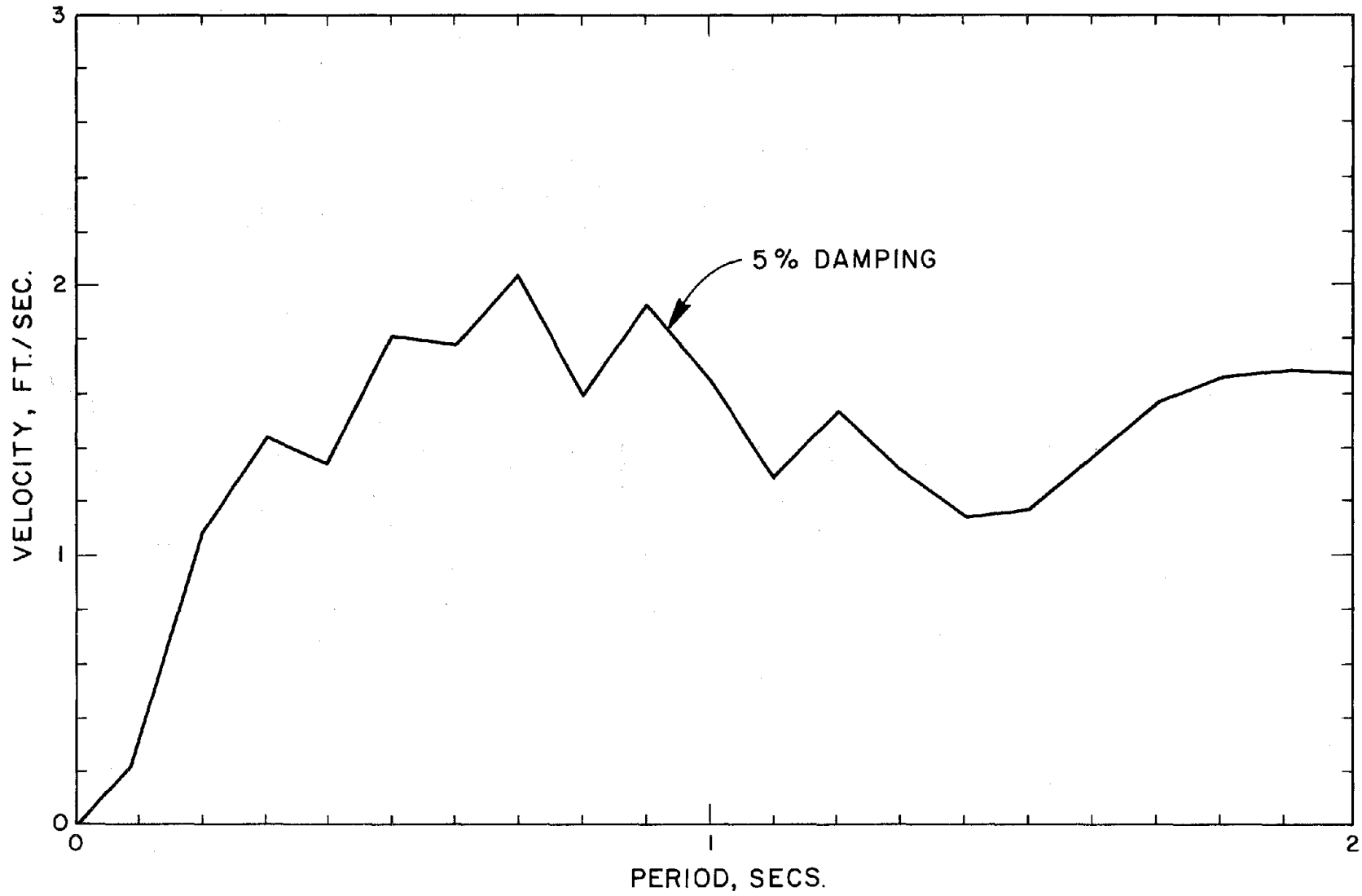


FIG. 4.23 VELOCITY RESPONSE SPECTRUM FOR GROUND ACCELERATION OF FIG. 4.22

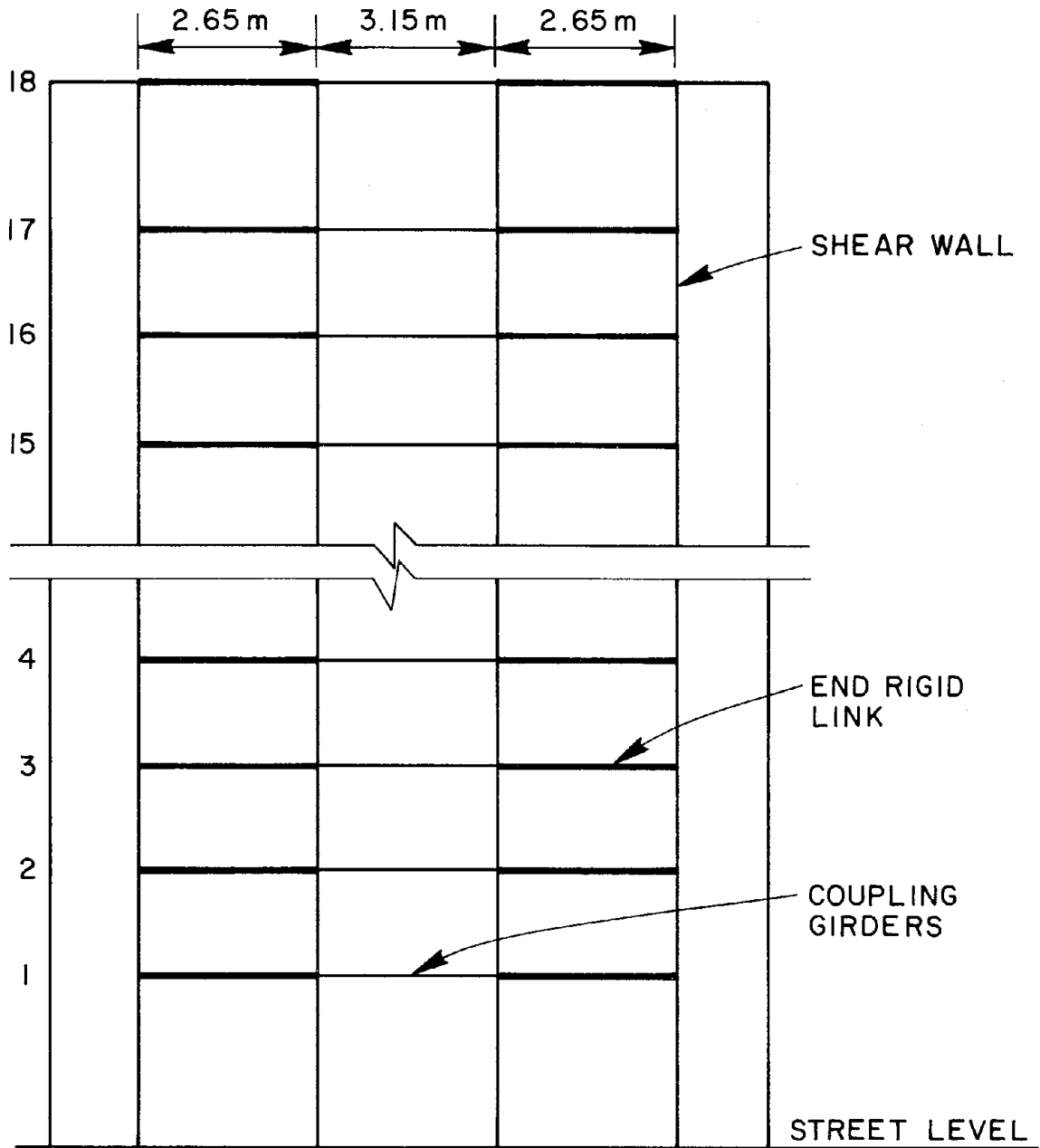


FIG. 4.24 BANCO DE AMERICA BUILDING: STRUCTURAL IDEALIZATION

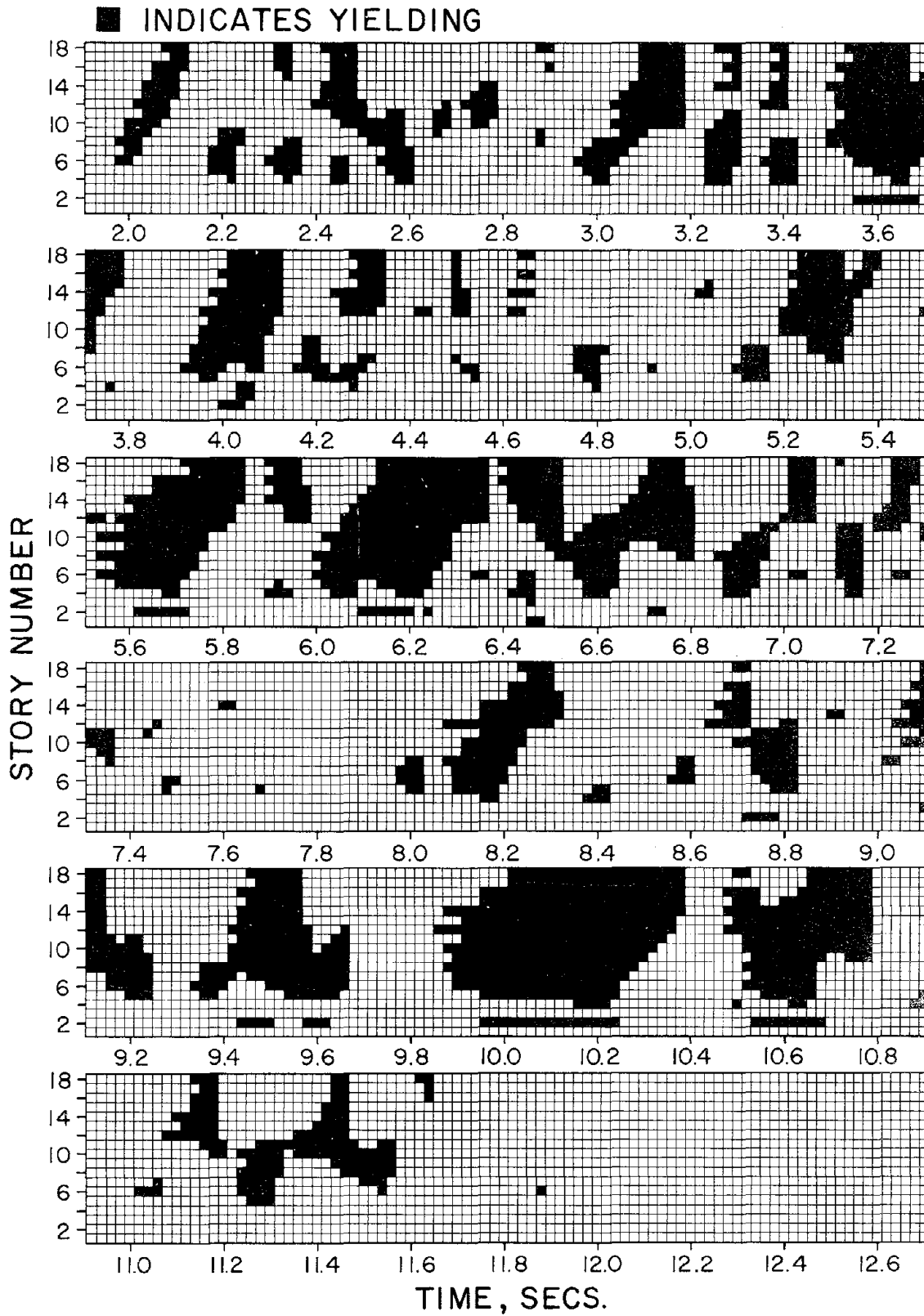


FIG. 4.25 BANCO DE AMERICA BUILDING: YIELDING HISTORY OF COUPLING GIRDERS

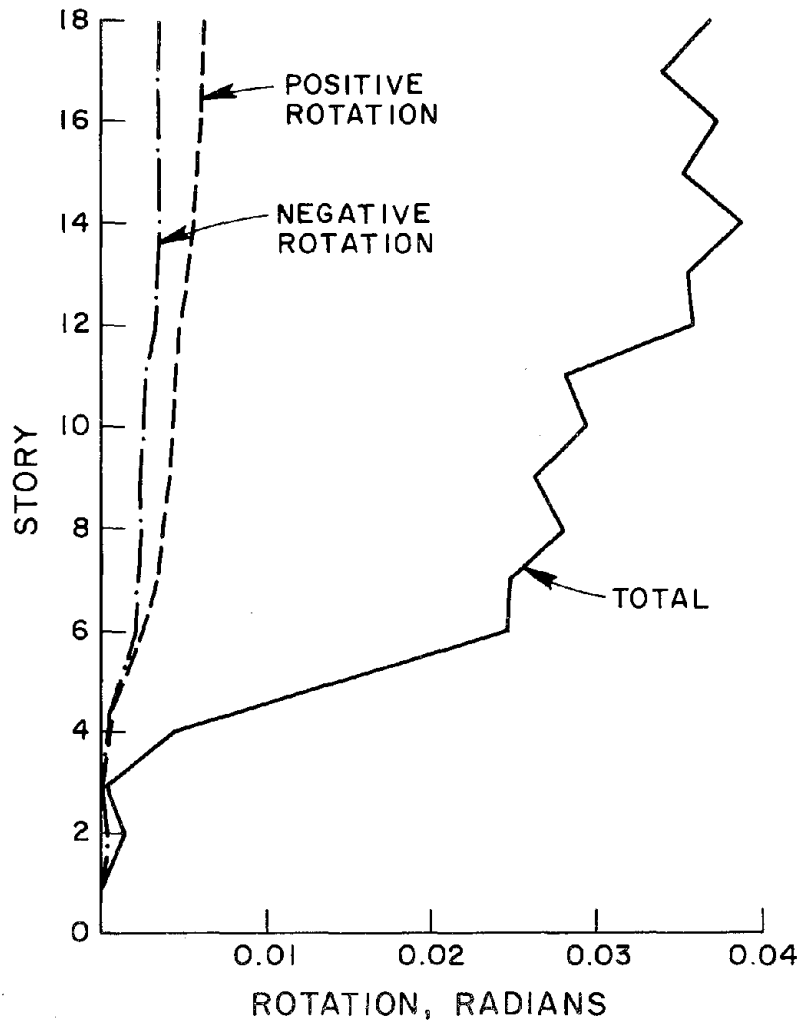


FIG. 4.26 ENVELOPES OF MAXIMUM PLASTIC ROTATIONS

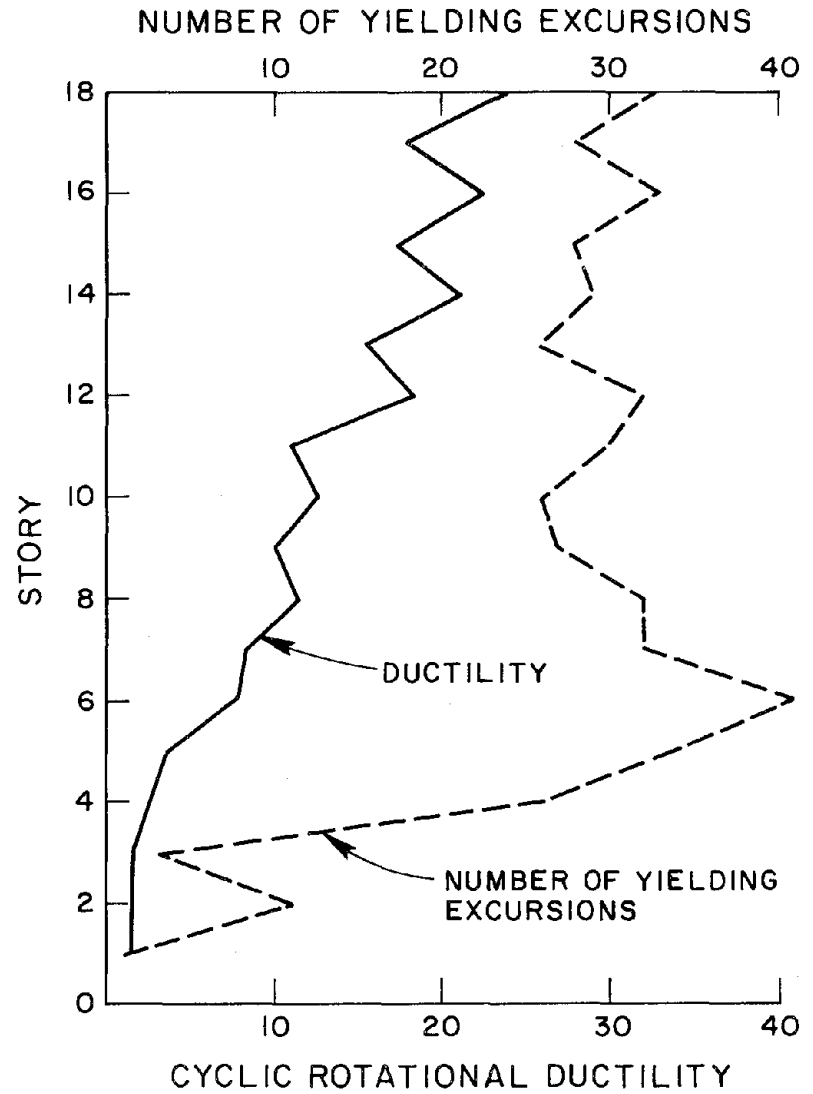


FIG. 4.27 CYCLIC ROTATIONAL DUCTILITY REQUIREMENTS AND NUMBER OF YIELDING EXCURSIONS

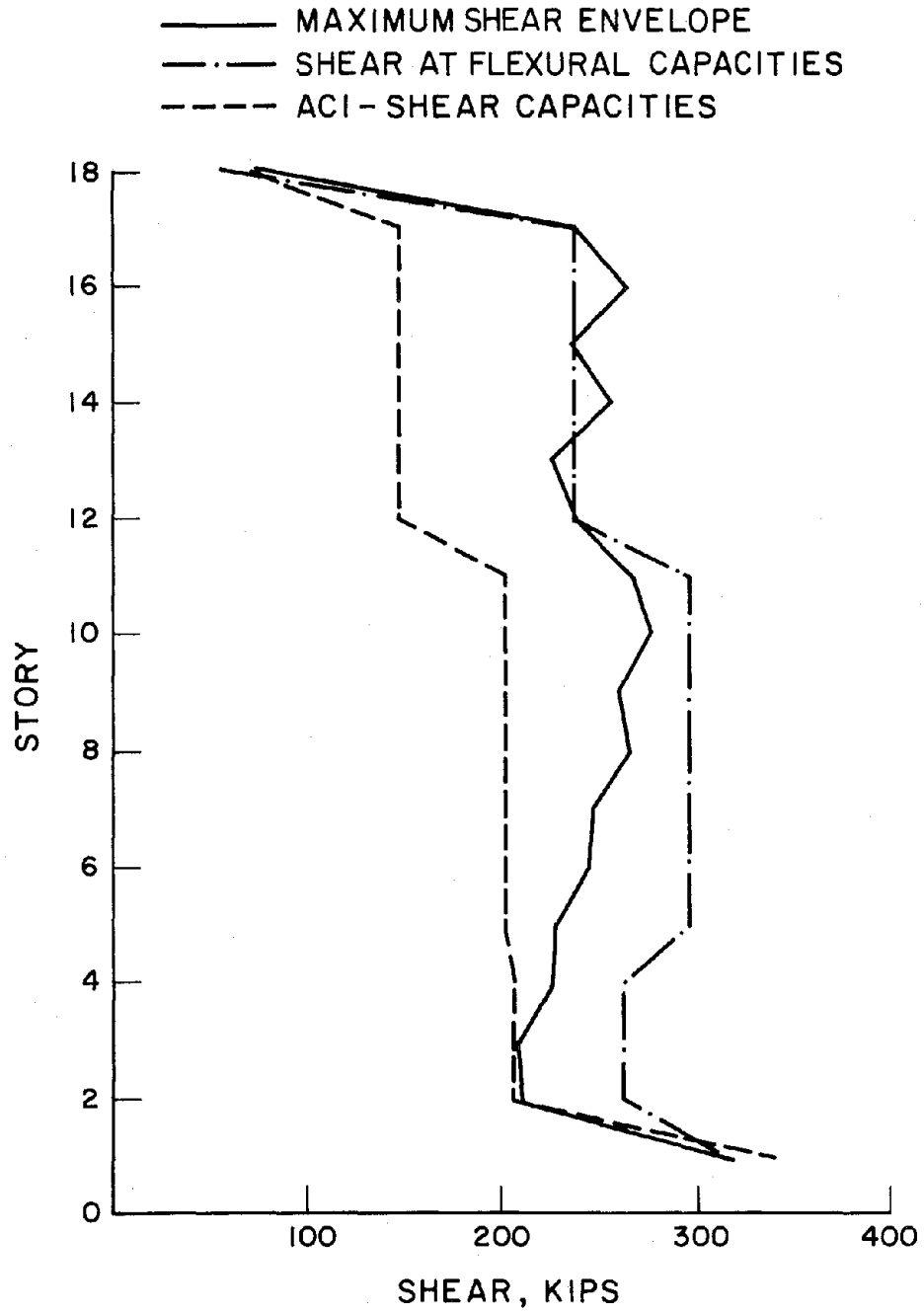


FIG. 4.28 ENVELOPE OF MAXIMUM GIRDER SHEARS

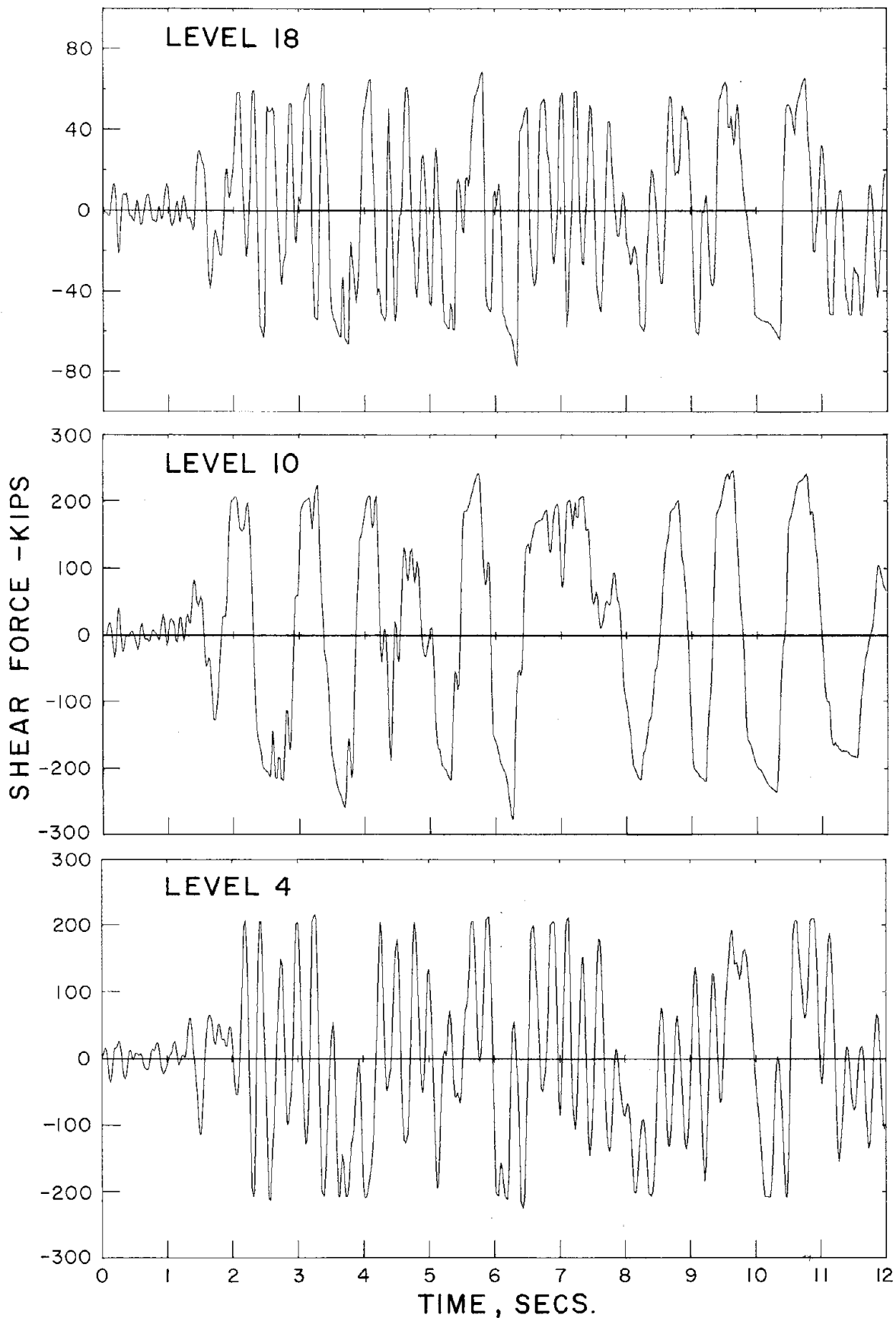


FIG. 4.29 HISTORY OF SHEAR FORCE IN GIRDERS AT FLOOR LEVELS 4, 10, AND 18

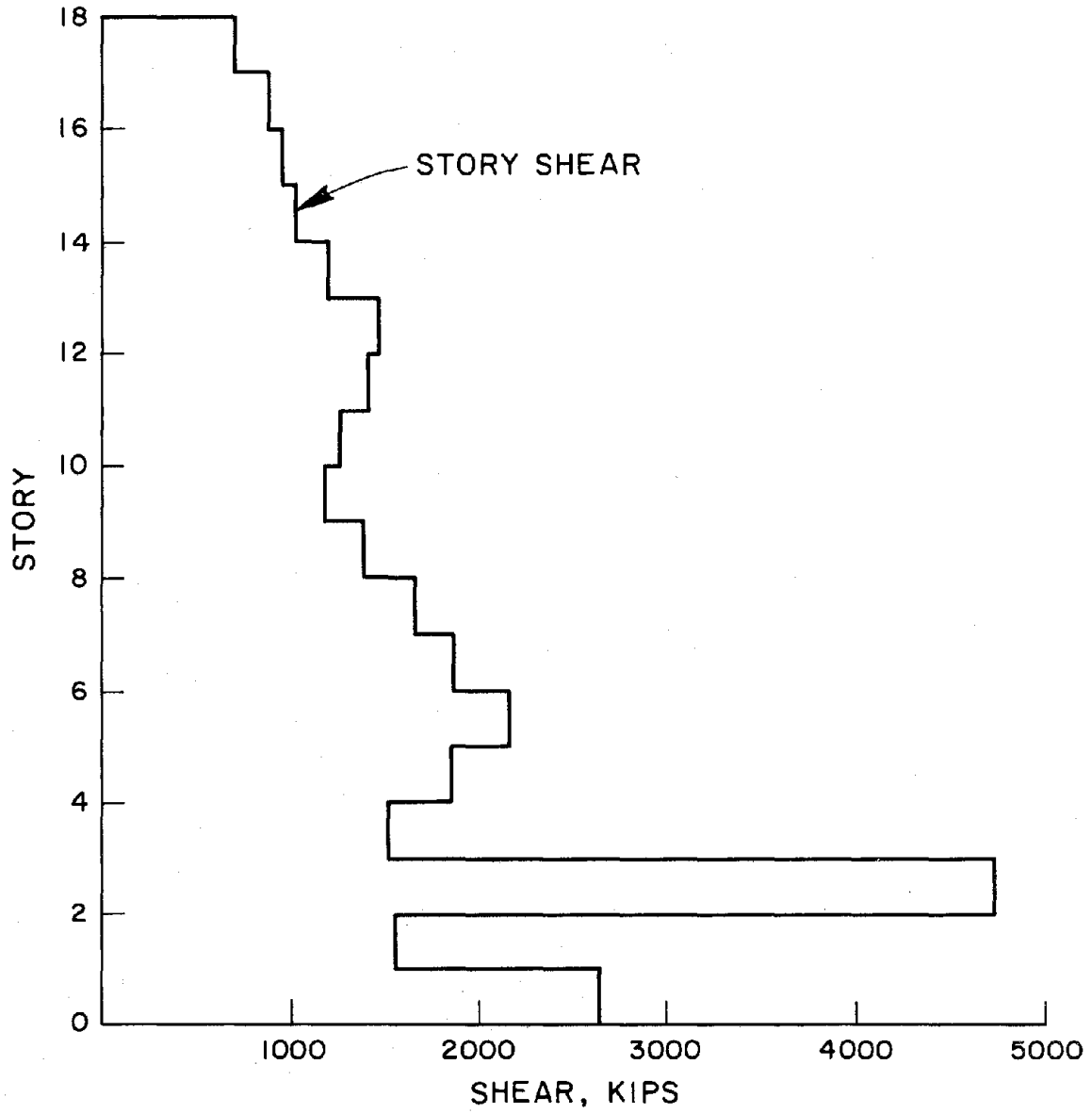


FIG. 4.30 ENVELOPE OF MAXIMUM STORY SHEAR



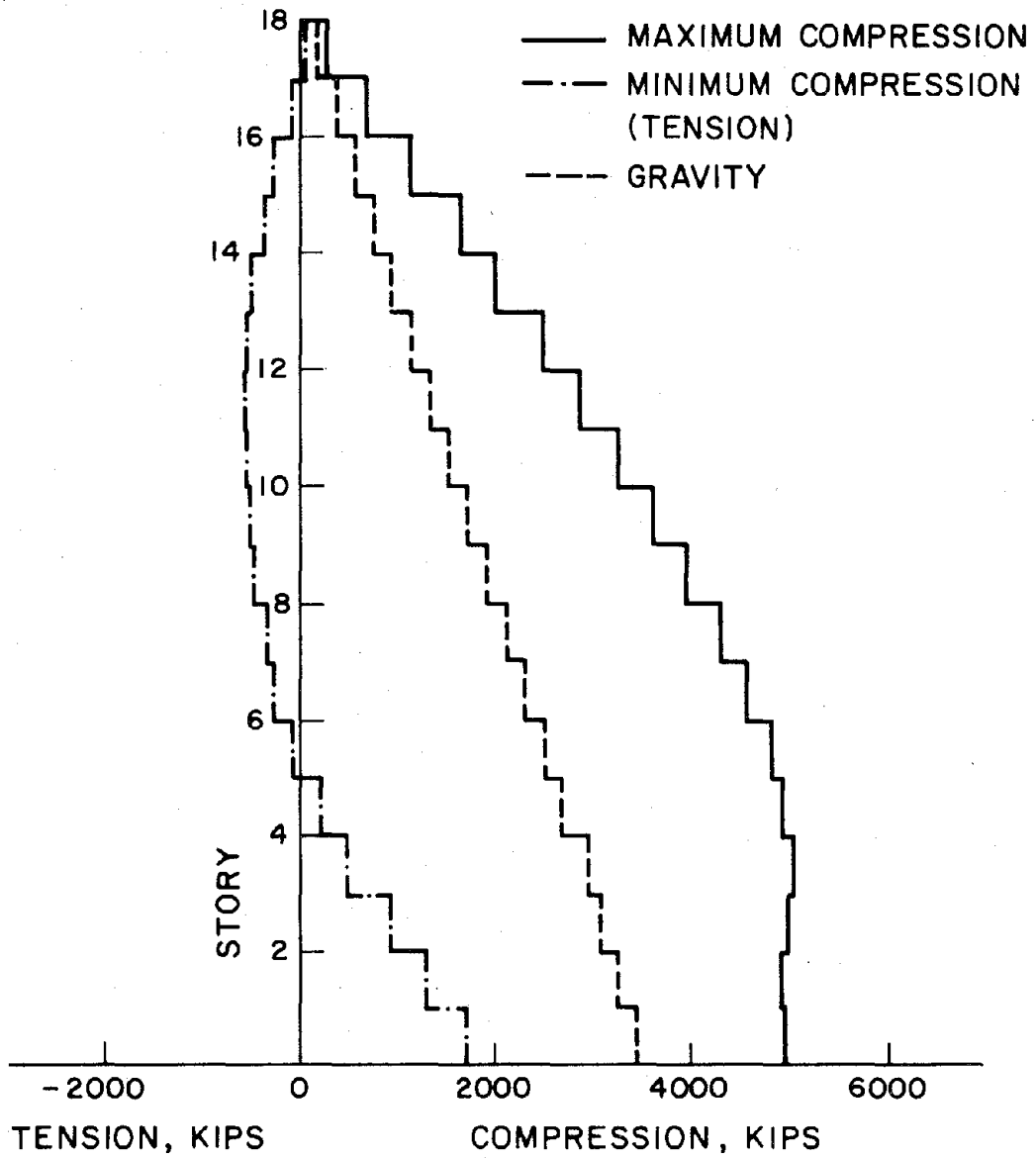


FIG. 4.32 ENVELOPES OF MAXIMUM AXIAL FORCE IN ONE CORE WALL

## APPENDIX I - NOTATION

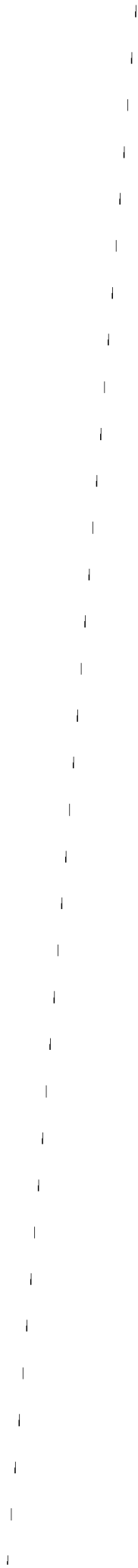
- $A_1^i, A_2^i$  =  $i^{\text{th}}$  story sectional area of wall 1 or wall 2;
- $A_b^i$  = sectional area of  $i^{\text{th}}$  story coupling beam;
- $\bar{A}_b^i$  = effective shear area of  $i^{\text{th}}$  story coupling beam;
- $a_1$  = distance between neutral axes of two adjacent walls;
- $\underline{C}, \tilde{\underline{C}}$  = damping matrix of system associated with nodal point and generalized coordinates, respectively;
- $\tilde{\underline{C}}_b^i$  =  $i^{\text{th}}$  story beam element damping matrix associated with generalized coordinates;
- $\tilde{\underline{C}}_w^i$  =  $i^{\text{th}}$  story wall element damping matrix associated with generalized coordinates;
- $d_1^i, d_2^i$  = effective length of rigid links connecting ends of  $i^{\text{th}}$  story beam to neutral axis of wall 1 or wall 2;
- $d_b^i$  = depth of  $i^{\text{th}}$  story coupling beam;
- $E_1^i, E_2^i$  = Young's modulus of material at  $i^{\text{th}}$  story wall 1 or wall 2;
- $E_b^i$  = Young's modulus of  $i^{\text{th}}$  story coupling beam;
- $\underline{F}_{-b1}^i, \underline{F}_{-b2}^i$  = subvectors associated with beam element as defined in Eq. (2.6j);
- $\underline{F}_b^i = \begin{bmatrix} \underline{F}_{-b1}^T & \underline{F}_{-b2}^T \end{bmatrix}^T$ ;
- $\underline{F}_{-w1}^i, \underline{F}_{-w2}^i$  = subvectors associated with wall element as defined in Eqs. (2.11k and 2.11l);
- $\underline{F}_w^i = \begin{bmatrix} \underline{F}_{-w1}^T & \underline{F}_{-w2}^T \end{bmatrix}^T$ ;
- $G_b^i$  = Shear modulus of  $i^{\text{th}}$  story coupling beam;

- $\underline{H}$  = transformation matrix;
- $h_i$  = height of  $i^{\text{th}}$  story;
- $\underline{h}_{-b}^i$  = element transformation matrix for  $i^{\text{th}}$  story coupling beam;
- $\underline{h}_{-w}^i$  = element transformation matrix for  $i^{\text{th}}$  story wall element;
- $I_1^i, I_2^i$  =  $i^{\text{th}}$  story sectional moment of inertia of wall 1 or 2;
- $I_b^i$  = sectional moment of inertia of  $i^{\text{th}}$  story coupling beam;
- $\underline{K}, \underline{\tilde{K}}$  = stiffness matrix of system associated with nodal point and generalized coordinates, respectively;
- $\underline{k}_b^{11}, \underline{k}_b^{12}, \underline{k}_b^{21}, \underline{k}_b^{22}$  = submatrices of beam element stiffness matrix;
- $\underline{k}_b^i, \underline{\tilde{k}}_b^i$  = element stiffness matrix of  $i^{\text{th}}$  story beam associated with nodal point and generalized coordinates, respectively;
- $\underline{k}_{-w}^{11}, \underline{k}_{-w}^{12}, \underline{k}_{-w}^{21}, \underline{k}_{-w}^{22}$  = submatrices of wall element stiffness matrix;
- $\underline{k}_{-w}^i, \underline{\tilde{k}}_{-w}^i$  = element stiffness matrix of  $i^{\text{th}}$  story wall associated with nodal point and generalized coordinates, respectively;
- $l$  = total height of structure;
- $\underline{M}, \underline{\tilde{M}}$  = mass matrix of system associated with nodal point and generalized coordinates, respectively;
- $M_{y1}, M_{y2}$  = yielding moment capacity of coupling beam sections at left and right ends, respectively;
- $M_1, M_2$  = moment of coupling beam sections at left and right ends, respectively;
- $\underline{m}_{-b}^{11}, \underline{m}_{-b}^{12}, \underline{m}_{-b}^{21}, \underline{m}_{-b}^{22}$  = submatrices of beam element mass matrix;

- $\underline{m}_b^i, \tilde{\underline{m}}_b^i$  = element mass matrix of  $i^{\text{th}}$  story beam associated with nodal point and generalized coordinates, respectively;
- $\underline{m}_w^{11}, \underline{m}_w^{12}, \underline{m}_w^{21}, \underline{m}_w^{22}$  = submatrices of wall element mass matrix;
- $\underline{m}_w^i, \tilde{\underline{m}}_w^i$  = element mass matrix of  $i^{\text{th}}$  story wall associated with nodal point and generalized coordinates, respectively;
- $M(x)$  = bending moment along axis of a coupling beam;
- $P_y$  = span shear corresponding to initial yielding of coupling beam;
- $P(x)$  = axial force along axis of a coupling beam;
- $\underline{R}, \tilde{\underline{R}}$  = effective load vector of system associated with nodal point and generalized coordinates, respectively;
- $\underline{R}_b^i, \tilde{\underline{R}}_b^i$  = element effective load vector of  $i^{\text{th}}$  story beam associated with nodal point and generalized coordinates, respectively;
- $\underline{R}_w^i, \tilde{\underline{R}}_w^i$  = element effective load vector of  $i^{\text{th}}$  story wall associated with nodal point and generalized coordinates, respectively;
- $\underline{r}_j^i$  = vector of nodal point displacements at  $i^{\text{th}}$  story of  $j^{\text{th}}$  wall;
- $\underline{r}_b^i$  = vector of nodal point displacements associated with  $i^{\text{th}}$  story coupling beam;
- $\underline{r}_w^i$  = vector of nodal point displacements associated with  $i^{\text{th}}$  story wall element;
- $\underline{r}$  = vector of nodal point displacements of system;
- $s$  = span between end rigid links of a coupling beam;
- $T_i$  = kinetic energy of  $i^{\text{th}}$  structural element;
- $T_b^i$  = kinetic energy of  $i^{\text{th}}$  story coupling beam;

- $T_w^i$  = kinetic energy of  $i^{\text{th}}$  story wall element;
- $t$  = time variable;
- $U_i$  = strain energy of  $i^{\text{th}}$  structural element;
- $U_b^i$  = strain energy of  $i^{\text{th}}$  story coupling beam;
- $U_w^i$  = strain energy of  $i^{\text{th}}$  story wall element;
- $\underline{u}_j$  = vector of horizontal displacements and rotations of nodal points in  $j^{\text{th}}$  wall;
- $u_j^i, \dot{u}_j^i, \ddot{u}_j^i$  = horizontal displacement, velocity, and acceleration of nodal point at  $i^{\text{th}}$  story of  $j^{\text{th}}$  wall, relative to ground motion;
- $\underline{u}_j^{-i}$  = horizontal displacement at left end of effective clear span of  $i^{\text{th}}$  story beam, relative to ground motion;
- $\dot{u}_g, \ddot{u}_g$  = velocity and acceleration, respectively, of horizontal component of ground motion;
- $\underline{v}_j$  = vector of vertical displacements of nodal points in  $j^{\text{th}}$  wall;
- $v_j^i, \dot{v}_j^i, \ddot{v}_j^i$  = vertical displacement, velocity, and acceleration of nodal point at  $i^{\text{th}}$  story of  $j^{\text{th}}$  wall, relative to ground motion;
- $\underline{v}_j^{-i}$  = vertical displacement at left end of effective clear span of  $i^{\text{th}}$  story beam, relative to ground motion;
- $\dot{v}_g, \ddot{v}_g$  = velocity and acceleration, respectively, of vertical component of ground motion;
- $V(x)$  = shear force along axis of a coupling beam;
- $w$  = distance from beam-wall surface of a wall to its neutral axis;
- $x$  = coordinate variable along axis of a wall element or a coupling beam;

- $z_{Hj}^m, z_{vj}^m$  = generalized coordinates associated with generalized functions which are  $m^{\text{th}}$  lateral and  $m^{\text{th}}$  vertical mode shapes of uncoupled wall  $j$ , respectively;
- $\underline{z}$  = vector of generalized coordinates of reduced system;
- $\alpha_m, \alpha_k$  = respectively, mass and stiffness proportional constants for Rayleigh damping;
- $\beta_i$  =  $\sqrt{1 + (12 E_b^i I_b^i / s^2 G_b^i A_b^i)}$ ;
- $\lambda$  =  $w/d_b^i$ ;
- $\delta$  = relative transverse displacement of two ends of effective clear span of a coupling beam;
- $\rho_j^i$  = mass per unit volume of  $i^{\text{th}}$  story element of  $j^{\text{th}}$  wall;
- $\rho_b^i$  = mass per unit volume of  $i^{\text{th}}$  story beam;
- $\theta$  = relative end rotations of two ends of effective clear span of a coupling beam;
- $\theta_j^i$  = rotation of nodal point at  $i^{\text{th}}$  story of  $j^{\text{th}}$  wall;
- $\underline{\psi}_{-vj}^m, \underline{\psi}_{-Hj}^m$  = vector of nodal point displacements corresponding to  $m^{\text{th}}$  vertical and  $m^{\text{th}}$  lateral mode shapes, respectively, of individual uncoupled wall  $j$ ;
- $\zeta(x), \eta(x)$  = respectively, longitudinal and transverse displacement along axis of a beam or wall element;
- $\xi_i$  =  $(70 \beta_i^4 + 7 \beta_i^2 + 1) / 210 \beta_i^4$ ;
- $\Delta$  = relative longitudinal displacements of two ends of effective clear span of a coupling beam.



## EARTHQUAKE ENGINEERING RESEARCH CENTER REPORTS

- EERC 67-1 "Feasibility Study Large-Scale Earthquake Simulator Facility," by J. Penzien, J. G. Bouwkamp, R. W. Clough and D. Rea - 1967 (PB 187 905)
- EERC 68-1 Unassigned
- EERC 68-2 "Inelastic Behavior of Beam-to-Column Subassemblages Under Repeated Loading," by V. V. Bertero - 1968 (PB 184 888)
- EERC 68-3 "A Graphical Method for Solving the Wave Reflection-Refraction Problem," by H. D. McNiven and Y. Mengi 1968 (PB 187 943)
- EERC 68-4 "Dynamic Properties of McKinley School Buildings," by D. Rea, J. G. Bouwkamp and R. W. Clough - 1968 (PB 187 902)
- EERC 68-5 "Characteristics of Rock Motions During Earthquakes," by H. B. Seed, I. M. Idriss and F. W. Kiefer - 1968 (PB 188 338)
- EERC 69-1 "Earthquake Engineering Research at Berkeley," - 1969 (PB 187 906)
- EERC 69-2 "Nonlinear Seismic Response of Earth Structures," by M. Dibaj and J. Penzien - 1969 (PB 187 904)
- EERC 69-3 "Probabilistic Study of the Behavior of Structures During Earthquakes," by P. Ruiz and J. Penzien - 1969 (PB 187 886)
- EERC 69-4 "Numerical Solution of Boundary Value Problems in Structural Mechanics by Reduction to an Initial Value Formulation," by N. Distefano and J. Schujman - 1969 (PB 187 942)
- EERC 69-5 "Dynamic Programming and the Solution of the Biharmonic Equation," by N. Distefano - 1969 (PB 187 941)

---

Note: Numbers in parenthesis are Accession Numbers assigned by the National Technical Information Service. Copies of these reports may be ordered from the National Technical Information Service, 5285 Port Royal Road, Springfield, Virginia, 22161. Accession Numbers should be quoted on orders for the reports (PB --- ---) and remittance must accompany each order. (Foreign orders, add \$2.50 extra for mailing charges.) Those reports without this information listed are not yet available from NTIS. Upon request, EERC will mail inquirers this information when it becomes available to us.

- EERC 69-6 "Stochastic Analysis of Offshore Tower Structures,"  
by A. K. Malhotra and J. Penzien - 1969 (PB 187 903)
- EERC 69-7 "Rock Motion Accelerograms for High Magnitude  
Earthquakes," by H. B. Seed and I. M. Idriss - 1969  
(PB 187 940)
- EERC 69-8 "Structural Dynamics Testing Facilities at the  
University of California, Berkeley," by R. M. Stephen,  
J. G. Bouwkamp, R. W. Clough and J. Penzien - 1969  
(PB 189 111)
- EERC 69-9 "Seismic Response of Soil Deposits Underlain by  
Sloping Rock Boundaries," by H. Dezfulian and  
H. B. Seed - 1969 (PB 189 114)
- EERC 69-10 "Dynamic Stress Analysis of Axisymmetric Structures  
under Arbitrary Loading," by S. Ghosh and E. L.  
Wilson - 1969 (PB 189 026)
- EERC 69-11 "Seismic Behavior of Multistory Frames Designed by  
Different Philosophies," by J. C. Anderson and  
V. V. Bertero - 1969 (PB 190 662)
- EERC 69-12 "Stiffness Degradation of Reinforcing Concrete  
Structures Subjected to Reversed Actions," by  
V. V. Bertero, B. Bresler and H. Ming Liao - 1969  
(PB 202 942)
- EERC 69-13 "Response of Non-Uniform Soil Deposits to Travel  
Seismic Waves," by H. Dezfulian and H. B. Seed - 1969  
(PB 191 023)
- EERC 69-14 "Damping Capacity of a Model Steel Structure," by  
D. Rea, R. W. Clough and J. G. Bouwkamp - 1969  
(PB 190 663)
- EERC 69-15 "Influence of Local Soil Conditions on Building  
Damage Potential during Earthquakes," by H. B. Seed  
and I. M. Idriss - 1969 (PB 191 036)
- EERC 69-16 "The Behavior of Sands under Seismic Loading  
Conditions," by M. L. Silver and H. B. Seed - 1969  
(AD 714 982)
- EERC 70-1 "Earthquake Response of Concrete Gravity Dams," by  
A. K. Chopra - 1970 (AD 709 640)
- EERC 70-2 "Relationships between Soil Conditions and Building  
Damage in the Caracas Earthquake of July 29, 1967," by  
H. B. Seed, I. M. Idriss and H. Dezfulian - 1970  
(PB 195 762)

- EERC 70-3 "Cyclic Loading of Full Size Steel Connections," by E. P. Popov and R. M. Stephen - 1970 (PB 213 545)
- EERC 70-4 "Seismic Analysis of the Charaima Building, Caraballeda, Venezuela," by Subcommittee of the SEAONC Research Committee: V. V. Bertero, P. F. Fratessa, S. A. Mahin, J. H. Sexton, A. C. Scordelis, E. L. Wilson, L. A. Wyllie, H. B. Seed and J. Penzien, Chairman - 1970 (PB 201 455)
- EERC 70-5 "A Computer Program for Earthquake Analysis of Dams," by A. K. Chopra and P. Chakrabarti - 1970 (AD 723 994)
- EERC 70-6 "The Propagation of Love Waves across Non-Horizontally Layered Structures," by J. Lysmer and L. A. Drake - 1970 (PB 197 896)
- EERC 70-7 "Influence of Base Rock Characteristics on Ground Response," by J. Lysmer, H. B. Seed and P. B. Schnabel - 1970 (PB 197 897)
- EERC 70-8 "Applicability of Laboratory Test Procedures for Measuring Soil Liquefaction Characteristics under Cyclic Loading," by H. B. Seed and W. H. Peacock - 1970 (PB 198 016)
- EERC 70-9 "A Simplified Procedure for Evaluating Soil Liquefaction Potential," by H. B. Seed and I. M. Idriss - 1970 (PB 198 009)
- EERC 70-10 "Soil Moduli and Damping Factors for Dynamic Response Analysis," by H. B. Seed and I. M. Idriss - 1970 (PB 197 869)
- EERC 71-1 "Koyna Earthquake and the Performance of Koyna Dam," by A. K. Chopra and P. Chakrabarti - 1971 (AD 731 496)
- EERC 71-2 "Preliminary In-Situ Measurements of Anelastic Absorption in Soils Using a Prototype Earthquake Simulator," by R. D. Borchardt and P. W. Rodgers - 1971 (PB 201 454)
- EERC 71-3 "Static and Dynamic Analysis of Inelastic Frame Structures," by F. L. Porter and G. H. Powell - 1971 (PB 210 135)
- EERC 71-4 "Research Needs in Limit Design of Reinforced Concrete Structures," by V. V. Bertero - 1971 (PB 202 943)
- EERC 71-5 "Dynamic Behavior of a High-Rise Diagonally Braced Steel Building," by D. Rea, A. A. Shah and J. G. Bouwkamp - 1971 (PB 203 584)

- EERC 71-6 "Dynamic Stress Analysis of Porous Elastic Solids Saturated with Compressible Fluids," by J. Ghaboussi and E. L. Wilson - 1971 (PB 211 396)
- EERC 71-7 "Inelastic Behavior of Steel Beam-to-Column Subassemblages," by H. Krawinkler, V. V. Bertero and E. P. Popov - 1971 (PB 211 335)
- EERC 71-8 "Modification of Seismograph Records for Effects of Local Soil Conditions," by P. Schnabel, H. B. Seed and J. Lysmer - 1971 (PB 214 450)
- EERC 72-1 "Static and Earthquake Analysis of Three Dimensional Frame and Shear Wall Buildings," by E. L. Wilson and H. H. Dovey - 1972 (PB 212 904)
- EERC 72-2 "Accelerations in Rock for Earthquakes in the Western United States," by P. B. Schnabel and H. B. Seed - 1972 (PB 213 100)
- EERC 72-3 "Elastic-Plastic Earthquake Response of Soil-Building Systems," by T. Minami - 1972 (PB 214 868)
- EERC 72-4 "Stochastic Inelastic Response of Offshore Towers to Strong Motion Earthquakes," by M. K. Kaul - 1972 (PB 215 713)
- EERC 72-5 "Cyclic Behavior of Three Reinforced Concrete Flexural Members with High Shear," by E. P. Popov, V. V. Bertero and H. Krawinkler - 1972 (PB 214 555)
- EERC 72-6 "Earthquake Response of Gravity Dams Including Reservoir Interaction Effects," by P. Chakrabarti and A. K. Chopra - 1972 (AD 762 330)
- EERC 72-7 "Dynamic Properties on Pine Flat Dam," by D. Rea, C. Y. Liaw and A. K. Chopra - 1972 (AD 763 928)
- EERC 72-8 "Three Dimensional Analysis of Building Systems," by E. L. Wilson and H. H. Dovey - 1972 (PB 222 438)
- EERC 72-9 "Rate of Loading Effects on Uncracked and Repaired Reinforced Concrete Members," by S. Mahin, V. V. Bertero, D. Rea and M. Atalay - 1972 (PB 224 520)
- EERC 72-10 "Computer Program for Static and Dynamic Analysis of Linear Structural Systems," by E. L. Wilson, K.-J. Bathe, J. E. Peterson and H. H. Dovey - 1972 (PB 220 437)

- EERC 72-11 "Literature Survey - Seismic Effects on Highway Bridges," by T. Iwasaki, J. Penzien and R. W. Clough - 1972 (PB 215 613)
- EERC 72-12 "SHAKE-A Computer Program for Earthquake Response Analysis of Horizontally Layered Sites," by P. B. Schnabel and J. Lysmer - 1972 (PB 220 207)
- EERC 73-1 "Optimal Seismic Design of Multistory Frames," by V. V. Bertero and H. Kamil - 1973
- EERC 73-2 "Analysis of the Slides in the San Fernando Dams during the Earthquake of February 9, 1971," by H. B. Seed, K. L. Lee, I. M. Idriss and F. Makdisi - 1973 (PB 223 402)
- EERC 73-3 "Computer Aided Ultimate Load Design of Unbraced Multistory Steel Frames," by M. B. El-Hafez and G. H. Powell - 1973
- EERC 73-4 "Experimental Investigation into the Seismic Behavior of Critical Regions of Reinforced Concrete Components as Influenced by Moment and Shear," by M. Celebi and J. Penzien - 1973 (PB 215 884)
- EERC 73-5 "Hysteretic Behavior of Epoxy-Repaired Reinforced Concrete Beams," by M. Celebi and J. Penzien - 1973
- EERC 73-6 "General Purpose Computer Program for Inelastic Dynamic Response of Plane Structures," by A. Kanaan and G. H. Powell - 1973 (PB 221 260)
- EERC 73-7 "A Computer Program for Earthquake Analysis of Gravity Dams Including Reservoir Interaction," by P. Chakrabarti and A. K. Chopra - 1973 (AD 766 271)
- EERC 73-8 "Behavior of Reinforced Concrete Deep Beam-Column Subassemblages under Cyclic Loads," by O. Kustu and J. G. Bouwkamp - 1973
- EERC 73-9 "Earthquake Analysis of Structure-Foundation Systems," by A. K. Vaish and A. K. Chopra - 1973 (AD 766 272)
- EERC 73-10 "Deconvolution of Seismic Response for Linear Systems," by R. B. Reimer - 1973 (PB 227 179)
- EERC 73-11 "SAP IV: A Structural Analysis Program for Static and Dynamic Response of Linear Systems," by K.-J. Bathe, E. L. Wilson and F. E. Peterson - 1973 (PB 221 967)
- EERC 73-12 "Analytical Investigations of the Seismic Response of Long, Multiple Span Highway Bridges," by W. S. Tseng and J. Penzien - 1973 (PB 227 816)

- EERC 73-13 "Earthquake Analysis of Multi-Story Buildings Including Foundation Interaction," by A. K. Chopra and J. A. Gutierrez - 1973 (PB 222 970)
- EERC 73-14 "ADAP: A Computer Program for Static and Dynamic Analysis of Arch Dams," by R. W. Clough, J. M. Raphael and S. Majtahedi - 1973 (PB 223 763)
- EERC 73-15 "Cyclic Plastic Analysis of Structural Steel Joints," by R. B. Pinkney and R. W. Clough - 1973 (PB 226 843)
- EERC 73-16 "QUAD-4: A Computer Program for Evaluating the Seismic Response of Soil Structures by Variable Damping Finite Element Procedures," by I. M. Idriss, J. Lysmer, R. Hwang and H. B. Seed - 1973 (PB 229 424)
- EERC 73-17 "Dynamic Behavior of a Multi-Story Pyramid Shaped Building," by R. M. Stephen and J. G. Bouwkamp - 1973
- EERC 73-18 "Effect of Different Types of Reinforcing on Seismic Behavior of Short Concrete Columns," by V. V. Bertero, J. Hollings, O. Kustu, R. M. Stephen and J. G. Bouwkamp - 1973
- EERC 73-19 "Olive View Medical Center Material Studies, Phase I," by B. Bresler and V. V. Bertero - 1973 (PB 235 986)
- EERC 73-20 "Linear and Nonlinear Seismic Analysis Computer Programs for Long Multiple-Span Highway Bridges," by W. S. Tseng and J. Penzien - 1973
- EERC 73-21 "Constitutive Models for Cyclic Plastic Deformation of Engineering Materials," by J. M. Kelly and P. P. Gillis - 1973 (PB 226 024)
- EERC 73-22 "DRAIN - 2D User's Guide," by G. H. Powell - 1973 (PB 227 016)
- EERC 73-23 "Earthquake Engineering at Berkeley - 1973" - 1973 (PB 226 033)
- EERC 73-24 Unassigned
- EERC 73-25 "Earthquake Response of Axisymmetric Tower Structures Surrounded by Water," by C. Y. Liaw and A. K. Chopra - 1973 (AD 773 052)
- EERC 73-26 "Investigation of the Failures of the Olive View Stairtowers during the San Fernando Earthquake and Their Implications in Seismic Design," by V. V. Bertero and R. G. Collins - 1973 (PB 235 106)

- EERC 73-27 "Further Studies on Seismic Behavior of Steel Beam-Column Subassemblages," by V. V. Bertero, H. Krawinkler and E. P. Popov - 1973 (PB 234 172)
- EERC 74-1 "Seismic Risk Analysis," by C. S. Oliveira - 1974 (PB 235 920)
- EERC 74-2 "Settlement and Liquefaction of Sands under Multi-Directional Shaking," by R. Pyke, C. K. Chan and H. B. Seed - 1974
- EERC 74-3 "Optimum Design of Earthquake Resistant Shear Buildings," by D. Ray, K. S. Pister and A. K. Chopra - 1974 (PB 231 172)
- EERC 74-4 "LUSH - A Computer Program for Complex Response Analysis of Soil-Structure Systems," by J. Lysmer, T. Udaka, H. B. Seed and R. Hwang - 1974 (PB 236 796)
- EERC 74-5 "Sensitivity Analysis for Hysteretic Dynamic Systems: Applications to Earthquake Engineering," by D. Ray - 1974 (PB 233 213)
- EERC 74-6 "Soil-Structure Interaction Analyses for Evaluating Seismic Response," by H. B. Seed, J. Lysmer and R. Hwang - 1974 (PB 236 519)
- EERC 74-7 Unassigned
- EERC 74-8 "Shaking Table Tests of a Steel Frame - A Progress Report," by R. W. Clough and D. Tang - 1974
- EERC 74-9 "Hysteretic Behavior of Reinforced Concrete Flexural Members with Special Web Reinforcement," by V. V. Bertero, E. P. Popov and T. Y. Wang - 1974 (PB 236 797)
- EERC 74-10 "Applications of Reliability-Based, Global Cost Optimization to Design of Earthquake Resistant Structures," by E. Vitiello and K. S. Pister - 1974 (PB 237 231)
- EERC 74-11 "Liquefaction of Gravelly Soils under Cyclic Loading Conditions," by R. T. Wong, H. B. Seed and C. K. Chan - 1974
- EERC 74-12 "Site-Dependent Spectra for Earthquake-Resistant Design," by H. B. Seed, C. Ugas and J. Lysmer - 1974

- EERC 74-13 "Earthquake Simulator Study of a Reinforced Concrete Frame," by P. Hidalgo and R. W. Clough - 1974 (PB 241 944)
- EERC 74-14 "Nonlinear Earthquake Response of Concrete Gravity Dams," by N. Pal - 1974 (AD/A006583)
- EERC 74-15 "Modeling and Identification in Nonlinear Structural Dynamics, I - One Degree of Freedom Models," by N. Distefano and A. Rath - 1974 (PB 241 548)
- EERC 75-1 "Determination of Seismic Design Criteria for the Dumbarton Bridge Replacement Structure, Vol. I: Description, Theory and Analytical Modeling of Bridge and Parameters," by F. Baron and S.-H. Pang - 1975
- EERC 75-2 "Determination of Seismic Design Criteria for the Dumbarton Bridge Replacement Structure, Vol. 2: Numerical Studies and Establishment of Seismic Design Criteria," by F. Baron and S.-H. Pang - 1975
- EERC 75-3 "Seismic Risk Analysis for a Site and a Metropolitan Area," by C. S. Oliveira - 1975
- EERC 75-4 "Analytical Investigations of Seismic Response of Short, Single or Multiple-Span Highway Bridges," by Ma-chi Chen and J. Penzien - 1975 (PB 241 454)
- EERC 75-5 "An Evaluation of Some Methods for Predicting Seismic Behavior of Reinforced Concrete Buildings," by Stephen A. Mahin and V. V. Bertero - 1975
- EERC 75-6 "Earthquake Simulator Study of a Steel Frame Structure, Vol. I: Experimental Results," by R. W. Clough and David T. Tang - 1975 (PB 243 981)
- EERC 75-7 "Dynamic Properties of San Bernardino Intake Tower," by Dixon Rea, C.-Y. Liaw, and Anil K. Chopra - 1975 (AD/A008406)
- EERC 75-8 "Seismic Studies of the Articulation for the Dumbarton Bridge Replacement Structure, Vol. I: Description, Theory and Analytical Modeling of Bridge Components," by F. Baron and R. E. Hamati - 1975
- EERC 75-9 "Seismic Studies of the Articulation for the Dumbarton Bridge Replacement Structure, Vol. 2: Numerical Studies of Steel and Concrete Girder Alternates," by F. Baron and R. E. Hamati - 1975

- EERC 75-10 "Static and Dynamic Analysis of Nonlinear Structures,"  
by Digambar P. Mondkar and Graham H. Powell - 1975  
(PB 242 434)
- EERC 75-11 "Hysteretic Behavior of Steel Columns," by E. P. Popov,  
V. V. Bertero and S. Chandramouli - 1975
- EERC 75-12 "Earthquake Engineering Research Center Library Printed  
Catalog" - 1975 (PB 243 711)
- EERC 75-13 "Three Dimensional Analysis of Building Systems,"  
Extended Version, by E. L. Wilson, J. P. Hollings and  
H. H. Dovey - 1975 (PB 243 989)
- EERC 75-14 "Determination of Soil Liquefaction Characteristics by  
Large-Scale Laboratory Tests," by Pedro De Alba, Clarence  
K. Chan and H. Bolton Seed - 1975
- EERC 75-15 "A Literature Survey - Compressive, Tensile, Bond and  
Shear Strength of Masonry," by Ronald L. Mayes and  
Ray W. Clough - 1975
- EERC 75-16 "Hysteretic Behavior of Ductile Moment Resisting Reinforced  
Concrete Frame Components," by V. V. Bertero and  
E. P. Popov - 1975
- EERC 75-17 "Relationships Between Maximum Acceleration, Maximum  
Velocity, Distance from Source, Local Site Conditions  
for Moderately Strong Earthquakes," by H. Bolton Seed,  
Ramesh Murarka, John Lysmer and I. M. Idriss - 1975
- EERC 75-18 "The Effects of Method of Sample Preparation on the Cyclic  
Stress-Strain Behavior of Sands," by J. Paul Mulilis,  
Clarence K. Chan and H. Bolton Seed - 1975
- EERC 75-19 "The Seismic Behavior of Critical Regions of Reinforced  
Concrete Components as Influenced by Moment, Shear and  
Axial Force," by B. Atalay and J. Penzien - 1975
- EERC 75-20 "Dynamic Properties of an Eleven Story Masonry Building,"  
by R. M. Stephen, J. P. Hollings, J. G. Bouwkamp and  
D. Jurukovski - 1975
- EERC 75-21 "State-of-the-Art in Seismic Shear Strength of Masonry -  
An Evaluation and Review," by Ronald L. Mayes and  
Ray W. Clough - 1975
- EERC 75-22 "Frequency Dependencies Stiffness Matrices for Viscoelastic  
Half-Plane Foundations," by Anil K. Chopra, P. Chakrabarti  
and Gautam Dasgupta - 1975
- EERC 75-23 "Hysteretic Behavior of Reinforced Concrete Framed Walls,"  
by T. Y. Wong, V. V. Bertero and E. P. Popov - 1975

- EERC 75-24 "Testing Facility for Subassemblages of Frame-Wall Structural Systems," by V. V. Bertero, E. P. Popov and T. Endo - 1975
- EERC 75-25 "Influence of Seismic History of the Liquefaction Characteristics of Sands," by H. Bolton Seed, Kenji Mori and Clarence K. Chan - 1975
- EERC 75-26 "The Generation and Dissipation of Pore Water Pressures during Soil Liquefaction," by H. Bolton Seed, Phillippe P. Martin and John Lysmer - 1975
- EERC 75-27 "Identification of Research Needs for Improving a Seismic Design of Building Structures," by V. V. Bertero - 1975
- EERC 75-28 "Evaluation of Soil Liquefaction Potential during Earthquakes," by H. Bolton Seed, I. Arango and Clarence K. Chan 1975
- EERC 75-29 "Representation of Irregular Stress Time Histories by Equivalent Uniform Stress Series in Liquefaction Analyses," by H. Bolton Seed, I. M. Idriss, F. Makdisi and N. Banerjee 1975
- EERC 75-30 "FLUSH - A Computer Program for Approximate 3-D Analysis of Soil-Structure Interaction Problems," by J. Lysmer, T. Udaka, C.-F. Tsai and H. B. Seed - 1975
- EERC 75-31 "ALUSH - A Computer Program for Seismic Response Analysis of Axisymmetric Soil-Structure Systems," by E. Berger, J. Lysmer and H. B. Seed - 1975
- EERC 75-32 "TRIP and TRAVEL - Computer Programs for Soil-Structure Interaction Analysis with Horizontally Travelling Waves," by T. Udaka, J. Lysmer and H. B. Seed - 1975
- EERC 75-33 "Predicting the Performance of Structures in Regions of High Seismicity," by Joseph Penzien - 1975
- EERC 75-34 "Efficient Finite Element Analysis of Seismic Structure - Soil - Direction," by J. Lysmer, H. Bolton Seed, T. Udaka, R. N. Hwang and C.-F. Tsai - 1975
- EERC 75-35 "The Dynamic Behavior of a First Story Girder of a Three-Story Steel Frame Subjected to Earthquake Loading," by Ray W. Clough and Lap-Yan Li - 1975
- EERC 75-36 "Earthquake Simulator Study of a Steel Frame Structure, Volume II - Analytical Results," by David T. Tang - 1975
- EERC 75-37 "ANSR-I General Purpose Computer Program for Analysis of Non-Linear Structure Response," by Digambar P. Mondkar and Graham H. Powell - 1975

- EERC 75-38 "Nonlinear Response Spectra for Probabilistic Seismic Design and Damage Assessment of Reinforced Concrete Structures," by Masaya Murakami and Joseph Penzien - 1975
- EERC 75-39 "Study of a Method of Feasible Directions for Optimal Elastic Design of Framed Structures Subjected to Earthquake Loading," by N. D. Walker and K. S. Pister - 1975
- EERC 75-40 "An Alternative Representation of the Elastic-Viscoelastic Analogy," by Gautam Dasgupta and Jerome L. Sackman - 1975
- EERC 75-41 "Effect of Multi-Directional Shaking on Liquefaction of Sands," by H. Bolton Seed, Robert Pyke and Geoffrey R. Martin - 1975
- EERC 76-1 "Strength and Ductility Evaluation of Existing Low-Rise Reinforced Concrete Buildings - Screening Method," by Tsuneo Okada and Boris Bresler - 1976
- EERC 76-2 "Experimental and Analytical Studies on the Hysteretic Behavior of Reinforced Concrete Rectangular and T-Beams," by Shao-Yeh Marshall Ma, Egor P. Popov and Vitelmo V. Bertero - 1976
- EERC 76-3 "Dynamic Behavior of a Multistory Triangular-Shaped Building," by J. Petrovski, R. M. Stephen, E. Gartenbaum and J. G. Bouwkamp - 1976
- EERC 76-4 "Earthquake Induced Deformations of Earth Dams," by Norman Serff and H. Bolton Seed - 1976
- EERC 76-5 "Analysis and Design of Tube-Type Tall Building Structures," by H. de Clercq and G. H. Powell - 1976
- EERC 76-6 "Time and Frequency Domain Analysis of Three-Dimensional Ground Motions, San Fernando Earthquake," by Tetsuo Kubo and Joseph Penzien - 1976
- EERC 76-7 "Expected Performance of Uniform Building Code Design Masonry Structures," by R. L. Mayes, Y. Omote, S. W. Chen and R. W. Clough - 1976
- EERC 76-8 "Cyclic Shear Tests on Concrete Masonry Piers, Part I - Test Results," by R. L. Mayes, Y. Omote and R. W. Clough 1976
- EERC 76-9 "A Substructure Method for Earthquake Analysis of Structure - Soil Interaction," by Jorge Alberto Gutierrez and Anil K. Chopra - 1976
- EERC 76-10 "Stabilization of Potentially Liquefiable Sand Deposits using Gravel Drain Systems," by H. Bolton Seed and John R. Booker - 1976

- EERC 76-11 "Influence and Analysis Assumptions on Computed Inelastic Response of Moderately Tall Frames," by G. H. Powell and D. G. Row - 1976
- EERC 76-12 "Sensitivity Analysis for Hysteretic Dynamic Systems: Theory and Applications," by D. Ray, K. S. Pister and E. Polak - 1976
- EERC 76-13 "Coupled Lateral Torsional Response of Buildings to Ground Shaking," by Christopher L. Kan and Anil K. Chopra - 1976
- EERC 76-14 "Seismic Analyses of the Banco de America," by V. V. Bertero, S. A. Mahin, and J. A. Hollings -1976
- EERC 76-15 "Reinforced Concrete Frame 2: Seismic Testing and Analytical Correlation," by Ray W. Clough and Jawahar Gidwani - 1976
- EERC 76-16 "Cyclic Shear Tests on Masonry Piers, Part II - Analysis of Test Results," by R. L. Mayes, Y. Omote and R. W. Clough 1976
- EERC 76-17 "Structural Steel Bracing Systems: Behavior Under Cyclic Loading," by E. P. Popov, K. Takanashi and C. W. Roeder 1976
- EERC 76-18 "Experimental Model Studies on Seismic Response of High Curved Overcrossings," by David Williams and William G. Godden - 1976
- EERC 76-19 "Effects of Non-Uniform Seismic Disturbances on the Dumbarton Bridge Replacement Structure," by Frank Baron and Raymond E. Hamati - 1976
- EERC 76-20 "Investigation of the Inelastic Characteristics of a Single Story Steel Structure using System Identification and Shaking Table Experiments," by Vernon C. Matzen and Hugh D. McNiven 1976
- EERC 76-21 "Capacity of Columns with Splice Imperfections," by E. P. Popov, R. M. Stephen and R. Philbrick - 1976
- EERC 76-22 "Response of the Olive View Hospital Main Building during the San Fernando Earthquake," by Stephen A. Mahin, Robert Collins, Anil K. Chopra and Vitelmo V. Bertero - 1976
- EERC 76-23 "A Study on the Major Factors Influencing the Strength of Masonry Prisms," by N. M. Mostaghel, R. L. Mayes, R. W. Clough and S. W. Chen - 1976
- EERC 76-24 "GADFLEA - A Computer Program for the Analysis of Pore Pressure Generation and Dissipation during Cyclic or Earthquake Loading," by J. R. Booker, M. S. Rahman and H. Bolton Seed - 1976

EERC 76-25 "Rehabilitation of an Existing Building: A Case Study,"  
by B. Bresler and J. Axley - 1976

EERC 76-26 "Correlative Investigations on Theoretical and Experimental  
Dynamic Behavior of a Model Bridge Structure," by  
Kazuhiko Kawashima and Joseph Penzien - 1976

EERC 76-27 "Earthquake Response of Coupled Shear Wall Buildings," by  
Thirawat Srichatrapimuk - 1976

